UNCLASSIFIED

AD NUMBER
AD860352
LIMITATION CHANGES

TO:

Approved for public release; distribution is unlimited.

FROM:

Distribution authorized to U.S. Gov't. agencies and their contractors; Critical Technology; JUL 1969. Other requests shall be referred to Army Aviation Materiel Laboratories, Fort Eustis, VA 23604. This document contains export-controlled technical data.

AUTHORITY

USAAMRDL ltr dtd 18 Jun 1971

THIS PAGE IS UNCLASSIFIED

AD 860352

AD

USAAVLABS TECHNICAL REPORT 69-39

SUPPRESSION OF TRANSMITTED HARMONIC VERTICAL AND INPLANE ROTOR LOADS BY BLADE PITCH CONTROL

By

John C. Balcerak
John C. Erickson, Jr.

July 1969

U. S. ARMY AVIATION MATERIEL LABORATORIES
FORT EUSTIS, VIRGINIA

U S ARMY MATERIEL COMMAND

D D C
RECEIVED
OCT 2 1 1969
B

104

This contract was initiated to investigate the feasibility of applying higher-harmonic blade pitch control solely at the blade root for the purpose of eliminating the transmission of helicopter rotor oscillatory shear forces to the fuselage. Numerical analyses were performed to estimate the pitch control inputs and the associated performance required for eliminating transmitted (noncancelling) harmonic vertical root shears alone, harmonic inplane root shears alone, and the principal vertical and inplane harmonic root shears simultaneously.

For the UH-1A rotor system with an assumed ideal control system, results indicate that, except for the first-harmonic inplane shear, harmonic root pitch control can be applied to eliminate transmitted harmonic root shears. Elimination of the higher-harmonic shears does not appear to be feasible: they are relatively small in magnitude and do not warrant the additional mechanical complexity. Although the use of a single root pitch mode would be preferable from a simplicity standpoint, evidence suggests that dual pitch controls with differential pitching motions of inboard and outboard blade sections are essential. Higher harmonic pitch control is a promising means of vibration suppression. However, application of harmonic pitch control solely at the blade root appears to be stymied by the following deficiencies:

- For the two-bladed teetering rotor system considered, the first-harmonic inplane shear is the largest transmitted harmonic root shear. It cannot be eliminated by root pitch control.

- Root pitch control requirements change appreciably with flight conditions.

- In eliminating certain harmonic root shears, harmonic root pitch control inputs incite aerodynamic-inertial interactions, causing large blade motions and large pitch angle excursions.

For these deficiencies, a form of dual pitch control with differential pitching motions of inboard and outboard blade sections is foreseen as a promising solution.

A feasibility study of a rotor system with dual pitch controls is currently under way. This initial feasibility study does not embody consideration of higher-harmonic pitch control.

SUPPRESSION OF TRANSMITTED
HARMONIC VERTICAL AND INPLANE
ROTOR LOADS BY BLADE PITCH CONTROL

Final Report

Cornell Aeronautical Laboratory, Inc. Report No. BB-2496-S-1

By

John C. Balcerak
John C. Erickson, Jr.

SUMMARY

A study was made of the possibility of using higher harmonic pitch-angle inputs to eliminate the transmission of oscillatory vertical and inplane forces from a helicopter rotor to its driving shaft. The aerodynamic loads were computed by using a realistic model which represented the rotor blades by bound vorticity distributions and the wake by a mesh of segmented vortex filaments.

The method which was developed computed the required pitch-angle inputs at the blade root which would eliminate the oscillatory vertical and inplane root shears. The oscillatory lift and drag were not constrained to be zero at all radial stations, and the inertia forces associated with blade dynamic responses which also produced root shears were taken into account in the computations. The computational procedure which was developed is capable of treating either the two-bladed teetering rotor or articulated rotors.

The computed results were based on a two-bladed teetering rotor which was approximately the same as that of the UH-1A configuration except for the assumed differences in pitch control. The required pitch angle inputs were determined for eliminating various combinations of harmonic root shears.

Variations in the required pitch inputs were found for the various flight conditions analyzed. For all flight conditions, however, the results showed that most of the oscillatory vertical root shear could be eliminated with blade root pitch inputs at the second and fourth harmonics. Root pitch control could be applied to eliminate all the harmonic transmitted shears except the first inplane harmonic. The first harmonic root pitch control was unavailable because it was necessary for providing ordinary cyclic pitch control of the tip-path plane. Of the transmitted inplane shears that could be eliminated, the largest could be eliminated with blade root pitch inputs at the third and seventh harmonics. For all cases investigated, the blade dynamics responses had an important effect on the required pitch inputs.

The simultaneous application of higher even harmonic and higher odd harmonic pitch control affected the performance characteristics of the rotor from those of conventional control to a larger extent than the individual application of either higher even harmonic or higher odd harmonic pitch control.

iii

FOREWORD

v

TABLE OF CONTENTS

TABLE OF CONTENTS (Cont'd)

LIST OF ILLUSTRATIONS

ix

LIST OF ILLUSTRATIONS (Cont'd)

LIST OF TABLES

LIST OF SYMBOLS

A_n — Glauert coefficients, ft/sec

$(A_n q_i)$, $(B_n q_i)$ — Fourier coefficients of $q_i(t)$

$A_{q_i \ddot{z}_j}$, $A_{q_i \dot{z}_j}$, $A_{q_i z_j}$ — quasi-steady aerodynamic coefficients

b — blade semichord, ft

C_{d_p} — profile drag coefficient

C_l, C_{l_α} — section lift coefficient and lift-curve slope

c_i — generalized coordinate for i^{th} control mode

d — blade section drag per unit span, lb/ft

$D(I, J, n)$ — dynamic response matrix

D_C — canceling inplane root shear of one blade, lb

D_N — noncanceling inplane root shear of one blade, lb

e_o — distance of blade pitch axis forward of midchord, ft

e — distance of blade elastic axis forward of midchord, ft

$[E]$ — matrix of aerodynamic coefficients used in estimating $\Delta^t[G]$

$f_{q_i}(r)$ — normalized deflection in the q_i^{th} mode

$[F]$ — response matrix used in iterative solution

G_{q_i} — generalized airload acting in the q_i^{th} mode

$\bar{G}_{q_i}$ — complex periodic variation of G_{q_i}

$g_{q_i q_j}$ — structural damping coefficient

$G_{q_i q_j}$ — generalized gyroscopic coupling coefficient

h — blade section plunging velocity relative to fixed axes, ft/sec

h_o — blade deflection relative to reference plane due to preconing and steady blade bending, ft

h_i	generalized coordinate for i^{th} vertical deflection mode, ft
H_i	generalized coordinate for i^{th} inplane deflection mode, ft
h_m	distance of midchord axis above reference plane, ft
I_k	quasi-steady part of Γ_k, ft^2/sec
I_x, I_y	moments of inertia about elastic axis due to horizontal and vertical mass distributions, respectively, lb-ft-sec^2
I, J	indices used to designate rows and columns of matrices
j	$\sqrt{-1}$ except when used as subscript
k	subscript denoting collocation points in rotor disc
ℓ	subscript denoting value at azimuth position, $\psi_\ell = 2\pi(\ell-1)/(NA)$
$K_{q_i q_j}$	generalized stiffness coefficient
ℓ	blade section lift per unit span, lb/ft
m	blade mass per unit span, lb-sec^2/ft^2
$M_{q_i q_j}$	generalized mass coefficient
m	blade section pitching moment about midchord per unit span, lb-ft/ft
m_e	blade section pitching moment about elastic axis per unit span, lb-ft/ft
NA	number of azimuth positions used in the computation
NR	number of blade radial segments used in the computation
NRA	total number of collocation points in rotor disc; $NRA = NR \times NA$
q_i	generalized coordinate for i^{th} vertical deflection, inplane deflection, torsional, or control mode

xiii

$\bar{q}_i$ complex periodic variation of q_i.

R total blade radius, ft

r radius to a blade section, ft

S_c canceling vertical root shear of one blade, lb

$\bar{S}_c$ complex periodic variation of S_c

S_N noncanceling vertical root shear of one blade, lb

$\bar{S}_N$ complex periodic variation of S_N

S_n coefficients giving induced velocities due to mesh of vortex filaments in wake

T_n coefficients giving induced velocities due to rolled-up tip vortices

$T_{q_i q_j}$ generalized centrifugal force coefficient

t time, sec

(t) superscript used to denote t^{th} approximation of iterative solution

v_k velocity relative to the surface of the airfoil due to plunging motion at the kth collocation position, ft/sec

V_f rotor translational (forward) velocity, ft/sec

V_1 component of total velocity of blade section perpendicular to the shaft and to the blade axes, ft/sec

W_b load/blade, lb

w_k normal induced velocity distribution at the kth collocation position, ft/sec

z chordwise coordinate; distance aft of midchord, ft

$[X(n, I)]$ column matrix of nth harmonic Fourier coefficients of root shears and generalized coordinates

$[YP(n, I)]$ column matrix of prescribed variables

$[Y(n, I)]$ column matrix on right hand of equations used in iterative solution for variables

$\bar{Z}_{q_i} - Z_{q_i}$	generalized centrifugal force acting in q_i^{th} mode due to built-in twist and preconing
α_e	effective angle of attack of blade section relative to V_f [cf Equation (45)]
α_g	geometric angle of attack of blade section relative to V_f
$\dot{\alpha}_g$	time rate of change of geometric angle of attack, $\sec^{-1}$
α_m	stall angle for airfoil section, $|\alpha_m| \leq \pi/2$
α_M	stall angle for airfoil section, $\pi/2 < |\alpha_M| \leq \pi$
α_s	shaft angle relative to plane perpendicular to rotor translational velocity
β	first harmonic flapping relative to a plane perpendicular to the shaft; $\beta = \beta_{1C} \cos \psi + \beta_{1S} \sin \psi$
β_c	preconing angle
Γ_k	total bound vorticity of blade section of kth segment, $\text{ft}^2/\sec$
$\bar{\Gamma}$	strength of rolled-up tip vortex, $\text{ft}^2/\sec$
γ_k	chordwise bound vorticity distribution at the kth collocation position, ft/sec
$\Delta^{(t)}[G]$	change in column matrix of generalized aerodynamic forces from $(t-1)^{th}$ to $(t)^{th}$ approximation
θ	angular coordinate used to specify chordwise position; $x = -b \cos \theta$
θ_B	built-in twist
θ_i	generalized coordinate for i^{th} torsion mode
μ	advance ratio
ρ	air density, $\text{lb-sec}^2/\text{ft}^4$
σ, τ	induced velocity coefficients of Γ-equations
$[\dot{\Phi}_G]$	column matrix of iteration factors applied in computation of generalized aerodynamic forces
$[\dot{\Phi}_X]$	column matrix of iteration factors applied in computation of generalized coordinates

ψ azimuth angle

Ω rotor angular velocity, $\sec^{-1}$

ω_{q_i} natural frequency of q_i^{th} mode, $\sec^{-1}$

INTRODUCTION

The reduction of high vibration levels of helicopters has been the object of rather intensive effort for many years. The primary source of the objectionable vibrations appears to stem from the forces generated by the rotor which are transmitted directly to the drive shaft through the blade root fittings and rotor hub. Many different methods have been advocated for reducing the vibratory shears which are transmitted in this manner. Among these methods have been attempts to shift the natural bending frequencies of the rotor blades so as to reduce the amplification of the dynamic response in the bending modes, and attempts to reduce the vibratory exciting forces (as well as to improve performance) by the application of second harmonic pitch control.

Neither of the methods of attack mentioned above, or others, appeared to be entirely satisfactory. Thus, a study was initiated at CAL to investigate the possibility of reducing transmitted rotor shaking forces by the application of a more general type of blade pitch-angle control (Reference 1). This study differed from preceding ones in that a more realistic model was used in computing the rotor aero-dynamic exciting forces. In the first part of this study, the required pitch angles were found which would eliminate the oscillatory lift loadings at all radial stations. In the computations for this case, an ideal control system was assumed such that continuous radial and azimuthal variations in blade pitch angle would be possible. The required pitch angles were computed to obtain a prescribed constant blade-lift distribution which did not vary with azimuth position. This inverse problem was solved by an extension of a program developed for predicting the aerodynamic loads and dynamic response of rotor blades (Reference 2). From the results, it was concluded that the design of a pitch control system for the elimination of all harmonic vertical blade loadings would be difficult because the radial variations in the required pitch angles varied considerably with azimuth position, and the amplitudes and phase angles of the required inputs changed with flight condition.

In the second part of the study, a method was developed for computing the pitch-angle inputs at the blade root which were required to eliminate the oscillatory transmitted vertical root shears without requiring a radial variation in pitch inputs. A series of computations was carried out for a two-bladed rotor approximately the same as that of the UH-1A configuration except for the assumed differences in pitch control. It was found that all noncanceling vertical root shears from the second through the twelfth harmonic could be eliminated with higher harmonic pitch-angle inputs introduced at the blade root. Further, the largest part of the oscillatory transmitted vertical root shears could be removed by using only second and fourth harmonic pitch-angle inputs.

1

These results gave definite encouragement to the possibility of obtaining significant reductions in the transmitted harmonic root shears by using blade root pitch inputs which could be introduced by a practical control system.

This initial effort, as reported in Reference 1, was limited to the consideration of the lift or vertical shear loads transmitted to the fuselage. It is well known that vibratory drag loads generated in the rotor system are also responsible for serious fuselage vibrations, and it was recognized that further effort would be required to determine the effect of blade pitch control on the drag or inplane shear loads as well.

On the basis of the encouraging results obtained in Reference 1, it was deemed logical to continue the effort for evaluating the possible application of blade pitch inputs for the elimination of transmitted harmonic rotor loads, with emphasis on (1) the investigation of instabilities in the iterative solution which had been encountered in the first study, (2) study of transmitted inplane forces, and (3) estimating the effect of higher pitch-control inputs on performance.

In the present report, the analytical method for determining the pitch-angle inputs that are necessary for eliminating oscillatory vertical and inplane root shears is described. Part of this description is a treatment of the iterative scheme of solution of the basic equations of motion, including the use of iteration factors and improved initial conditions to overcome the computational instabilities. Results are presented for the extensive numerical computations carried out to eliminate the noncanceling vertical and inplane oscillatory shears in various harmonic combinations for three flight conditions of the UH-1A rotor configuration. Included in these results is the effect of the resulting blade pitch-angle inputs on performance. The basic aerodynamic analysis, which differs only slightly from References 1 and 2, is presented for completeness in Appendix I.

METHOD FOR FINDING PITCH-ANGLE INPUTS
TO ELIMINATE OSCILLATORY ROOT SHEARS

In Reference 1, a computational procedure was developed for finding the required harmonic root pitch-control inputs to eliminate the transmitted harmonic vertical root shears. The computational procedure has been extended such that the control inputs required to eliminate the transmitted harmonic inplane root shears can also be determined. In both cases, the blade dynamic responses which are excited by the residual harmonic airloads and affect the root shears are included in the analysis.

Computations were made to determine the harmonic control inputs required to eliminate oscillatory root shears for a two-bladed teetering rotor configuration approximately the same as that of the UH-1A helicopter, under the following assumptions:

1. The flight condition is steady so that the blade dynamic responses can be assumed to be periodic.

2. The blade root shears due to combined aerodynamic and inertia force loadings are to be zero at the prescribed harmonics.

3. The tip-path plane is in a prescribed position.

4. The blade dynamic responses can be described by:

    a. Three symmetric flapwise bending modes.

    b. Teetering motion and two antisymmetric flapwise bending modes.

    c. Two symmetric torsion modes.

    d. Two antisymmetric torsion modes (with the same frequencies as the symmetric modes).

    e. Two symmetric chordwise bending modes.

    f. Two antisymmetric chordwise bending modes (with the same frequencies as the symmetric modes).

5. Control can be applied by:

    a. One symmetric and one antisymmetric pitch control mode, each giving uniform feathering along the blade span.

3

b. One symmetric and one antisymmetric pitch-control mode, each giving differential feathering of the inboard and outboard sections of the blade.

When the second and all higher even harmonic root shears are prescribed to be zero, the vertical root shear transmitted to the fuselage is a constant, independent of azimuth position. The harmonic inplane shears are transmitted to the fuselage at harmonics one above and one below the harmonic inplane root shear so that, when the third and all higher odd harmonic root shears are prescribed to be zero, the inplane shear transmitted to the fuselage consists of a constant and a second harmonic force.

The treatment of the aerodynamics of the rotor-wake system was basically the same as that used in Reference 1. Minor modifications of the aerodynamic analysis were made in conjunction with the inclusion of the inplane aerodynamic forces, and the entire analysis is reviewed in Appendix I.

ROTOR DYNAMIC RESPONSES

The dynamic response of the rotor was described by the modes indicated schematically in Figure 1, which are applicable to the case of a two-bladed teetering configuration. All of the modes can be handled simultaneously in the computer program which was developed in Reference 1 and extended to include the inplane degrees of freedom herein. The computational procedure is also capable of treating the case of articulated rotors, but no computations were performed for this configuration.

The vertical and inplane symmetric and antisymmetric modes were designated by even and odd subscripts, respectively. The vertical tip deflections due to bending in the first, second, and third symmetric flapwise bending modes were denoted by h_2, h_4 and h_6; the inplane tip deflections due to bending in the first and second symmetric bending modes were denoted by H_2 and H_4. The tip deflections represent the generalized coordinates in the various modes. The tip deflections h_1 , h_3 and h_5 were used as generalized coordinates for the teetering motion and the first and second antisymmetric flapwise bending modes, respectively, while the tip deflections H_1 and H_3 were used as generalized coordinates for the first and second antisymmetric chordwise bending modes, respectively. Since the deflections in the blade chordwise bending modes are assumed to be zero at the blade root, the deflection shapes for each blade are the same for the symmetric and antisymmetric chordwise bending modes.

A symmetric vertical rotor displacement mode h_{0S} and an antisymmetric inplane rotor displacement mode H_{0A} are included in the analysis. The former mode corresponds to vertical motion of the flapping hinge, and the latter mode corresponds to inplane motion of the lag hinge. Both are produced by fuselage and hub motion. The h_{0S} and H_{0A} modes are introduced because the sum of the generalized

4

aerodynamic and inertia forces acting in these degrees of freedom is equal in magnitude to the transmitted shear. The amplitudes of the h_{OS} and H_{OA} motions are assumed to be zero in the analysis; i. e., it is assumed that the h_{OS} and H_{OA} motions do not produce any blade plunging or inplane motions, respectively.

An antisymmetric blade vertical displacement mode h_{OA} is also shown in Figure 1. This mode has no physical significance in the case of a teetering rotor, and motions in this mode are set equal to zero in the calculations. In the case of an articulated rotor blade with an offset flapping hinge, this mode would correspond to a tilting of the shaft. The generalized forces acting in the antisymmetric h_{OA} mode produce canceling vertical root shears, but such shears can transmit moments to the shaft only when offset hinges are used. The analysis provides for the computation of these moments. Similarly, displacements in the symmetric blade inplane displacement mode H_{OS} are assumed to be zero, and the generalized forces in this mode produce canceling inplane root shears.

The generalized coordinates θ_1, θ_2, θ_3, and θ_4 used for the blade torsion modes are the angular deflections about the elastic axis at the blade tip. Since the pitching of the blade root is described by the control modes, the angular deflections in the blade torsion modes are assumed to be zero at the blade root. As a result, the deflection shapes for each blade are the same for the symmetric and antisymmetric torsion modes. The natural frequencies of the bending and torsion modes shown in Figure 1 are listed in Appendix II for the configuration studied.

The computational model permits the use of two symmetric and two antisymmetric pitch-control modes. Conventional collective pitch is the steady component of the motion in the first symmetric control mode C_2, while conventional cyclic pitch is the first harmonic motion in the first antisymmetric control mode C_1. Higher harmonic motions can be introduced in both the C_1 and C_2 modes in order to modify the root shears. The second symmetric and second antisymmetric control modes C_4 and C_3, shown schematically in Figure 1, are possible differential control motions in which the inner and outer sections of the blade pitch in opposite directions. The mode shapes shown for C_3 and C_4 could be replaced by other radial variations within the framework of the analysis. For example, a linear variation in pitch might be used which could be produced by a device introducing a moment at the blade tip.

The spanwise variations of the amplitude in each mode are represented by dimensionless functions as

$$f_{q_i}(r) q_i(t) \qquad = \text{amplitude of motion in } q^{th} \text{ mode at radial station } r \text{ and at time } t.$$

5

HARMONIC AND DISCRETE TIME TREATMENT OF VARIABLES

The investigation has been limited to considering steady flight conditions for which the rotor loads, rotor motions, and transmitted shears are assumed to be periodic. In carrying out the aerodynamic computations, including the effects of the wake vorticity distributions, it is convenient to utilize the values of the variables at discrete time increments similar to the treatment used in Reference 2. As discussed in Appendix I, the positions of the shed and trailing vortices in the wake are determined from uniform inflow theory for the given flight condition. When the values of V_f, α_y, $\dot{\alpha}_y$ and h in Equation (42) of Appendix I are given at the NRA blade segment positions in the rotor disc, the aerodynamic problem is completely defined. The solution of the aerodynamic problem gives the blade circulation, lift, and pitching moment at each of the blade segment positions. Since the profile and induced drag loads are also determined at each of the blade segment positions, the variations in the aerodynamic loads are, in effect, given at discrete azimuth or time increments. The transmitted shears and generalized forces acting in each of the flapwise bending, chordwise bending, and torsion modes at the discrete azimuth positions can be computed from the lift, drag, and moment distributions. In computing the dynamic responses to periodic forces, it is more desirable to use a harmonic description of the variables. The time variation of the q_i^{th} generalized coordinate can be approximated by a finite Fourier series as follows:

$$ q_i(t) = \sum_{n=0}^{NA/2} \left\{ (A_n q_i) \cos n\psi + (B_n q_i) \sin n\psi \right\}, \tag{1} $$

where

$$ (A_0 q_i) = \frac{1}{NA} \sum_{k=1}^{NA} (q_i)_k , $$

$$ \left. \begin{aligned} (A_n q_i) &= \frac{2}{NA} \sum_{k=1}^{NA} (q_i)_k \cos n\psi_k \\ (B_n q_i) &= \frac{2}{NA} \sum_{k=1}^{NA} (q_i)_k \sin n\psi_k \end{aligned} \right\} ; \qquad 1 \le n \le \left(\frac{NA}{2} - 1 \right) \tag{2} $$

$$ (A_n q_i) = \frac{1}{NA} \sum_{k=1}^{NA} (q_i)_k \cos(k-1)\pi ; \qquad n = \frac{NA}{2} . $$

The symbol $(A_n q_i)$ indicates the operation of multiplying $(q_i)_k$, the value of the generalized coordinates, at azimuth position $\psi_k = 2\pi(k-1)/NA$ by $(2/NA) \cos n\psi_k$ and summing for NA equally spaced azimuth positions. This is simply the coefficient of the nth harmonic cosine term. Similarly, $(B_n q_i)$ is the coefficient of the nth harmonic sine term.

6

DISCUSSION OF EQUATIONS OF MOTION AND ANALYTICAL PROBLEM

The equation of motion for each of the flapwise or chordwise linear deflection and torsion modes can be written in the general form

$$\sum_{j}\left\{ M_{q_i q_j}\ddot{\bar{q}}_j - 2\Omega G_{q_i q_j}\dot{\bar{q}}_j + \left(K_{q_i q_j} - \Omega^2 T_{q_i q_j}\right)\bar{q}_j + j(gK)_{q_i q_j}\left(\bar{q}_j - \bar{q}_{j avg}\right)\right\}$$

$$= \bar{G}_{q_i} + \bar{Z}_{q_i} - \left\{ \delta_{q_i, h_{os}}\bar{S}_N + \delta_{q_i, h_{oA}}\bar{S}_C - \delta_{q_i, H_{oA}}\bar{D}_N - \delta_{q_i, H_{os}}\bar{D}_C\right\} \qquad (3)$$

for the assumed complex periodic variations in the generalized coordinates and in all the generalized forces acting on the blade. In this expression, the $M_{q_i q_j}$'s are generalized mass coefficients, the $G_{q_i q_j}$'s are gyroscopic coupling coefficients, the $K_{q_i q_j}$'s are generalized stiffness coefficients, the $T_{q_i q_j}$'s are centrifugal force coefficients, and the $g_{q_i q_j}$'s are structural damping coefficients. Definitions of these coefficients are given in Appendix II. The quantities on the right-hand side are the complex generalized aerodynamic forces acting in the q_i^{th} mode $\bar{G}_{q_i}$; the generalized centrifugal forces arising from built-in twist and preconing $\bar{Z}_{q_i}$; the complex noncanceling vertical root shear $\bar{S}_N$; the complex canceling vertical root shear $\bar{S}_C$; the complex noncanceling inplane root shear $-\bar{D}_N$; and the complex canceling inplane root shear $-\bar{D}_C$. The shears $\bar{S}_N$, $\bar{S}_C$, $-\bar{D}_N$, $-\bar{D}_C$ act only in the h_{os}, h_{oA}, H_{oA}, and H_{os} modes, respectively, as indicated by the δ functions. All coefficients and generalized forces represent values per blade.

Complex vectors, indicated by bars, have been used in Equation (3), since they are convenient in writing the conventional expression for structural damping. The complex periodic variations of each generalized coordinate $(\bar{q}_i)$ are expressed in the form

$$\bar{q}_i = \sum_{n=0}^{NA/2}\left\{ (A_n q_i) - j(B_n q_i)\right\} e^{j\omega t}$$

$$= \sum_{n=0}^{NA/2}\left\{ (A_n q_i)\cos n\psi + (B_n q_i)\sin n\psi\right\}$$

$$+ j\sum_{n=0}^{NA/2}\left\{ -(B_n q_i)\cos n\psi + (A_n q_i)\sin n\psi\right\}, \qquad (4)$$

where the complex coefficients have been defined in such a manner that the real part of Equation (4) is identical to Equation (1). Similar expressions hold for the other complex periodic quantities $(\bar{G}_{q_i}, \bar{Z}_{q_i}, \bar{S}_N, \bar{S}_C, -\bar{D}_N, -\bar{D}_C)$.

Only the real part of Equation (3) is considered in the subsequent discussion because it suffices to describe the real physical motion. After substituting expressions of the type shown in Equation (4), the real part of Equation (3) can be arranged in the form of a sum of

7

harmonic terms, and the coefficient of each cosine and sine harmonic must vanish for the complete equation to be satisfied. The requirements on the coefficients of $\cos n\psi$ and $\sin n\psi$ in the equation for the q_i^{th} mode are

$$\sum_j \left\{ K_{q_i q_j} - \Omega^2 T_{q_i q_j} - n^2 \Omega^2 M_{q_i q_j} \right\} (A_n q_j) + \sum_j \left\{ (Kg)_{q_i q_j} - n\Omega^2 2 G_{q_i q_j} \right\} (B_n q_j)$$

$$+ \delta_{q_i, h_{OS}} (A_n S_N) + \delta_{q_i, h_{OA}} (A_n S_G) + \delta_{q_i, H_{OA}} (-A_n D_N) + \delta_{q_i, H_{OS}} (-A_n D_C)$$

$$= (A_n G_{q_i}) + (A_n Z_{q_i}), \qquad (5)$$

$$-\sum_j \left\{ (Kg)_{q_i q_j} - n\Omega^2 2 G_{q_i q_j} \right\} (A_n q_j) + \sum_j \left\{ K_{q_i q_j} - \Omega^2 T_{q_i q_j} - n^2 \Omega^2 M_{q_i q_j} \right\} (B_n q_j)$$

$$+ \delta_{q_i, h_{OS}} (B_n S_N) + \delta_{q_i, h_{OA}} (B_N S_G) + \delta_{q_i, H_{OA}} (-B_n D_N) + \delta_{q_i, H_{OS}} (-B_n D_C)$$

$$= (B_n G_{q_i}). \qquad (6)$$

In matrix form, these equations and certain auxiliary constraint equations are shown in the form in which they appear in the computer program on pages 9 and 10.

From the symmetry of the two-bladed teetering rotor, it follows that the generalized forces acting in the flapwise and torsional symmetric modes can only be of even or zero harmonic order, while those acting in the flapwise and torsional antisymmetric modes can only be of odd harmonic order. As a result, the response in the flapwise and torsional symmetric modes must be at zero or even harmonic orders, and the response in the flapwise and torsional antisymmetric modes must be at odd harmonic orders. The same condition holds for the inplane modes; i. e., the generalized forces acting in the chordwise symmetric modes can only be of even or zero harmonic order, while those acting in the chordwise antisymmetric modes can only be of odd harmonic order. The response in each of the various modes is indicated by the variables appearing on the left-hand side of Equations (7) and (8). The fact that the responses in the various modes occur as described above does not mean that the two sets of equations are decoupled, since coupling can occur among harmonic coefficients of all orders through the generalized aerodynamic forces. For example, the combination of even harmonic blade motion and the flow dissymmetry due to forward flight can produce odd harmonic generalized aerodynamic forces.

The first four rows in Equation (7) represent the equilibrium of the nth harmonic cosine components of the generalized forces in the symmetric vertical deflection modes (h_{03}, h_2, h_4, h_6). The fifth and sixth rows represent the equilibrium of the cosine components of the

8

FORM OF EQUATIONS FOR EVEN HARMONICS, n = 2,4,......12 (ALSO APPLICABLE FOR n = 0 AS DISCUSSED BELOW):

$$\frac{1}{\Omega^2}
\begin{bmatrix}
D(I,J,n) = \frac{K_{q_iq_j}}{\Omega^2} - n^2 W_{q_iq_j} & 0 & D(I,J,n) = \frac{(K_\theta)_{q_iq_j} - 2nG_{q_iq_j}}{\Omega^2} = \text{\textcircled{B}} \\
0 & -T_{q_iq_j} = \text{\textcircled{A}} & D(I,J,n) \approx \text{\textcircled{A}} & D(I,J,n) \approx \text{\textcircled{B}} \\
D(I,J,N) = {}^1/\Omega^2 \text{ IF } J = JP(n,I) \quad = 0 \text{ OTHERWISE} \\
0 & \frac{1}{\Omega^2} & D(I,J,n) = -D(I-8,J+8,n) & 0 & D(I,J,N) = D(I-8,J-8,n) \approx \text{\textcircled{A}} & D(I,J,n) \approx -\text{\textcircled{B}} \\
D(I,J,n) = {}^1/\Omega^2 \text{ IF } J = JP(n,I) \quad = 0 \text{ OTHERWISE} \\
0 & \frac{1}{\Omega^2} D(I,J,n) \approx \text{\textcircled{A}} & D(I,J,n) \approx \text{\textcircled{B}} & 0 & D(I,J,n) \approx \text{\textcircled{B}} \\
0 & D(I,J,n) \approx \text{\textcircled{B}} & D(I,J,n) \approx \text{\textcircled{A}} & \frac{1}{\Omega^2}D(I,J,n) & D(I,J,n) \approx \text{\textcircled{A}}
\end{bmatrix}
\begin{Bmatrix}
A_n S_n \\ h_2 \\ h_4 \\ h_6 \\ \theta_2 \\ \theta_4 \\ C_2 \\ C_4 \\
B_n S_n \\ h_2 \\ h_4 \\ h_6 \\ \theta_2 \\ \theta_4 \\ C_2 \\ C_8 \\
-A_n D_c \\ H_2 \\ H_4 \\
-B_n D_c \\ H_2 \\ H_4
\end{Bmatrix}
= \frac{1}{\Omega^2}
\begin{Bmatrix}
A_n G_{HOS} \\ G_{h_2} \\ G_{h_4} \\ G_{h_6} \\ G_{\theta_2} \\ G_{\theta_4} \\ 0 \\ 0 \\
B_n G_{HOS} \\ G_{h_2} \\ G_{h_4} \\ G_{h_6} \\ G_{\theta_2} \\ G_{\theta_4} \\ 0 \\ 0 \\
A_n G_{HOS} \\ G_{H_2} \\ G_{H_4} \\
B_n G_{HOS} \\ G_{H_2} \\ G_{H_4}
\end{Bmatrix}
+ \frac{1}{\Omega^2}
\begin{Bmatrix}
0 \\ Z_{q_i}(n) \\ 0 \\ 0 \\ 0 \\ 0 \\ 0 \\ 0 \\ 0 \\ 0 \\ 0 \\ 0 \\ 0 \\ 0 \\ 0 \\ 0 \\ 0 \\ 0 \\ 0 \\ 0 \\ 0 \\ 0 \\ 0
\end{Bmatrix}
+ \frac{1}{\Omega^2}
\begin{Bmatrix}
0 \\ 0 \\ 0 \\ 0 \\ 0 \\ 0 \\ YP(n,7) \\ YP(n,8) \\ 0 \\ 0 \\ 0 \\ 0 \\ 0 \\ 0 \\ YP(n,15) \\ YP(n,16) \\ 0 \\ 0 \\ 0 \\ 0 \\ 0 \\ 0 \\ 0
\end{Bmatrix}
\qquad (7)$$

9

FORM OF EQUATIONS FOR ODD HARMONICS, $n = 1,3,\ldots,11$:

generalized moments in the symmetric torsion modes $(\theta_2 \cdot, \theta_4)$. Simi-larly, the ninth to the fourteenth rows represent the equilibrium of the sine components of the generalized forces in the symmetric vertical modes and the generalized moments in the symmetric torsional modes. The seventeenth, eighteenth, and nineteenth rows represent the equilib-rium of the nth harmonic cosine components of the generalized forces in the symmetric inplane modes, while the twentieth, twenty-first and twenty-second rows represent the equilibrium of the sine compo-nents of the generalized forces in the symmetric inplane modes. The choice of this representation was a logical extension of the represen-tation presented in Reference 1.

Twenty-two variables have been listed in the column matrix on the left-hand side of Equation (7). The deflections in the h_{os} and H_{os} modes are assumed to be zero, but the noncanceling vertical har-monic shear coefficients $(A_n S_n)$, $(B_n S_n)$ and the canceling inplane harmonic shear coefficients $(-A_n D_c)$, $(-B_n D_c)$ which are associated with these modes are treated as variables in the problem. The remaining variables are the cosine and sine components of the deflec-tions in the symmetric flapwise bending modes, symmetric torsion modes, symmetric control modes and symmetric chordwise bending modes. No equations of motion are included for the equilibrium of the control modes since the characteristics of the control system have not been included in the study. The seventh, eighth, fifteenth, and sixteenth rows of Equation (7) are four constraint equations which are added to the dynamic equations in order to make the number of equations equal to the number of unknowns in the column matrix on the left-hand side. Since constraint equations are included in the equation set for each harmonic, a well-defined problem results for the complete system of equations having the same number of equations as unknowns.

The implementation of a pitch control system for the elim-ination of root shears might be based on several different concepts. One such system might apply a higher harmonic pitch control schedule which would be selected in accordance with the flight condition (i. e., flight velocity, rotor speed, etc.). Solutions based on the method given in this section indicate the pitch control schedules which should be used. In another possible system, the output of a sensor measuring the blade root shears might be used as a feedback in a pitch-control servo. The application of such a servo system would be dependent upon obtaining a design in which the dynamic responses of the coupled rotor - servo system would be stable. A more extensive computer program would be required to study this problem, which would include the dynamics of both the rotor and servo systems.

A general element of the 22-by-22 dynamic response matrix on the left-hand side of Equation (7) is denoted by $D(I, J, n)$, where I and J denote the row and column, respectively, and n the applicable harmonic order. The $[D]$ matrix has been partitioned, and the forms of typical elements in the submatrices are shown. The specific form of the 22-by-22 matrix was obtained by bordering on the 16-by-16 matrix

11

of Reference 1. The elements of the submatrices $[D]$ referring to the inplane degrees of freedom can be expressed in the same general form as those for the flapwise and torsional degrees of freedom, and they would become part of either principal submatrix by suitable rearrangement of the equations.

The nth harmonic generalized aerodynamic forces acting in the symmetric modes are listed in the first column matrix on the right-hand side of Equation (7). In the next column matrix, a list is given of the generalized centrifugal forces ($Z_{q_i}(n)$) associated with preconing and built-in twist. These are steady forces, and $Z_{q_i}(n)$ is zero unless $n = 0$. The last column matrix in the right-hand side of Equation (7) is used in the computer program to prescribe the values of four variables (for $n = 0$, only two of the cosine coefficients need be prescribed since all the sine coefficients are zero).

Two examples are given below in order to clarify the meaning of the notation used in the constraint equations. If it were desired to use the seventh equation to put a constraint on $(A_n S_n)$ (i.e., the nth harmonic cosine coefficient of noncanceling root shear), a setting

$$JP(n, I = 7) = 1 \qquad (9)$$

would be used in the inputs to the computer program. This means the only element of the $[D]$ matrix in the seventh row ($I = 7$) would be in the first column ($J = 1$), resulting in the equation

$$\frac{1}{\Omega^2}(A_n S_n) = \frac{1}{\Omega^2} YP(n, 7). \qquad (10)$$

Thus, for $JP(n, 7) = 1$, the input $YP(n, 7)$ would be set equal to zero if a solution were desired with the nth harmonic noncanceling vertical root shear equal to zero.

If it were desired to use the seventh equation to put a constraint on $(-A_n D_n)$ (i.e., the nth harmonic cosine coefficient of noncanceling inplane shear), a setting

$$JP(n, I = 7) = 17 \qquad (11)$$

would be used in the inputs to the computer program. This means that the only element of the $[D]$ matrix in the seventh row ($I = 7$) would be in the seventeenth column ($J = 17$), resulting in the equation

$$\frac{1}{\Omega^2}(-A_n D_N) = \frac{1}{\Omega^2} YP(n, 7), \qquad (12)$$

and for $JP(n, 7) = 17$, the input $YP(n, 7)$ would be set equal to zero if a solution were desired with the nth harmonic noncanceling inplane shear equal to zero.

12

Except for the latter example, the preceding discussion has been given relative to the even harmonic equations, but analogous considerations hold for the odd harmonic equations. Although the expressions for the matrix elements appear to be the same in Equations (7) and (8), different $K_{q_i q_j}$, $M_{q_i q_j}$, $T_{q_i q_j}$, $(Kg)_{q_i q_j}$ and $G_{q_i q_j}$ coefficients are involved because symmetric and antisymmetric modes occur in the two cases, respectively. For $n = 0$, there are no sine component generalized forces or generalized coordinates, and somewhat different treatment is required. It was desired to use matrices of the same order for all harmonics in the computer program for convenience. The $n = 0$ case was brought into this framework by retaining only diagonal terms in the ninth to sixteenth and twentieth to twenty-second rows of the matrix and setting the right-hand side of the corresponding equations equal to zero. Thus, the same matrix inversion program could be used for $n = 0$ as for the other harmonics.

The set of equations of motion and constraint equations for even or odd harmonics can be written symbolically in the form

$$\left[D(I,J,n)\right]\left[X(n,J)\right] = \frac{1}{\Omega^2}\left[G(n,I)\right] + \frac{1}{\Omega^2}\left[Z(n,I)\right] + \frac{1}{\Omega^2}\left[YP(n,I)\right], \qquad (13)$$

where appropriate symbols have been introduced for the column matrices in Equations (7) and (8). The $\left[X(n,J)\right]$ matrix is composed of variables corresponding to symmetric modes for zero and even harmonics and is composed of variables corresponding to antisymmetric modes for odd harmonics. The nth harmonic generalized aerodynamic forces are functions of the lift, moment, and drag on the blade which depend on all the harmonics of the motion as mentioned previously. That is,

$$\left[G(n,I)\right] = \left[f\left\{(A_0 h_2), \cdots (A_0 H_4); (A_1 h_1), \cdots (A_1 H_3);\right.\right.$$

$$\left.\left.(B_1 h_1), \cdots (B_1 H_3); \cdots; (A_{12} h_2), \cdots (A_{12} H_4)\right\}\right]. \qquad (14)$$

An explicit expression for the generalized forces in the form of Equation (14) is not available, but such a relationship can be obtained from the solution of the aerodynamic problem as discussed in Appendix I. For given harmonic coefficients, the azimuthal variations of the generalized coordinates can be computed using Equation (1). The input variables α_g, $\dot{\alpha}_g$, and h in Equation (34), Appendix I, can then be expressed in terms of the generalized coordinates for blade motion by referring to Figures 2 and 3, again making small-angle approximations. The geometric angle of attack at each blade segment azimuthal position k relative to the local velocity is

$$\alpha_{g_k} = \left\{\theta_s + \sum_\tau f_{c_\tau} c_\tau + \sum_\gamma f_{\theta_\gamma} \theta_\gamma\right\}_k, \qquad (15)$$

13

where θ_{g} is the built-in twist and the control modes are as shown in Figure 1. The relative angular velocity due to the motion of the blade is

$$\dot{\alpha}_{g_{K}} = \left\{ \sum_{\tau} f_{c_{\tau}} \dot{c}_{\tau} + \sum_{\tau} f_{\theta_{\tau}} \dot{\theta}_{\tau} + \Omega \left(\beta_{c} + \sum_{s} h_{s} \frac{df_{h_{s}}}{dr} \right) \right\}_{K}. \qquad (16)$$

The last term is due to the small component of the shaft angular velocity along the blade axis and was neglected in the computations. The component of velocity normal to V_{f} and the blade axis is

$$\dot{h}_{K} = \left\{ V_{f} \sin \alpha_{s} + (V_{f} \cos \alpha_{s}) (\cos \psi) \left(\beta_{c} + \sum_{s} h_{s} \frac{df_{h_{s}}}{dr} \right) \right.$$

$$\left. + \sum_{s} f_{h_{s}} \dot{h}_{s} - e \sum_{\tau} f_{\theta_{\tau}} \dot{\theta}_{\tau} - e_{o} \sum_{\tau} f_{c_{\tau}} \dot{c}_{\tau} \right\}_{K}, \qquad (17)$$

where e is the distance between the midchord and the elastic axis and e_{o} is the distance between the midchord and the pitch axis (Appendix II). The summations in Equations (15), (16), and (17) are over all the symmetric and antisymmetric modes of bending, torsion, and control motion.

Once the $\alpha_{g_{K}}{}'s$, $\dot{\alpha}_{g_{K}}{}'s$, and $\dot{h}_{K}{}'s$ have been determined, Equation (41), Appendix I, can be solved for the bound vortices and the corresponding Glauert coefficients at all blade segment positions in the rotor disc. The lift (l), pitching moment (m), and drag loadings (d) can be computed by Equations (48), (49), and (52), respectively, of Appendix I. The generalized forces in each of the vertical, torsion and chordwise displacement modes can be determined from the relations

$$\left(G_{h_{i}} \right)_{l} = \int l_{l}(r) f_{h_{i}}(r) dr, \qquad (18)$$

$$\left(G_{\theta_{i}} \right)_{l} = \int \left[m_{l}(r) - e(r) l_{l}(r) \right] f_{\theta_{i}}(r) dr, \qquad (19)$$

and

$$\left(G_{H_{i}} \right)_{l} = - \int d_{l}(r) f_{H_{i}}(r) dr, \qquad (20)$$

where the subscript l refers to the indicated quantities at azimuth angle ψ_{l}. The harmonic analysis of the results obtained from Equations (18), (19), and (20) is the final step in relating the harmonic coefficients of the generalized aerodynamic forces and the harmonic coefficients of the generalized coordinates of the blade motions as indicated in Equation (14).

A schematic diagram of the analytical problem which must be solved to evaluate the pitch-angle inputs necessary to eliminate oscillatory root shears is shown in Figure 4. The diagram indicates the relationships among the various parts of the problem in the approach

14

which has been discussed. The overall diagram has been divided into two boxes indicated by the dashed lines -- one showing the solution of the aerodynamics of the rotor-wake systems, and the other showing the solution for the blade dynamic response, required pitch angles and residual root shears. Again, it is pointed out that the aerodynamic part of the problem is treated by using the values of the variables at discrete time or azimuth-angle increments, while the solutions for the dynamic responses and shears a e created in terms of their harmonic coefficients.

ITERATIVE SCHEME OF SOLUTION FOR HARMONIC MOTIONS AND ROOT SHEARS

It is evident from the schematic diagram shown in Figure 4 that the dependencies of the aerodynamic loadings on the dynamic blade responses are very involved. The loads for specified input motions are obtained only after an iterative solution for the bound vortices as discussed in Appendix I. Consequently, a direct solution for the harmonic blade motions and root shears due to the aerodynamic loadings cannot be carried out, and an iterative scheme of solution was adopted for their determination as well.

In discussing this iterative scheme of solution, superscripts are used to denote the values of the variables in a particular iteration. Equation (13) can then be written as

$$\left[D(I,J,n)\right]\left[X^{(t)}(n,J)\right] = \frac{1}{\Omega^2}\left[G^{(t-1)}(n,I)\right] + \frac{1}{\Omega^2}\Delta^{(t)}\left[G(n,I)\right] + \frac{1}{\Omega^2}\left[Z(n,I)\right] + \frac{1}{\Omega^2}\left[YP(n,I)\right], \quad (21)$$

where $\left[X^{(t)}(n,J)\right]$ is the tth approximation for the column matrix of the generalized coordinates, $\left[G^{(t-1)}(n,I)\right]$ is the column matrix of generalized aerodynamic forces based on the preceding approximation for the column matrix of generalized coordinates, and $\Delta^{(t)}\left[G(n,I)\right]$ is the increment in the column matrix of generalized forces from the $(t-1)^{th}$ to the tth approximation. That is,

$$\Delta^{(t)}\left[G(n,I)\right] = \left[G^{(t)}(n,I)\right] - \left[G^{(t-1)}(n,I)\right]. \quad (22)$$

No superscripts are shown for the $[D]$, $[Z]$, and $[YP]$ matrices because they remain constant in the iterative solution.

As a reminder that the $[G(n,I)]$ are complicated functions of the lift, drag, and pitching moments on the blades, which, in turn, depend upon all harmonics of the generalized coordinates, the $(t-1)^{th}$ approximation can be written in the sense of Equation (14) as

$$\left[G^{(t-1)}(n,I)\right] = \left[f\left\{X^{(t-1)}(0,1), \cdots, X^{(t-1)}(12,22)\right\}\right]. \quad (23)$$

15

The most direct iterative procedure would be to assume $\Delta^{(t)}[G]$ to be zero in computing the tth approximation for the column matrix of generalized coordinates, $[X^{(t)}]$, and to use these coordinates to compute the tth approximation for the generalized aerodynamic forces, $[G^{(t)}]$; these, in turn, would be used to compute $[X^{(t+1)}]$ neglecting $\Delta^{(t+1)}[G]$, etc. Unfortunately, as Equation (21) stands, the $[D]$ matrix becomes singular when constraints are placed upon the various harmonics in order to control or suppress the transmitted vertical or inplane shears. This occurs because the coupling among many of the modes is aerodynamic in nature, but not inertial or elastic, so that this coupling appears on the right-hand side of the equations but not on the left-hand side in $[D]$.

Coupling among the modes can be achieved on the left-hand side of the equations together with an expected improvement in the rate of convergence by estimating the increments in the generalized aerodynamic forces from iteration to iteration. A relatively simple estimate of $\Delta^{(t)}[G]$ can be made based on the assumption that the changes in the aerodynamic lifts, drags, and pitching moments from one iteration to the next are linear functions of the corresponding changes in the harmonic coefficients of the blade motions. Accordingly, $\Delta^{(t)}[G]$ is approximated by an expression of the following form:

$$\frac{1}{\Omega^2}\Delta^{(t)}\Big[G(n,I)\Big] = -\Big[E(I,J,n)\Big]\Big\{\Big[X^{(t)}(n,J)\Big]-\Big[X^{(t-1)}(n,J)\Big]\Big\}, \qquad (24)$$

where $[E]$ is a square matrix depending upon harmonic number n. This approximation to $\Delta^{(t)}[G]$ neglects the interharmonic coupling that is present [see Equation (23)] but should provide an estimate of the principal coupling in the nth harmonic. Expressions for the elements of $[E]$, which are based upon quasi-steady aerodynamics, are presented in Appendix III.

After substituting Equation (24) into Equation (21), the following equation results:

$$\Big[F(I,J,n)\Big]\Big[X^{(t)}(n,J)\Big] = \Big[Y^{(t)}(n,I)\Big], \qquad (25)$$

where

$$\Big[F(I,J,n)\Big] = \Big[D(I,J,n)\Big]+\Big[E(I,J,n)\Big], \qquad (26)$$

$$\Big[Y^{(t)}(n,I)\Big] = \frac{1}{\Omega^2}\Big[G^{(t-1)}(n,I)\Big]+\Big[E(I,J,n)\Big]\Big[X^{(t-1)}(n,I)\Big]+\frac{1}{\Omega^2}\Big[Z(n,I)\Big]+\frac{1}{\Omega^2}\Big[YP(n,I)\Big]. \quad (27)$$

Equation (25) is solved at each harmonic n by finding $[F^{-1}]$, the matrix inverse of $[F]$. The inverse exists now because the $[E]$ matrix has been so constructed that, when added to $[D]$, the total $[F]$ is regular. Therefore, the solution is

$$\Big[X^{(t)}(n,J)\Big] = \Big[F^{-1}(I,J,n)\Big]\Big[Y^{(t)}(n,I)\Big]. \qquad (28)$$

16

Once the $[x^{(t)}]$ matrices have been determined, the next approximation for the generalized aerodynamic forces can be computed by performing the operations indicated by Equation (23). The entire process can then be continued until convergence is achieved.

Unfortunately, the initial investigation of transmitted shear suppression reported in Reference 1 showed that the above-described iterative scheme did not always converge. When it did converge, the rate of convergence was often very slow. Convergence was obtained in one case (Run B-6 of Reference 1) by examining a nonconvergent run and adjusting certain elements in $[E]$ accordingly. In that case, as well as others, it was observed that some of the modes have natural frequencies that are very close to the aerodynamic exciting forces which occur at harmonics of the blade rotational frequency (see Appendix II). It was also found that the iteration would converge when the torsion modes were ignored but would diverge when these modes were introduced.

Consequently, the above iterative method of solution was closely scrutinized from several points of view. Attempts were made to develop general criteria which would insure convergence in advance. These attempts were unsuccessful due, in large part, to the complexity of the aerodynamic, inertial, and elastic interactions as expressed, say, by the operations implied in Equation (23).

The above-mentioned closeness of some of the natural mode frequencies to those of the exciting forces led to examination of the magnitudes of the determinants of the $[F]$ matrices. These varied greatly in magnitude; at some harmonics, they were as large as 10^{-1} but at others were as small as 10^{-8}. Surprisingly, the third harmonic, which was the smallest, did not differ at all between a rapidly convergent iteration and a divergent one. An increase of about 4 percent, from 5.14Ω to 5.33Ω, in the natural frequency of the first symmetric and antisymmetric torsion modes increased the magnitude of the determinants of the fifth and lower-order harmonics by as much as 39 percent on the one hand but decreased the magnitude of the determinants of the sixth and higher-order harmonics by as much as 33 percent on the other. A substantial improvement was gained, though, by increasing the frequencies of the same modes to 25.0Ω; i.e., well beyond the twelfth harmonic. The magnitudes of the smallest determinants increased in this case by factors of over 10^3. It was concluded that nothing practically useful could be done in the way of small frequency adjustments to avoid resonance.

A series of numerical experiments with the use of "iteration factors" or "gain factors" showed sufficient promise that this approach was selected to provide convergent iterations. In addition, a method for determining improved initial conditions for the iteration was developed. These two steps, which are described below, permitted all cases to be iterated successfully.

17

Iteration factors were applied to the iterative scheme in two ways; first, in the computation of the generalized aerodynamic forces $[G]$ and, second, in the computation of the generalized coordinates $[x]$. First, Equation (23) for the generalized forces can be rewritten as

$$\left[G^{(t-1)}(n,I) \right] = \left[1 - \mathcal{P}_G(I) \right]\left[G^{(t-2)}(n,I) \right]$$

$$+ \left[\mathcal{P}_G(I) \right]\left[f \left\{ x^{(t-1)}(0,1), \cdots, x^{(t-1)}(12,22) \right\} \right], \quad (29)$$

where $\left[\mathcal{P}_G \right]$ is a column matrix of iteration factors that differ for each mode but are independent of n, and $\left[1 - \mathcal{P}_G \right]$ is a column matrix whose elements are one minus the iteration factors. If the elements of $\left[\mathcal{P}_G \right]$ are all unity, Equation (29) reduces to Equation (23). In the limit when a solution is achieved, $[f]$ becomes equal to $\left[G^{(t-2)} \right]$ and Equation (23) is also recovered. When Equation (29) is substituted on the right-hand side of Equation (27), it becomes effectively an additional quasi-steady aerodynamic term which can be determined empirically from observation of the trend of successive iterations. Secondly, Equation (28) can be rewritten in a similar way as

$$\left[x^{(t)}(n,J) \right] = \left[1 - \mathcal{P}_x(J) \right]\left[x^{(t-1)}(n,J) \right]$$

$$+ \left[\mathcal{P}_x(J) \right]\left[F^{-1}(I,J,n) \right]\left[Y^{(t)}(n,I) \right], \quad (30)$$

where $\left[\mathcal{P}_x \right]$ is a column matrix of iteration factors that differ for each mode but are independent of n, and $\left[1 - \mathcal{P}_x \right]$ is a column matrix whose elements are one minus the iteration factors. Again, if the elements of $\left[\mathcal{P}_x \right]$ are all unity, Equation (30) reduces to Equation (28) and, in the limit when a solution is achieved, $\left[F^{-1} \right]\left[Y^{(t)} \right]$ becomes equal to $\left[x^{(t-1)} \right]$ and Equation (28) is recovered.

Figure 5 is a schematic diagram of the complete computational procedure showing the solution for the harmonic motions, required pitch angles, and residual root shears. The overall process is repeated until the percentage variations in the generalized coordinates from one overall iteration to the next are below prescribed values.

The use of the iteration factors was implemented by adapting the computer program to run a prescribed number of iterations with a given set of iteration factors and then to stop with all the results saved on tape. This permits resumption of the iteration, starting with the saved results but a different set of iteration factors. Furthermore, the results of the converged solutions can be saved from one case and used as initial conditions in subsequent cases, thus providing a significant improvement in initial conditions for the iteration of cases with higher harmonic shear suppression.

In Appendix IV, examination is made of the actual procedures that were used in obtaining solutions for the various cases at one flight condition.

18

RESULTS OF COMPUTATIONS FOR PITCH-ANGLE INPUTS REQUIRED TO ELIMINATE NONCANCELING OSCILLATORY ROOT SHEARS

SCOPE OF NUMERICAL ANALYSIS

Computations to eliminate noncanceling vertical and/or inplane root shears were performed for rotor configurations similar to that of the UH-1A helicopter corresponding to Flight Conditions DN65A, DN66A and DN67A of Reference 6. In all computations, the flexural motions of the blade were represented by the first two symmetric and the first two antisymmetric bending modes, and the first two torsional modes. Pitch deflections were represented by the first symmetric and the first antisymmetric pitch modes (C_2 and C_1), while deflections in the differential pitch-control modes (C_3 and C_4) were specified to be zero.

The deflections in the differential pitch-control modes were set equal to zero by the application of two of the four constraint equations for each harmonic number n [see Equations (7) and (8)]. At $n = 0$, since the sine coefficients are zero, the one remaining constraint equation was used to prescribe the desired thrust load per blade (a value of 3200 pounds was used in all computations). At $n = 1$, the two remaining prescribed variables are the cosine and sine components of the teetering motion which were used to establish the desired tip-path-plane position. For $n > 1$, the constraints are that either the harmonic coefficients of the root shears or the harmonic coefficients of the first control mode are to be zero. In particular, at the even harmonics,

$$\text{or} \quad \left.\begin{array}{l} (A_n S_N) = 0 \\ (B_n S_N) = 0 \\ (A_n C_2) = 0 \\ (B_n C_2) = 0 \end{array}\right\} \quad n = 2, 4, 6, 8, 10, 12$$

and at the odd harmonics,

$$\text{or} \quad \left.\begin{array}{l} (-A_n D_N) = 0 \\ (-B_n D_N) = 0 \\ (A_n C_1) = 0 \\ (B_n C_1) = 0 \end{array}\right\} \quad n = 3, 5, 7, 9, 11.$$

For rotor configurations corresponding to Flight Conditions DN65A ($\mu = 0.076$) and DN67A ($\mu = 0.259$), pitch-control inputs and root shears were computed for conventional control and for five other configurations for which various harmonic noncanceling root shears were prescribed to be zero. For the rotor configuration corresponding to Flight Condition DN66A ($\mu = 0.215$), data were computed for conventional control and one other configuration for which various harmonic noncanceling root shears were prescribed to be zero. A listing of pertinent flight condition parameters is given

19

in Table I, while a listing of the various configurations for which numerical analyses were performed is given in Table II, which also lists the rotor performance data for the cases analyzed. Listings of the harmonic root shears and the required rotor blade pitch angles for each of the cases analyzed are given in Tables III through VIII.

RESULTS OF NUMERICAL ANALYSIS -- FLIGHT CONDITION DN67A, $\mu = 0.259$

The vertical and inplane harmonic root shears for all cases investigated for Flight Condition DN67A are listed in Table III. Table IV lists the corresponding data on the harmonic pitch-angle inputs required to eliminate noncanceling vertical and inplane root shears along with the conventional control pitch schedule. Comparisons of the azimuthal variations of the noncanceling vertical root shears, collective pitch-control schedules, noncanceling inplane shears, and cyclic pitch-control schedules are shown in Figures 6, 7, 8, and 9, respectively.

The largest transmitted vertical harmonic shears for this flight condition occur at the second and fourth harmonics (Figure 6). Thus, the application of second and fourth harmonic pitch control eliminates the principal part of the oscillatory vertical root shear. When higher harmonic pitch control is applied at $n = 2$, 4, 6, 8, 10, and 12, a constant value of $A_n S_N = 3200$ is maintained throughout the azimuth (not shown in Figure 6 for clarity). The pitch-angle requirements for eliminating the second and fourth harmonic vertical root shears remain approximately the same whether or not the noncanceling vertical shears for the sixth through twelfth harmonics are eliminated. Comparatively large collective pitch inputs are required through the tenth harmonic to eliminate the vertical root shears, while the twelfth harmonic vertical shear could be eliminated by comparatively small pitch inputs. The presence of the comparatively large pitch inputs at the harmonics greater than the fourth yields a somewhat irregular collective pitch schedule in comparison to that required for eliminating only the second and fourth harmonic vertical shears as shown in Figure 7. The pitch-control schedule for eliminating the second and fourth harmonic vertical shears is approximately the same as that presented in Reference 1 (where the torsional responses were neglected), while that for eliminating all noncanceling vertical shears varies from that of Reference 1 principally in the sixth and tenth harmonics. The primary reason for the difference in the results is believed to stem from the inclusion of the torsional degrees of freedom in the analysis conducted herein rather than from the inclusion of the inplane degrees of freedom. In Reference 1, it was found that the inclusion of the torsional modes effected only small changes in the harmonic root shears and pitch schedule for conventional control. Quite likely, a similar result would have been obtained herein, since the dynamic response in the torsional modes was comparatively small for conventional control. When higher harmonic pitch-control inputs are applied, the dynamic

20

response in the torsional modes increases significantly, and the required pitch-control inputs must be correspondingly altered to compensate for the extraneous angle-of-attack changes effected by the response in the torsional modes. Figures 10 and 11 show comparisons of the tip responses in the first antisymmetric and symmetric torsion modes, respectively, for conventional control and several other higher pitch-control configurations, and the influence of the higher pitch-control inputs on the torsional response is quite evident.

As had been found in Reference 1, the requirement for the comparatively large higher harmonic pitch inputs to eliminate comparatively small harmonic vertical shears stems from the effect of the dynamic response of the rotor. When higher harmonic pitch control was applied at $n > 2$, it was found that, for most of the higher harmonics, the contribution of the aerodynamic forces to the root shears increased considerably. Thus, a compensating increase in the inertia forces was required to render the resultant shear zero. For the second harmonic pitch-control inputs, the contribution of the aerodynamic forces to the vertical root shear decreased to about one-half its value for conventional control such that a comparatively small second harmonic pitch-control input was required to eliminate the largest of the transmitted vertical shears. The desirability of eliminating transmitted vertical shears above the second harmonic by means of higher harmonic pitch control at the blade root is thus questionable. As suggested in Reference 1, the situation might be improved by the application of a different control mode, such as differential rotation of the inner and outer sections of the blade, which might change the relative magnitudes of the aerodynamic and inertia root shears.

The pitch-control schedules required to eliminate the transmitted inplane root shears are also listed in Table IV, and the corresponding vertical and inplane harmonic root shears are listed in Table III. Azimuthal variations of the noncanceling inplane root shears are shown in Figure 8. Root pitch control can be applied to eliminate all the harmonic transmitted shears except the first inplane harmonic. The first harmonic root pitch control is unavailable because it is necessary for providing ordinary cyclic pitch control of the tip-path plane. Of the transmitted inplane shears that can be eliminated, the largest occur at the third and seventh harmonics. The magnitudes of the third and seventh harmonic inplane shears are about equal, and the seventh harmonic inplane shear is larger than the fifth, probably because of the proximity of the frequency of the second chordwise bending mode to the seventh harmonic of the rotor speed. As seen in Figure 9, the third and seventh harmonic pitch-control schedules were relatively unaffected when fifth, ninth, and eleventh harmonic pitch control were applied to eliminate the corresponding harmonic inplane root shears. The third harmonic pitch-control input is significantly

21

greater than those for the higher harmonics, and those of the ninth and eleventh harmonics are quite small. The conventional cyclic pitch-control schedule is also practically unaffected by the application of higher odd harmonic pitch-control inputs. As had been found in the case of the vertical shears for even harmonics, the application of higher harmonic pitch-control inputs leads to an increase in the contribution of the aerodynamic forces to the root shear for most of the odd harmonics; again, a compensating increase in the inertia forces is required to render the transmitted inplane forces zero.

The application of higher even harmonic pitch-control inputs to eliminate transmitted oscillatory vertical root shears also effects changes in the magnitude of the harmonic components of the inplane shears. The converse is also true; that is, the application of higher odd harmonic pitch-control inputs to eliminate transmitted oscillatory inplane root shears effects changes in the magnitude of the harmonic components of the vertical root shears. Some of these changes in magnitude of the root shears were quite significant. For example, in Table III, it is found that the seventh harmonic of the inplane shear for conventional control has a value of 33.0 pounds. When second and fourth harmonic pitch-control inputs are used to eliminate the second and fourth harmonics of the vertical shear, the seventh harmonic inplane shear increases in magnitude to a value of approximately 160 pounds. If higher harmonic pitch inputs are applied at all even harmonics from $n = 2$ to $n = 12$ to render the total vertical shear constant throughout the azimuth, the value of the seventh harmonic inplane shear increases further to a value of approximately 485 pounds. The increase was noted to occur principally in the inertia forces. The azimuthal variations of the inplane shear for these two conditions are shown in Figure 8, and it is seen that the seventh harmonic of the inplane shear has a magnitude of approximately one-third that of the first harmonic (which is transmitted to the drive shaft as a steady component and at 2/rev) when higher harmonic pitch inputs are applied at all even harmonics from $n = 2$ to $n = 12$. The penalty in applying pitch control at harmonics above $\eta = 2$ is thus reflected in the root shears not only by significant increases in the transmitted aerodynamic forces but also by significant increases in the transmitted inertia forces.

When odd harmonic pitch control was applied at $n = 3$ and 7, the fourth harmonic vertical shear increased from 57.3 pounds to 114.5 pounds, while the second harmonic vertical shear decreased from 250 pounds to 184 pounds. The changes in all other noncanceling vertical shears were less pronounced, and the application of higher harmonic pitch control at all odd harmonics from $n = 3$ through $n = 11$ did not effect further significant changes in the noncanceling vertical shears (see Figure 6).

22

When higher harmonic pitch-control inputs were applied at n = 2, 3, 4,and 7 to eliminate the largest noncanceling vertical and inplane shears simultaneously, the magnitudes of the required harmonic collective pitch control inputs at n = 2 and 4 were found to be larger than those for the case where the noncanceling vertical shears were eliminated only at n = 2 and 4 (see Figure 7). In particular, the requirement for the amplitude of the fourth harmonic pitch-control input increased from 0.7 degree to 1.29 degrees. The harmonic cyclic pitch-control input at n = 3 was somewhat less than that for the case where the noncanceling inplane shears were eliminated only at n = 3 and 7, while the harmonic cyclic pitch-control input at n = 7 increased significantly from 0.23 degree to 1.36 degrees, leading to the rather irregular cyclic pitch-control schedule shown in Figure 9. These results are not surprising in view of the preceding discussion with regard to the effect of higher harmonic pitch-control input on the generalized aerodynamic forces and root shears. For example, when higher harmonic pitch control was applied at n = 2 and 4, the magnitude of the inplane root shear at the seventh harmonic increased from a conventional-control value of 33 pounds to a value of 160 pounds. Also, when higher harmonic pitch control was applied at n = 3 and 7, the magnitude of the vertical root shear at the fourth harmonic increased from a conventional-control value of 57 pounds to a value of 115 pounds. The cited increase in the inplane shear was due primarily to an increase in the inertia forces associated with the increased response in the second chordwise bending mode, while the cited increase in the vertical shear at n = 4 was due primarily to an increase in the generalized aerodynamic forces.

COMPARISON OF RESULTS -- FLIGHT CONDITIONS DN67A, DN66A, AND DN65A

In the preceding section, a detailed discussion was presented of the results of the computations to eliminate noncanceling root shears for Flight Condition DN67A, for which the advance ratio μ = 0.259. The scope of the computations for Flight Condition DN65A, for which μ = 0.076, was the same as that of Flight Condition DN67A. For Flight Condition DN66A, for which μ = 0.215, only two cases were investigated; namely, that of conventional control and the condition in which both the two largest vertical and the two largest inplane transmitted shears were eliminated simultaneously. The rotor rotational speed was the same for all flight conditions.

A listing of the harmonic root shears for all cases investigated for Flight Condition DN65A is given in Table V, while Table VI lists the corresponding required pitch angles. The harmonic root shears for both cases investigated for Flight Condition DN66A are listed in Table VII, and Table VIII lists the corresponding required pitch angles. Comparisons of the azimuthal variations of the noncanceling vertical root

23

shears, collective pitch-control schedules, noncanceling inplane shears, and cyclic pitch-control schedules are shown in Figures 12, 13, 14 and 15, respectively, for $\mu = 0.076$. In the same order, comparisons of the data for $\mu = 0.215$ are shown in Figures 16 through 19.

Comparison of the collective pitch-angle inputs for Flight Conditions DN65A ($\mu = 0.076$) and DN67A ($\mu = 0.259$), for the cases in which the second and fourth vertical harmonic shears were eliminated, shows a decrease in the pitch-angle requirement at $n = 2$ as the advance ratio decreases but an increase in the fourth harmonic pitch angle requirement. This requirement appears to be associated with the increase in the fourth harmonic vertical shear and the fourth harmonic generalized aerodynamic force, which are greater at $\mu = 0.076$ than they are at $\mu = 0.259$. The second harmonic pitch-angle requirement at $\mu = 0.076$ is approximately one-half that at $\mu = 0.259$, and the smaller magnitude of the pitch-control requirement at $\mu = 0.076$ again appears to be associated with the smaller vertical shear and the smaller generalized aerodynamic force.

The collective pitch-angle requirements to eliminate the harmonics of the transmitted shears above $n = 4$ at $\mu = 0.076$ are quite small (Figure 13) and appear to be related to the magnitudes of the vertical shears for these harmonics. When the second and fourth harmonic vertical shears are eliminated, the azimuthal history of the vertical shear, shown in Figure 12, is virtually constant. Comparison of the collective pitch-control schedules between the case for which all transmitted vertical shears were eliminated and that for which only the second and fourth harmonic vertical shears were eliminated shows very little difference in the pitch-control schedules at $\mu = 0.076$ (Figure 13). In contrast, at $\mu = 0.259$, the collective pitch-control schedule for eliminating all transmitted harmonic vertical shears showed significant amounts of pitch-control inputs above $n = 4$ in comparison to those at $n = 2$ and 4 (Figure 7).

The magnitudes of the harmonic components of the transmitted inplane shears decrease substantially as the advance ratio decreases from 0.259 to 0.076, although the third and seventh harmonics remain the two largest components for both advance ratios. At $\mu = 0.076$, the third harmonic pitch-control input appears to be quite large in comparison to the magnitude of the third harmonic inplane shear, and also in comparison to the seventh harmonic pitch control input required to eliminate an inplane shear of comparable magnitude. The pitch-angle requirements to eliminate the remaining odd harmonic inplane shears are quite small, thus being comparable in magnitude to the harmonic components of the inplane shears. Also, at $\mu = 0.076$, the pitch-angle requirements at the third and seventh harmonics remained practically the same whether or not the remaining odd harmonic shears were eliminated (Figure 15), whereas small changes were shown for these

24

conditions at $\mu = 0.259$. Because of the comparatively low harmonic content in the inplane shear above the first harmonic, the azimuthal history of the total noncanceling inplane shear per blade (Figure 14) is dominated by its first harmonic content.

At $\mu = 0.259$, a pronounced effect was found of higher even harmonic pitch-control inputs on the harmonic components of the total inplane shear. At $\mu = 0.076$, this coupling effect was substantially diminished such that the azimuthal variation of the inplane shear was essentially the same as that for the conventional control (Figure 14) in contrast to that at $\mu = 0.259$ (Figure 8).

The collective and cyclic pitch-control schedules to eliminate the second and fourth harmonic vertical shears and the third and seventh harmonic inplane shears simultaneously are shown in Figures 13 and 15, respectively, for $\mu = 0.076$. The second harmonic pitch-control input decreases somewhat from the case where only the second and fourth harmonic vertical shears are eliminated, while the fourth harmonic control input shows a nominal increase. The cyclic pitch-control inputs at the third harmonic show a somewhat larger increase from the case where only the third and seventh harmonics of the inplane shear were eliminated, while the increase in the seventh harmonic pitch-control input is nominal. The change in amplitude in the third harmonic was also accompanied by a change in phase of approximately 85 degrees, which led to a somewhat pronounced difference in the cyclic pitch-control schedule for the two cases (Figure 15). At $\mu = 0.259$, a phase shift of approximately 120 degrees also occurred, but the change in amplitude of the seventh harmonic pitch-control input obscured the phase shift of the third harmonic in the comparison of the pitch control schedules (Figure 9).

Comparison of the azimuthal variations of the noncanceling vertical root shears for Flight Condition DN66A, $\mu = 0.215$, for conventional control and higher harmonic pitch control at $n = 2, 3, 4,$ and 7 is shown in Figure 16. Similar comparison of the collective pitch-control schedules is shown in Figure 17, the inplane shear in Figure 18, and the cyclic pitch-control schedule in Figure 19.

As might have been expected, the largest transmitted vertical shears occurred at the second and fourth harmonics, and the largest transmitted inplane shears occurred at the third and seventh harmonics. The second and fourth harmonic vertical shears, however, were smaller for this flight condition ($\mu = 0.215$) than for either of the other two cases investigated ($\mu = 0.076$ and $\mu = 0.259$). In contrast, the seventh harmonic inplane shear for this case was the largest of the three cases, while the third harmonic inplane shear had an intermediate value. The collective and cyclic pitch-control inputs to eliminate the second, third, fourth, and seventh harmonic transmitted shears simultaneously were not as severe as for $\mu = 0.259$, as might be expected.

25

The various comparisons of the cyclic and collective pitch control schedules for all cases investigated suggest that an optimization procedure would be required to implement a suitable pitch-control schedule which would minimize rather than eliminate the transmitted vertical and inplane shears.

It is also quite evident that certain penalties exist in applying a higher harmonic root pitch-control system to eliminate some of the transmitted vertical and inplane shears. Further computational effort would be required to assess the effects of certain problem areas in the application of higher harmonic pitch-control inputs. For example, it may be desired to eliminate only the second harmonic vertical root shear rather than both the second and the fourth. This collective pitch schedule could minimize the penalties sustained with respect to the generalized aerodynamic forces and inertia forces in the harmonic vertical and inplane root shears above $n = 2$. A less ambitious simultaneous elimination of transmitted harmonic vertical and inplane shears also appeared to be desirable, particularly at the high advance ratios. The pitch angle requirement to eliminate the seventh harmonic inplane shear at $\mu = 0.076$ was 0.16 degree. At $\mu = 0.215$, it was 0.27 degree, but at $\mu = 0.259$, it rose to 1.36 degrees. Thus, at $\mu = 0.259$, the pitch-angle requirement would appear to be disproportionate in comparison to those at the lower advance ratios.

Several factors not analyzed under the study conducted herein could also cause significant differences in the pitch-schedule requirements. Among these are the rotor rotational speed and the associated change in frequency of the various vibration modes. The response in the first torsion mode, for example, produces a substantial angle-of-attack change, particularly in the highly loaded outboard section of the blade, which, in turn, effects a change in the pitch-angle requirement at the blade root. The proximity of the frequency of the second chordwise bending mode to the seventh harmonic of the rotor rotational speed was also instrumental in effecting large seventh harmonic pitch-angle requirements to eliminate the transmitted inertial forces associated with this mode.

26

ESTIMATED EFFECT OF HIGHER HARMONIC
PITCH CONTROL ON PERFORMANCE

A summary of the performance characteristics for conventional and higher harmonic pitch control for all cases and flight conditions investigated is given in Table II. The required thrust load per blade for each configuration was constrained to equal the steady component of the root shear per blade, and a value of 3200 pounds was used in all cases.

At the lowest advance ratio ($\mu = 0.076$), the total drag per blade and, hence, the associated rotor torque are almost invariant with respect to the type of harmonic pitch control applied at the blade root. Also, at $\mu = 0.215$, the total drag per blade for conventional control is practically the same as that for the case of higher harmonic pitch control applied at $n = 2$, 3, 4, and 7. At $\mu = 0.259$, the total drag per blade for higher harmonic pitch control applied at $n = 2$ and 4, $n = 3$ and 7, and $n = 3$, 5, 7, 9, and 11 was again approximately the same as that for conventional control. For higher harmonic pitch control applied at $n = 2$, 4, 6, 8, 10, and 12 at $\mu = 0.259$, the total drag per blade increased by approximately 5 percent from that at conventional control; when higher harmonic pitch control was applied at $n = 2$, 3, 4, and 7, the total drag increased by more than 20 percent from its value at conventional control. The sharp increase in the total drag for the latter case is attributed to the high instantaneous blade angles of attack associated with this case, and the corresponding nonlinear variation of the drag with angle of attack. The high instantaneous angles of attack stem primarily from two sources; namely, the root pitch-control inputs (Figures 7 and 9) and the responses in the antisymmetric and symmetric torsional modes (Figures 10 and 11). In these figures, it is seen that the peak values of the angles of attack are much larger for higher harmonic pitch control applied at $n = 2$, 3, 4, and 7 than for any other case investigated.

The mean effective angle of attack (Figure 20 and Table IX) exhibits little change with the type of pitch control applied at the blade root at each advance ratio investigated. This result is not surprising since the mean effective angle of attack is closely associated with the total lift carried by each rotor blade, which was constrained to a constant value for all cases investigated.

At $\mu = 0.259$, the mean effective angle of attack drops sharply at the inboard section of the blade. The resultant total drag is relatively unaffected, however, because the drag coefficient does not change appreciably for comparatively large changes in angle of attack at the low Mach numbers.

27

Surprisingly, the required control moment shows more variation among the various types of pitch control at $\mu = 0.076$ than at $\mu = 0.259$, except for the case of higher harmonic pitch control applied at $n = 2$, 3, 4, and 7. A detailed examination of the constituent terms [Equation (55)] shows that the significant part in any variation of the control moment from that of conventional control was due to the change in response of the antisymmetric chordwise bending modes, which exert a moment about the rotor hub because of preconing.

At $\mu = 0.076$, the side force increases by approximately 8 percent from its conventional-control value when even higher harmonic pitch control is applied or when both even and odd higher harmonic pitch controls are applied simultaneously. The side force decreases by approximately 3 percent when odd higher harmonic pitch control is applied. At $\mu = 0.259$, the side force decreases by approximately 9 percent from its conventional-control value when even or odd higher harmonic pitch control is applied, and it decreases by about 14 percent when even and odd higher harmonic pitch controls are applied simultaneously. At $\mu = 0.215$, the side force decreased by approximately 9 percent from its conventional-control value when higher harmonic pitch control was applied at $n = 2$, 3, 4, and 7. In all cases, the change in the side force was due primarily to changes in the contributions from the inertia forces of the rotor blades to the side force [Equation (56)] rather than from changes in the contributions from the aerodynamic forces.

At $\mu = 0.076$, the longitudinal force [x-Force, Equation (57)] remained unchanged from its conventional-control value when odd higher harmonic pitch control was applied, and it decreased by approximately 5 percent when even higher harmonic pitch control was applied. At $\mu = 0.259$, the longitudinal force increased slightly from its conventional-control value when even higher harmonic pitch control was applied and decreased slightly when odd higher harmonic pitch control was applied. When higher harmonic pitch control was applied at $n = 2$, 3, 4, and 7, the longitudinal force decreased from its conventional-control value by approximately 8 percent at $\mu = 0.076$, by approximately 6 percent at $\mu = 0.215$, and by approximately 50 percent at $\mu = 0.259$. The differences in the effect of higher harmonic pitch controls on the longitudinal forces at the various advance ratios are associated with the amplitudes of the applied higher harmonic pitch controls, which also correspond more closely to the magnitudes of the dynamic responses of the rotor blades than to the magnitudes of the aerodynamic forces. Examination of the constituent terms in the longitudinal force [Equation (57)] shows that the differences in the longitudinal forces are due primarily to changes in the contributions from the inertia forces rather than from the aerodynamic forces. In particular, for higher harmonic pitch control applied at $n = 2$, 3, 4, and 7 at $\mu = 0.259$, the response in the first antisymmetric inplane bending mode was approximately one-half that of the conventional-control value, which accounted for the 50-percent change in the longitudinal force.

28

From the limited analysis which had been conducted herein
with respect to flight conditions, rotor rotational speed, etc., it
appears that the most severe penalty of applying a higher harmonic
pitch-control system would lie in the increased power required to
overcome the increased drag forces. The higher drag forces, in
turn, stem from the higher angles of attack required to eliminate
certain of the transmitted shears. Since the inertia forces contribute
substantially to the transmitted shears in many cases, further inves-
tigation would be required to evaluate the effect of dynamic parameters
on the performance characteristics of rotors with higher harmonic
pitch control.

CONCLUSIONS AND RECOMMENDATIONS

The following specific conclusions were reached on the basis of this investigation:

1. All noncanceling vertical root shears of the two-bladed teetering rotor from the second through twelfth harmonics can be eliminated with higher harmonic pitch-angle control introduced at the blade root (as in conventional control systems) for all flight conditions investigated. The largest part of the oscillatory transmitted vertical root shears can be removed by using pitch-angle inputs only at the second and fourth harmonics.

2. All noncanceling inplane root shears of the two-bladed teetering rotor from the third through eleventh harmonics can be eliminated with higher harmonic pitch-angle control introduced at the blade root for all flight conditions investigated. The largest of these oscillatory transmitted inplane root shears can be removed by using pitch-angle inputs at the third and seventh harmonics.

3. For the two-bladed teetering rotor, the first harmonic inplane shear (the largest transmitted shear) cannot be eliminated by root pitch control. The first harmonic root pitch control is unavailable because it is necessary for ordinary cyclic pitch control of the tip-path plane.

4. Except for the first harmonic inplane shear, the largest of the cited oscillatory transmitted vertical and inplane root shears can be eliminated simultaneously with second, third, fourth, and seventh harmonic pitch-angle control introduced at the blade root. The resulting pitch-angle requirements are different from those cited in Conclusions 1 and 2 for the same flight condition.

5. The amplitudes and phase angles of the pitch inputs required to eliminate only the noncanceling vertical root shears, only the noncanceling inplane root shears, and both simultaneously also vary appreciably with flight condition. In general, the higher harmonic pitch-angle requirements for eliminating transmitted harmonic root shears become more severe with increasing advance ratio.

30

6. It appears undesirable to attempt to eliminate all noncanceling harmonic vertical and inplane root shears using a control system with pitch inputs introduced at the blade root. The higher harmonic pitch inputs, which are introduced to eliminate transmitted root shears, excite dynamic blade motions, and the inertia forces due to these motions also produce root shears. At some harmonic numbers (depending on blade parameters and flight condition), the root shears due to the inertia forces are almost equal and opposite to the root shears due to the corresponding aerodynamic forces. Consequently, large pitch-angle inputs and large blade dynamic motions may result from the pitch-angle inputs designed to eliminate comparatively small root shears. Under these conditions, it would be undesirable to introduce control inputs at certain harmonic numbers.

7. The effect of higher harmonic pitch control on rotor performance was small for most of the cases analyzed. Under certain conditions, however, the high instantaneous angles of attack required to eliminate certain of the transmitted root shears produced much larger drag forces on the rotor.

8. Instabilities in the iterative solution of the equations of motion may stem from the involved dependencies of the aerodynamic loadings on the blade dynamic motions. It has been found possible to iterate the equations of motion successfully to solution by providing improved initial conditions on the generalized forces and coordinates, and by using "iteration factors" on them as well. These factors could be chosen differently for each mode and were found to depend on the flight condition and the type of harmonic pitch control applied.

The results of this study, which indicate that appropriate pitch-angle inputs can produce significant reductions in the transmitted oscillatory root shears, offer definite encouragement toward the application of this approach to reduce fuselage vibrations. To further this goal, additional research is recommended to:

1. Extend the present numerical analysis to rotor configurations other than the UH-1A two-bladed teetering rotor.

31

2. Study the application of symmetric and antisymmetric differential pitch-control motions of the inner and outer sections of the blade to eliminate transmitted harmonic shears, particularly the first harmonic shear of the two-bladed teetering rotor and at harmonics where pitch inputs at the blade root tend to excite large dynamic responses.

3. Extend the analysis to determine the pitch-control configurations which would provide the optimal rotor characteristics with respect to transmitted shears, blade dynamic motions, and performance.

4. Study the application of a servo system for controlling the pitch inputs which would use measured transmitted shears as a feedback signal. This effort is recommended since large differences in the higher harmonic pitch-angle inputs are required at different flight conditions.

LITERATURE CITED

1. Daughaday, H., SUPPRESSION OF TRANSMITTED HARMONIC ROTOR LOADS BY BLADE PITCH CONTROL, Cornell Aeronautical Laboratory, Inc.; USAAVLABS Technical Report 67-14, U. S. Army Aviation Materiel Laboratories, Fort Eustis, Virginia, November 1967, AD 665430.

2. Piziali, R. A., A METHOD FOR PREDICTING THE AERO-DYNAMIC LOADS AND DYNAMIC RESPONSE OF ROTOR BLADES, Cornell Aeronautical Laboratory, Inc.; USAAVLABS Technical Report 65-74, U. S. Army Aviation Materiel Laboratories, Fort Eustis, Virginia, January 1966, AD 628583.

3. Chang, T. T., A METHOD FOR PREDICTING THE TRIM CONSTANTS OF A SINGLE-ROTOR HELICOPTER AND THE ROTOR-BLADE LOADINGS AND RESPONSES, Cornell Aeronautical Laboratory, Inc.; USAAVLABS Technical Report 67-71, U. S. Army Aviation Materiel Laboratories, Fort Eustis, Virginia, November 1967, AD 666802.

4. Targoff, W. P., THE BENDING VIBRATIONS OF A TWISTED ROTATING BEAM, Cornell Aeronautical Laboratory, Inc.; WADC Technical Report 56-27, Wright Air Development Center, Wright-Patterson Air Force Base, Ohio, December 1955.

5. Graham, D. J., Nitzberg, G. E., and Olson, R. N., A SYSTEM-ATIC INVESTIGATION OF PRESSURE DISTRIBUTIONS AT HIGH SPEEDS OVER FIVE REPRESENTATIVE NACA LOW-DRAG AND CONVENTIONAL AIRFOIL SECTIONS, NACA Technical Report 832, National Advisory Committee for Aeronautics, Moffett Field, California, 1945.

6. MEASUREMENT OF DYNAMIC AIRLOADS IN A FULL-SCALE SEMIRIGID ROTOR, Bell Helicopter Report No. 525-009-001; TCREC Technical Report 62-42, U. S. Army Transportation Research Command, Fort Eustis, Virginia, December 1962.

7. DuWaldt, F. A., Gates, C. A., and Piziali, R. A., INVESTI-GATION OF THE FLUTTER OF A MODEL HELICOPTER ROTOR BLADE IN FORWARD FLIGHT, Cornell Aeronautical Laboratory, Inc.; WADD Technical Report 60-479, Wright Air Development Division, Wright-Patterson Air Force Base, Ohio, July 1960.

Table I

PARAMETERS FOR ADJUSTED FLIGHT CONDITIONS

PARAMETERS	ADJUSTED FLIGHT CONDITION*		
	DN65A	DN66A	DN67A
V_f = FORWARD VELOCITY, ft/sec	55.1	155.4	188.0
knots	32.6	92.1	111.4
Ω = ROTOR ANGULAR VELOCITY, rad/sec	32.8	32.8	32.8
rpm	313	313	313
μ = ADVANCE RATIO	0.076	0.215	0.259
ρ = AIR DENSITY, slugs/ft^3	0.002150	0.002155	0.002155
W_b = LOAD/BLADE, lb	3200	3200	3200
α_s = SHAFT ANGLE, deg	4.5	4.6	6.5
TIP-PATH-PLANE POSITION RELATIVE TO SHAFT:			
β_{1C} = FORWARD TILT, deg	-2.02	-0.74	-0.65
β_{1S} = LEFT TILT, deg	-0.50	0.68	1.80

*THE ADJUSTED FLIGHT CONDITIONS DN65A, DN66A, AND DN67A ARE SLIGHTLY DIFFERENT FROM THE CORRESPONDING CONDITIONS OF REFERENCE 6.

Table II

PERFORMANCE CHARACTERISTICS FOR CONVENTIONAL AND
HIGHER HARMONIC PITCH-CONTROL FLIGHT CONDITIONS

FLIGHT CONDITION	μ	COMPUTER RUN	HIGHER HARMONIC PITCH CONTROL AT n =	CONTROL MOMENT (ft-lb)	DRAG (ONE BLADE) (lb)	ROTOR TORQUE (ft-lb)	ROTOR (hp)	SIDE FORCE (lb)	X FORCE (lb)
DN65A	0.076	G1B	(CONVENTIONAL CONTROL)	-811	212	6371	382	-444	1217
		G2F	2,4	-738	211	6340	380	-476	1163
		G3C	2,4,6,8,10,12	-745	211	6332	380	-476	1160
		G6B	3,7	-801	213	6389	383	-43G	1215
		G7B	3,5,7,9,11	-803	213	6394	384	-430	1217
		G8C	2,3,4,7	-727	213	6388	383	-482	1115
DN66A	0.215	F1B	(CONVENTIONAL CONTROL)	-849	226	6958	415	-892	767
		F8D	2,3,4,7	-636	227	7000	417	-812	723
DN67A	0.259	E2C	(CONVENTIONAL CONTROL)	-1036	305	9661	576	-1479	987
		E4E	2,4	-1047	308	9821	585	-1336	1013
		E3E	2,4,6,8,10,12	-1070	322	10252	611	-1334	1008
		E6C	3,7	-1021	309	9729	580	-1361	965
		E7C	3,5,7,9,11	-1008	308	9706	579	-1340	949
		E8D	2,3,4,7	-612	371	11801	703	-1262	419

35

Table II

EFFECT OF HIGHER HARMONIC PITCH-A

FLIGHT CONDITION DN6

	COMPUTER RUN E2C				COMPUTER RUN E4E				COMPUTER RUN E3E				H
	CONVENTIONAL CONTROL				HIGHER HARMONIC PITCH CONTROL AT n = 2,4				HIGHER HARMONIC PITCH CONTROL AT n = 2,4,6,8,10,12				H
	HARMONIC ROOT SHEAR* (ONE BLADE)				HARMONIC ROOT SHEAR* (ONE BLADE)				HARMONIC ROOT SHEAR* (ONE BLADE)				HARMONI
	VERTICAL		INPLANE		VERTICAL		INPLANE		VERTICAL		INPLANE		VER
n	AMPLITUDE (lb)	PHASE ANGLE (deg)	AMPLITUDE (lb)	PHASE ANGLE (deg)	AMPLITUDE (lb)	PHASE ANGLE (deg)	AMPLITUDE (lb)	PHASE ANGLE (deg)	AMPLITUDE (lb)	PHASE ANGLE (deg)	AMPLITUDE (lb)	PHASE ANGLE (deg)	AMPLITUI (lb)
0	3200.0	0	508.6	0	3200.0	0	515.5	0	3200.0	0	538.2	0	3200.0
1	2741.0	-109.2	1537.0	-144.0	2764.0	-109.2	1435.0	-139.7	2760.0	-109.2	1435.0	-139.9	2746.0
2	250.5	163.0	74.0	104.4	0	0	84.0	166.6	0	0	100.7	163.7	183.9
3	213.1	150.5	38.6	162.6	100.6	127.5	29.9	-122.0	105.1	131.4	41.4	-118.4	299.4
4	57.3	56.5	12.8	143.4	0	0	19.3	33.5	0	0	26.5	38.1	114.5
5	68.0	-25.3	13.1	-131.2	91.2	13.3	15.2	83.3	104.7	52.3	46.5	72.9	75.0
6	15.1	-112.4	23.8	-136.7	20.4	-108.9	34.2	-148.6	0	0	96.5	-158.8	18.3
7	5.5	35.7	33.0	161.4	4.3	33.3	159.6	166.2	7.8	96.5	484.9	-138.6	5.6
8	18.3	126.1	7.6	62.7	19.5	127.8	13.5	156.6	0	0	92.1	149.1	22.3
9	2.0	-55.1	4.4	158.1	1.3	-71.6	8.0	55.9	5.0	-55.3	33.8	172.0	2.0
10	20.1	-61.0	4.9	113.1	18.5	-59.9	0.4	-143.3	0	0	21.2	-22.8	19.6
11	1.9	127.7	1.8	-98.3	2.2	107.2	2.7	156.9	4.7	135.8	6.0	-34.3	2.3
12	2.6	0	1.6	178.3	1.8	-0.1	0.2	-179.3	0	0	7.2	178.5	1.5

*VERTICAL ROOT SHEARS ARE NONCANCELING FOR n = 0 OR n = EVEN AND ARE CANCELING FOR n = ODD.

INPLANE ROOT SHEARS ARE NONCANCELING FOR n = ODD AND ARE CANCELING FOR n = 0 OR n = EVEN.

AZIMUTHAL VARIATION OF nth HARMONIC ROOT SHEAR = (AMPLITUDE) x $\cos(n\psi + \text{PHASE ANGLE})$.

Table III

HIGHER HARMONIC PITCH-ANGLE INPUTS ON ROOT SHEARS,
FLIGHT CONDITION DN67A, $\mu = 0.259$

RUN E3E		COMPUTER RUN E6C				COMPUTER RUN E7C				COMPUTER RUN E8D			
HARMONIC PITCH 2,4,6,8,10,12		HIGHER HARMONIC PITCH CONTROL AT n = 3,7				HIGHER HARMONIC PITCH CONTROL AT n = 3,5,7,9,11				HIGHER HARMONIC PITCH CONTROL AT n = 2,3,4,7			
SHEAR* (ONE BLADE)		HARMONIC ROOT SHEAR' (ONE BLADE)				HARMONIC ROOT SHEAR* (ONE BLADE)				HARMONIC ROOT SHEAR* (ONE BLADE)			
INPLANE		VERTICAL		INPLANE		VERTICAL		INPLANE		VERTICAL		INPLANE	
AMPLITUDE (lb)	PHASE ANGLE (deg)	AMPLITUDE (lb)	PHASE ANGLE (deg)	AMPLITUDE (lb)	PHASE ANGLE (deg)	AMPLITUDE (lb)	PHASE ANGLE (deg)	AMPLITUDE (lb)	PHASE ANGLE (deg)	AMPLITUDE (lb)	PHASE ANGLE (deg)	AMPLITUDE (lb)	PHASE ANGLE (deg)
538.2	0	3200.0	0	513.1	0	3200.0	0	512.3	0	3200.0	0	617.9	0
1435.0	-139.9	2746.0	-109.2	1430.0	-141.9	2744.0	-109.3	1403.0	-141.9	2761.0	-109.2	1079.0	-161.9
100.7	163.7	183.9	173.5	14.9	157.4	183.7	176.3	7.4	173.8	0	0	152.6	167.1
41.4	-118.4	299.4	146.0	0	0	308.6	143.2	0	0	128.6	34.3	0	0
26.5	38.1	114.5	102.8	23.4	108.3	102.4	92.6	12.0	96.4	0	0	28.2	67.8
46.5	72.9	75.0	-27.5	18.5	-166.2	38.3	-121.9	0	0	139.0	5.8	26.9	84.6
96.5	-158.8	18.3	-96.1	31.6	-136.8	11.0	-92.1	23.6	-163.3	40.2	-86.4	113.3	-64.6
484.9	-138.6	5.6	32.0	0	0	6.5	32.1	0	0	4.1	-59.6	0	0
92.1	149.1	22.3	127.9	9.2	36.5	22.9	129.1	3.4	-62.5	38.8	117.8	140.1	-75.1
33.8	172.0	2.0	-70.8	5.3	133.1	2.1	-78.8	0	0	0.5	-24.5	18.3	-124.1
21.2	-22.8	19.6	-56.8	6.2	120.5	19.1	-52.3	6.7	93.3	18.9	-53.6	22.2	120.2
6.0	-34.3	2.3	117.8	2.8	-107.3	2.4	120.4	0	0	2.6	114.7	3.5	70.4
7.2	178.5	1.5	0	1.2	178.0	1.0	0.2	1.7	178.2	1.6	179.9	5.7	-1.0

D.

Table IV
REQUIRED PITCH ANGLES TO ELIMINATE NONCANCELING ROOT SHEARS, FLIGHT CONDITION DN67A, μ = 0.259

n	COMPUTER RUN E2C PITCH ANGLES WITH CONVENTIONAL CONTROL		COMPUTER RUN E4E PITCH ANGLES TO ELIMINATE ROOT SHEARS AT n = 2,4		COMPUTER RUN E3E PITCH ANGLES TO ELIMINATE ROOT SHEARS AT n = 2,4,6,8,10,12	
	AMPLITUDE (deg)	PHASE ANGLES (deg)	AMPLITUDE (deg)	PHASE ANGLES (deg)	AMPLITUDE (deg)	PHASE ANGLES (deg)
0	19.40	0	19.54	0	19.54	0
1	6.28	59.2	6.77	59.5	6.76	59.4
2			1.09	153.6	1.11	153.7
3			0	0	0	0
4			0.70	65.6	0.73	68.9
5					0	0
6					0.67	-10.4
7					0	0
8					0.90	-134.5
9					0	0
10					0.55	48.5
11					0	0
12					0.20	-106.2

n	COMPUTER RUN E6C PITCH ANGLES TO ELIMINATE ROOT SHEARS AT n = 3,7		COMPUTER RUN E7C PITCH ANGLES TO ELIMINATE ROOT SHEARS AT n = 3,5,7,9,11		COMPUTER RUN E8D PITCH ANGLES TO ELIMINATE ROOT SHEARS AT n = 2,3,4,7	
	AMPLITUDE (deg)	PHASE ANGLES (deg)	AMPLITUDE (deg)	PHASE ANGLES (deg)	AMPLITUDE (deg)	PHASE ANGLES (deg)
0	19.42	0	19.42	0	19.54	0
1	6.31	58.9	6.31	58.8	6.80	59.6
2	0	0	0	0	1.29	160.1
3	1.17	50.5	1.26	44.0	0.94	-69.5
4	0	0	0	0	1.29	44.8
5	0	0	0.33	98.5	0	0
6	0	0	0	0	0	0
7	0.23	178.8	0.34	-179.7	1.36	139.2
8			0	0		
9			0.04	109.3		
10			0	0		
11			0.05	-115.1		
12						

AZIMUTHAL VARIATION OF nth HARMONIC PITCH ANGLE =

(AMPLITUDE) x $\cos(n\psi + $ PHASE ANGLE$)$

	COMPUTER RUN G1B				COMPUTER RUN G2F				COMPUTER RUN G3C				
	CONVENTIONAL CONTROL				HIGHER HARMONIC PITCH CONTROL AT n = 2,4				HIGHER HARMONIC PITCH CONTROL AT n = 2,4,6,8,10,12				
	HARMONIC ROOT SHEAR* (ONE BLADE)				HARMONIC ROOT SHEAR* (ONE BLADE)				HARMONIC ROOT SHEAR* (ONE BLADE)				HARM
	VERTICAL		INPLANE		VERTICAL		INPLANE		VERTICAL		INPLANE		V
n	AMPLITUDE (lb)	PHASE ANGLE (deg)	AMPLITUDE (lb)	PHASE ANGLE (deg)	AMPLITUDE (lb)	PHASE ANGLE (deg)	AMPLITUDE (lb)	PHASE ANGLE (deg)	AMPLITUDE (lb)	PHASE ANGLE (deg)	AMPLITUDE (lb)	PHASE ANGLE (deg)	AMPLIT (lb
0	3200.0	0	344.8	0	3200.0	0	343.4	0	3200.0	0	343.1	0	3200.
1	2440.0	169.5	1097.0	-116.8	2440.0	169.4	1065.0	-119.7	2440.0	169.4	1060.0	-119.7	2442.
2	160.3	8.2	1.6	137.8	0	0	14.7	14.7	0	0	15.1	13.6	170.
3	60.1	100.3	8.2	-130.4	61.5	120.8	11.6	-65.0	61.3	121.1	11.8	-64.1	117.
4	69.7	24.2	3.8	-176.0	0	0	11.9	90.0	0	0	12.5	88.2	78.
5	26.6	-18.8	1.0	101.7	47.1	-15.0	8.8	140.5	49.8	-11.6	11.2	145.0	18.
6	3.7	-166.4	2.6	36.0	5.5	-177.7	1.6	-88.5	0	0	7.7	-81.2	4.
7	2.2	32.8	5.8	6.7	2.9	16.9	10.9	4.2	3.2	10.2	29.7	4.3	2.
8	0.8	167.7	1.2	-175.0	0.5	123.1	3.6	67.3	0	0	2.9	94.0	0.
9	0.6	-161.4	0.4	2.3	0.6	-168.4	0.8	137.4	0.7	-170.7	1.1	177.9	0.
10	0.9	6.0	0.1	18.8	1.0	-1.7	0.9	-152.8	0	0	1.2	-122.3	1.
11	0.3	-6.3	0.1	17.5	0.3	-0.1	0.7	-72.1	0.3	7.2	0.7	-55.8	0.
12	0.1	-179.9	0.1	178.6	0.2	-179.8	0.1	-1.3	0	0	0.1	-1.3	0.

*VERTICAL ROOT SHEARS ARE NONCANCELING FOR n = 0 OR n = EVEN AND ARE CANCELING FOR n = ODD.
INPLANE ROOT SHEARS ARE NONCANCELING FOR n = ODD AND ARE CANCELING FOR n = 0 OR n = EVEN.
AZIMUTHAL VARIATION OF nth HARMONIC ROOT SHEAR = (AMPLITUDE) x $\cos(n\psi + $ PHASE ANGLE).

A

Table V

HIGHER HARMONIC PITCH-ANGLE INPUTS ON ROOT SHEARS, FLIGHT CONDITION DN65A, μ = 0.076

| G3C ...PITCH ,6,8,10,12 (ONE BLADE) INPLANE		COMPUTER RUN G6B — HIGHER HARMONIC PITCH CONTROL AT n = 3,7 — HARMONIC ROOT SHEAR* (ONE BLADE)				COMPUTER RUN G7B — HIGHER HARMONIC PITCH CONTROL AT n = 3,5,7,9,11 — HARMONIC ROOT SHEAR* (ONE BLADE)				COMPUTER RUN G8C — HIGHER HARMONIC PITCH CONTROL AT n = 2,3,4,7 — HARMONIC ROOT SHEAR* (ONE BLADE)			
		VERTICAL		INPLANE		VERTICAL		INPLANE		VERTICAL		INPLANE	
AMPLITUDE (lb)	PHASE ANGLE (deg)	AMPLITUDE (lb)	PHASE ANGLE (deg)	AMPLITUDE (lb)	PHASE ANGLE (deg)	AMPLITUDE (lb)	PHASE ANGLE (deg)	AMPLITUDE (lb)	PHASE ANGLE (deg)	AMPLITUDE (lb)	PHASE ANGLE (deg)	AMPLITUDE (lb)	PHASE ANGLE (deg)
43.1	0	3200.0	0	345.9	0	3200.0	0	346.2	0	3200.0	0	346.1	0
60.0	-119.7	2442.0	169.4	1089.0	-116.2	2442.0	169.4	1090.0	-116.2	2440.0	169.3	1027.0	-121.4
15.1	13.6	170.6	3.7	11.0	-51.7	170.7	3.6	11.1	-52.7	0	0	30.8	26.4
11.8	-64.1	117.2	74.6	0	0	117.9	73.9	0	0	95.7	-19.3	0	0
12.5	88.2	78.3	30.5	6.5	169.1	78.0	30.4	6.0	169.0	0	0	15.8	-107.9
11.2	145.0	18.8	-9.2	1.0	-81.2	15.3	13.4	0	0	59.0	-1.1	9.7	152.2
7.7	-81.2	4.4	-173.3	3.9	37.4	4.2	-173.6	3.4	46.9	6.5	170.4	5.5	-33.9
29.7	4.3	2.1	37.4	0	0	2.1	37.3	0	0	2.8	26.2	0	0
2.9	94.0	0.4	-174.3	0.8	114.9	0.5	-178.2	0.8	120.9	0.7	-11.3	4.5	40.8
1.1	177.9	0.6	-164.3	0.2	65.7	0.6	-163.7	0	0	0.6	-170.5	0.8	-168.8
1.2	-122.3	1.0	4.2	0.4	-143.6	1.1	4.4	0.2	-148.4	1.0	-1.6	0.8	-73.9
0.7	-55.8	0.3	-14.3	0.4	-67.0	0.3	-15.4	0	0	0.3	-17.5	0.8	-65.9
0.1	-1.3	0.2	-179.9	0.1	-1.3	0.2	180.0	0.1	-1.0	0.2	179.9	0.4	-1.4

B

Table VI
REQUIRED PITCH ANGLES TO ELIMINATE NONCANCELING ROOT SHEARS, FLIGHT CONDITION DN65A, $\mu = 0.076$

n	COMPUTER RUN G1B PITCH ANGLES WITH CONVENTIONAL CONTROL		COMPUTER RUN G2F PITCH ANGLES TO ELIMINATE ROOT SHEARS AT n = 2,4		COMPUTER RUN G3C PITCH ANGLES TO ELIMINATE ROOT SHEARS AT n = 2,4,6,8,10,12	
	AMPLITUDE (deg)	PHASE ANGLES (deg)	AMPLITUDE (deg)	PHASE ANGLES (deg)	AMPLITUDE (deg)	PHASE ANGLES (deg)
0	17.45	0	17.42	0	17.42	0
1	1.71	-13.0	1.77	-15.1	1.77	-15.1
2			0.59	2.2	0.59	2.3
3			0	0	0	0
4			0.81	13.9	0.80	15.4
5					0	0
6					0.10	-96.9
7					0	0
8					0.01	-141.3
9					0	0
10					0.02	77.3
11					0	0
12					0.004	-106.4

n	COMPUTER RUN G6B PITCH ANGLES TO ELIMINATE ROOT SHEARS AT n = 3,7		COMPUTER RUN G7B PITCH ANGLES TO ELIMINATE ROOT SHEARS AT n = 3,5,7,9,11		COMPUTER RUN G8C PITCH ANGLES TO ELIMINATE ROOT SHEARS AT n = 2,3,4,7	
	AMPLITUDE (deg)	PHASE ANGLES (deg)	AMPLITUDE (deg)	PHASE ANGLES (deg)	AMPLITUDE (deg)	PHASE ANGLES (deg)
0	17.46	0	17.47	0	17.44	0
1	1.70	-12.6	1.70	-12.7	1.76	-12.6
2	0	0	0	0	0.49	1.9
3	0.52	-0.7	0.52	-0.7	0.97	-65.5
4	0	0	0	0	1.05	6.5
5	0	0	0.03	35.9	0	0
6	0	0	0	0	0	0
7	0.05	19.9	0.05	25.4	0.16	38.4
8			0	0		
9			0.01	62.4		
10			0	0		
11			0.01	-135.4		
12						

AZIMUTHAL VARIATION OF nth HARMONIC PITCH ANGLE

$$(\text{AMPLITUDE}) \times \cos(n\psi + \text{PHASE ANGLE})$$

43

Table VII

EFFECT OF HIGHER HARMONIC PITCH-ANGLE INPUTS ON ROOT SHEARS,
FLIGHT CONDITION DM66A, $\mu = 0.215$

	COMPUTER RUN F1B				COMPUTER RUN F8D			
	CONVENTIONAL CONTROL				HIGHER HARMONIC PITCH CONTROL AT n = 2,3,4,7			
	HARMONIC ROOT SHEAR* (ONE BLADE)				HARMONIC ROOT SHEAR* (ONE BLADE)			
	VERTICAL		INPLANE		VERTICAL		INPLANE	
n	AMPLITUDE (lb)	PHASE ANGLE (deg)	AMPLITUDE (lb)	PHASE ANGLE (deg)	AMPLITUDE (lb)	PHASE ANGLE (deg)	AMPLITUDE (lb)	PHASE ANGLE (deg)
0	3200.0	0	371.4	0	3200.0	0	373.4	0
1	1552.0	-129.3	1039.0	-139.9	1562.0	-129.2	951.0	-138.6
2	118.2	164.7	41.2	92.3	0	0	25.9	127.0
3	302.0	147.9	17.4	168.7	113.3	98.1	0	0
4	24.8	42.2	19.4	152.7	0	0	23.4	90.6
5	152.4	-73.7	8.8	51.4	159.9	-43.4	17.8	110.6
6	11.3	-107.5	27.5	-121.7	17.3	-105.5	40.5	-123.9
7	6.8	-9.9	44.0	-165.2	7.8	-13.6	0	0
8	4.7	-102.2	10.1	70.4	4.6	-145.2	8.8	-13.8
9	7.2	-107.8	1.6	-74.0	7.6	-107.0	2.2	-33.1
10	21.8	2.8	4.4	-156.2	23.3	2.9	4.4	173.9
11	5.3	87.7	7.4	103.2	5.7	89.2	7.4	107.2
12	6.7	180.0	1.4	-1.2	7.5	180.0	1.5	-1.1

*VERTICAL ROOT SHEARS ARE NONCANCELING FOR n = 0 OR n = EVEN AND ARE CANCELING FOR n = ODD. INPLANE ROOT SHEARS ARE NONCANCELING FOR n = ODD AND ARE CANCELING FOR n = 0 OR n = EVEN. AZIMUTHAL VARIATION OF nth HARMONIC ROOT SHEAR = (AMPLITUDE) x $\cos(n\psi + \text{PHASE ANGLE})$.

Table VIII

REQUIRED PITCH ANGLES TO ELIMINATE NONCANCELING ROOT SHEARS, FLIGHT CONDITION DN66A, $\mu = 0.215$

n	COMPUTER RUN F1B PITCH ANGLES WITH CONVENTIONAL CONTROL		COMPUTER RUN F8D PITCH ANGLES TO ELIMINATE ROOT SHEARS AT n = 2, 3, 4, 7	
	AMPLITUDE (deg)	PHASE ANGLES (deg)	AMPLITUDE (deg)	PHASE ANGLES (deg)
0	18.00	0	18.08	0
1	4.51	61.0	4.74	61.5
2			0.62	165.9
3			0.73	-67.2
4			0.97	29.5
5			0	0
6			0	0
7			0.27	153.6

AZIMUTHAL VARIATION OF nth HARMONIC PITCH ANGLE =
(AMPLITUDE) x $\cos(n\psi + $ PHASE ANGLE)

Table IX
RADIAL DISTRIBUTION OF MEAN EFFECTIVE ANGLE OF ATTACK

FLIGHT CONDITION	μ	COMPUTER RUN	HIGHER HARMONIC PITCH CONTROL AT n =	MEAN EFFECTIVE ANGLE OF ATTACK, deg, AT r/R =							
				0.213	0.400	0.588	0.750	0.850	0.900	0.950	0.988
DN65A	0.076	G1B	CONVENTIONAL CONTROL	7.92	8.55	7.50	6.63	5.77	5.24	4.68	4.34
		G2F	2,4	7.87	8.56	7.52	6.66	5.75	5.22	4.67	4.33
		G3C	2,4,6,8,10,12	7.87	8.57	7.53	6.66	5.75	5.22	4.67	4.33
		G6B	3,7	7.90	8.53	7.48	6.62	5.79	5.26	4.71	4.37
		G7B	3,5,7,9,11	7.90	8.53	7.48	6.62	5.79	5.26	4.71	4.37
		G8C	2,3,4,7	7.81	8.56	7.53	6.67	5.75	5.21	4.66	4.33
DN66A	0.215	F1B	CONVENTIONAL CONTROL	9.48	10.83	8.74	7.17	6.09	5.52	4.90	4.52
		F8D	2,3,4,7	9.94	10.69	8.68	7.22	6.14	5.57	4.95	4.57
DN67A	0.259	E2C	CONVENTIONAL CONTROL	-2.61	10.18	9.06	7.56	6.54	5.98	5.37	5.02
		E4E	2,4	-3.03	10.16	9.12	7.65	6.65	6.08	5.48	5.13
		E3E	2,4,6,8,10,12	-2.82	10.13	9.11	7.64	6.63	6.07	5.47	5.12
		E6C	3,7	-2.65	10.11	9.06	7.57	6.57	6.00	5.39	5.05
		E7C	3,5,7,9,11	-2.74	10.10	9.07	7.58	6.57	6.00	5.39	5.05
		E8D	2,3,4,7	-3.59	10.03	8.99	7.56	6.59	6.06	5.46	5.11

VERTICAL DEFLECTION MODES
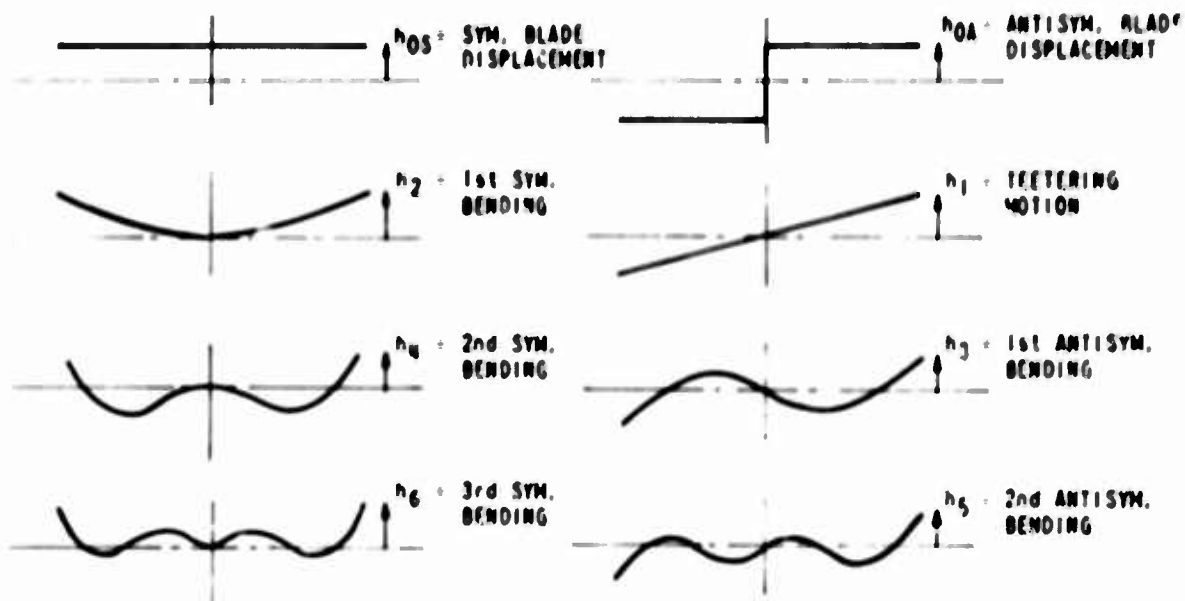
INPLANE DEFLECTION MODES
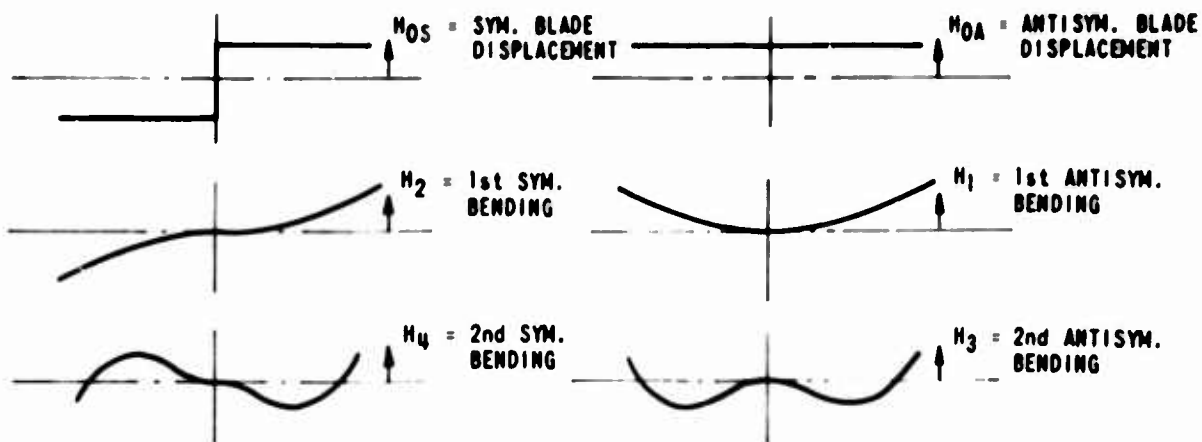
Figure 1. SCHEMATIC DIAGRAM OF MODES USED TO DESCRIBE
MOTIONS OF A TWO-BLADED TEETERING ROTOR

47

TORSION MODES
(about elastic axis)

(SAME PITCH CHANGE
ON BOTH BLADES)

(OPPOSITE PITCH CHANGE
ON OPPOSITE BLADES)

θ_2 = 1st SYM. TORSION

θ_1 = 1st ANTISYM. TORSION

θ_4 = 2nd SYM. TORSION

θ_3 = 2nd ANTISYM. TORSION

CONTROL MODES
(cyclic and collective rotations about same feathering axis)

C_2 = 1st SYM. PITCH

C_1 = 1st ANTISYM. PITCH

C_4 = 2nd SYM. PITCH

C_3 = 2nd ANTISYM. PITCH
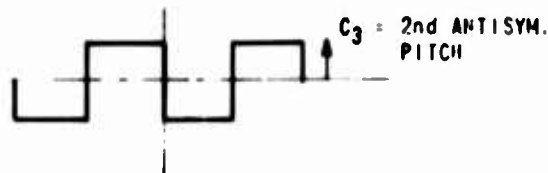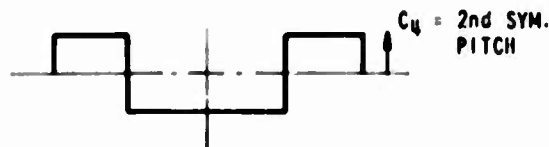
B
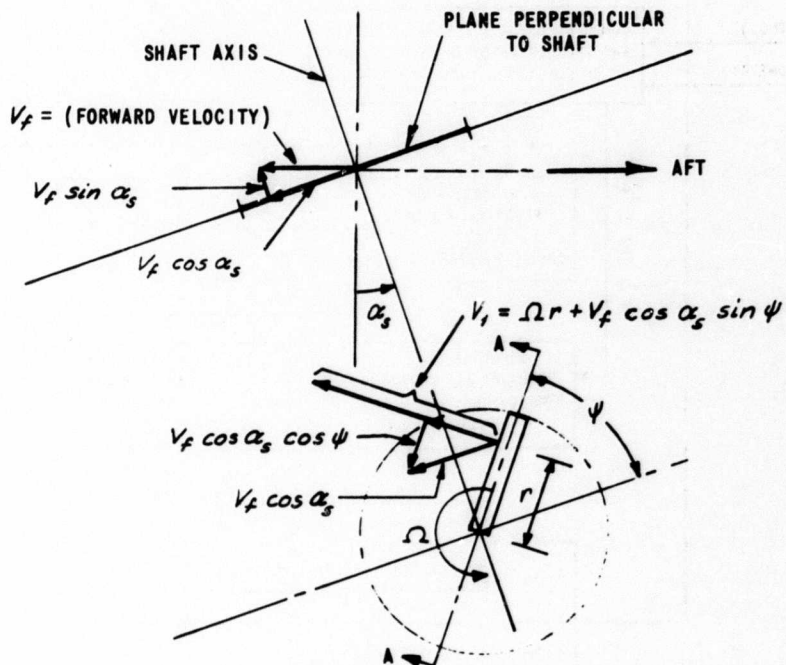
Figure 2. RELATIVE VELOCITIES DUE TO FORWARD MOTION AND BLADE
ROTATION (REFERRED TO A SHAFT-ORIENTED REFERENCE SYSTEM)
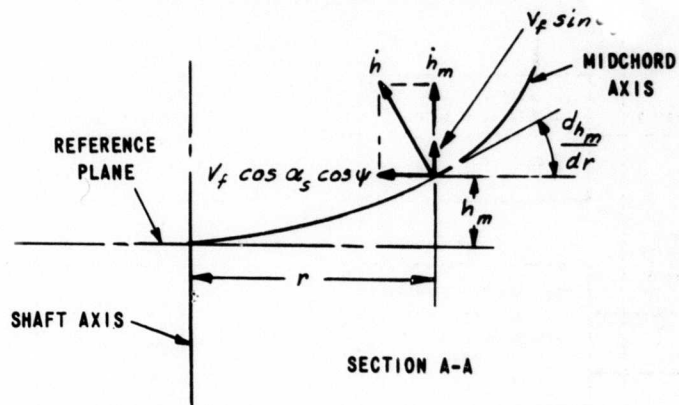
Figure 3. TRANSVERSE VELOCITY OF BLADE MIDCHORD AXIS RELATIVE
TO AIR (INDUCED VELOCITIES NOT INCLUDED)

49
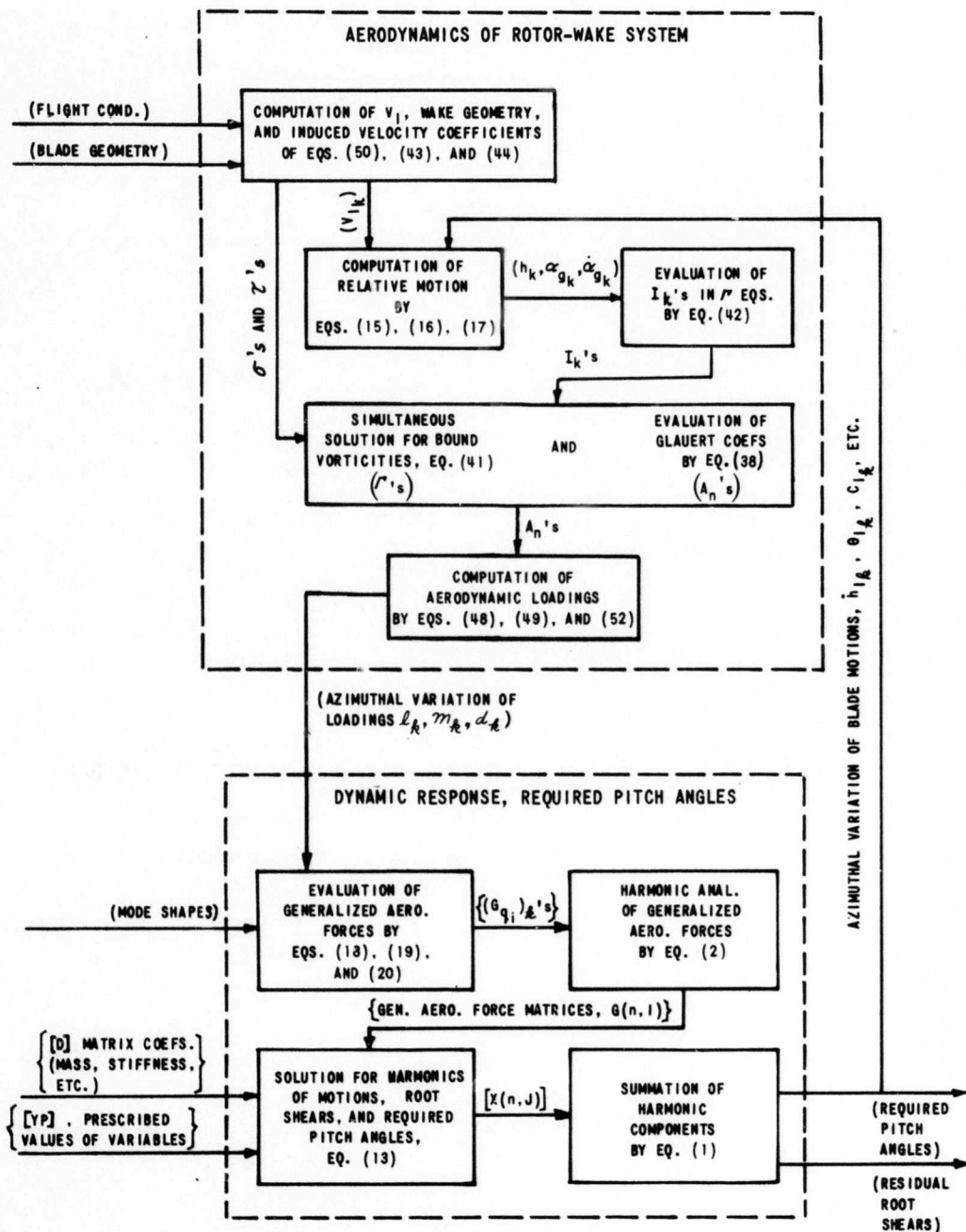
Figure 4. SCHEMATIC DIAGRAM OF THE ANALYTICAL PROBLEM OF EVALUATING
PITCH-ANGLE INPUTS TO ELIMINATE OSCILLATORY ROOT SHEARS
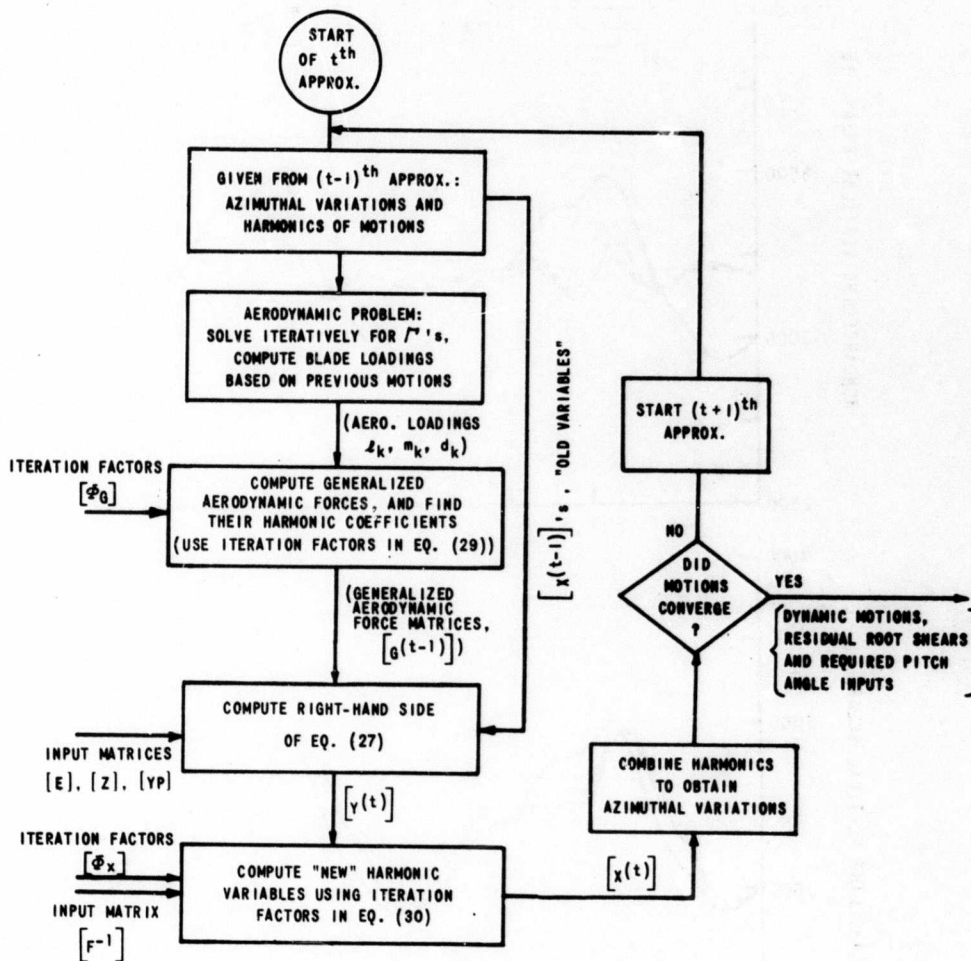
Figure 5. SCHEMATIC DIAGRAM OF PRINCIPAL STEPS IN ITERATIVE SOLUTION
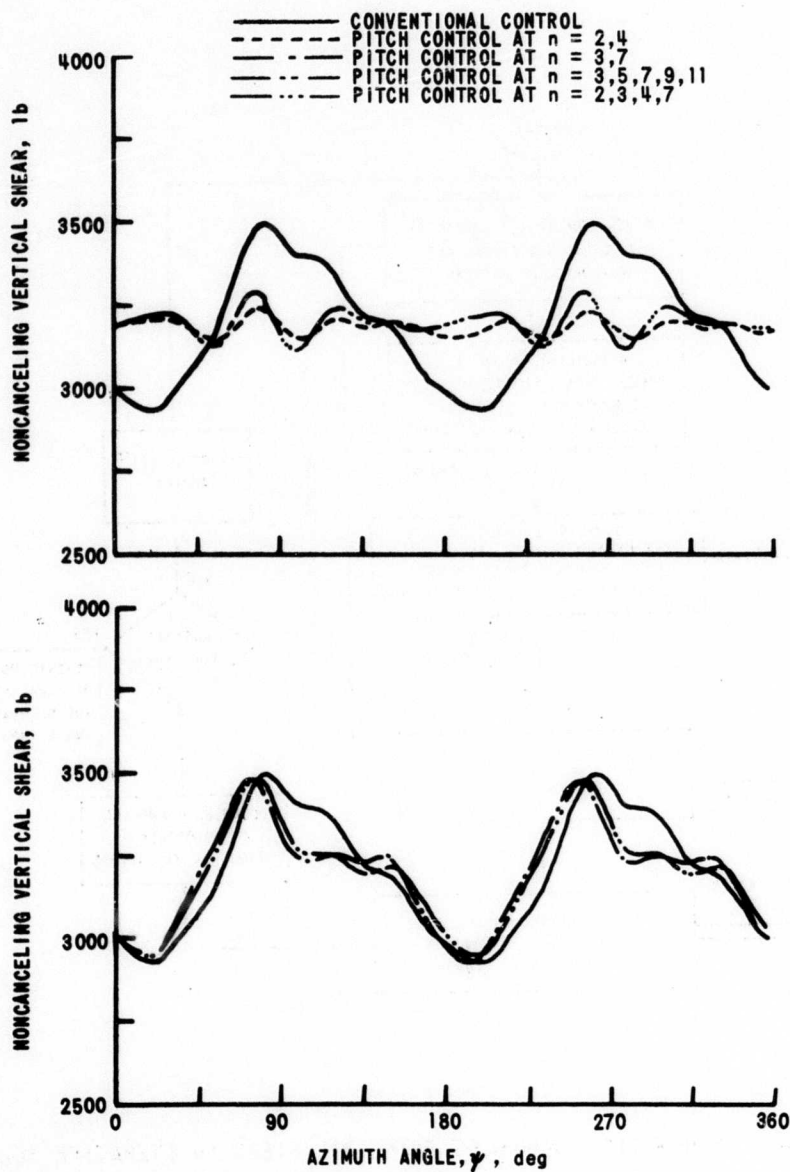
Figure 6. COMPARISONS OF AZIMUTHAL VARIATIONS OF NONCANCELING
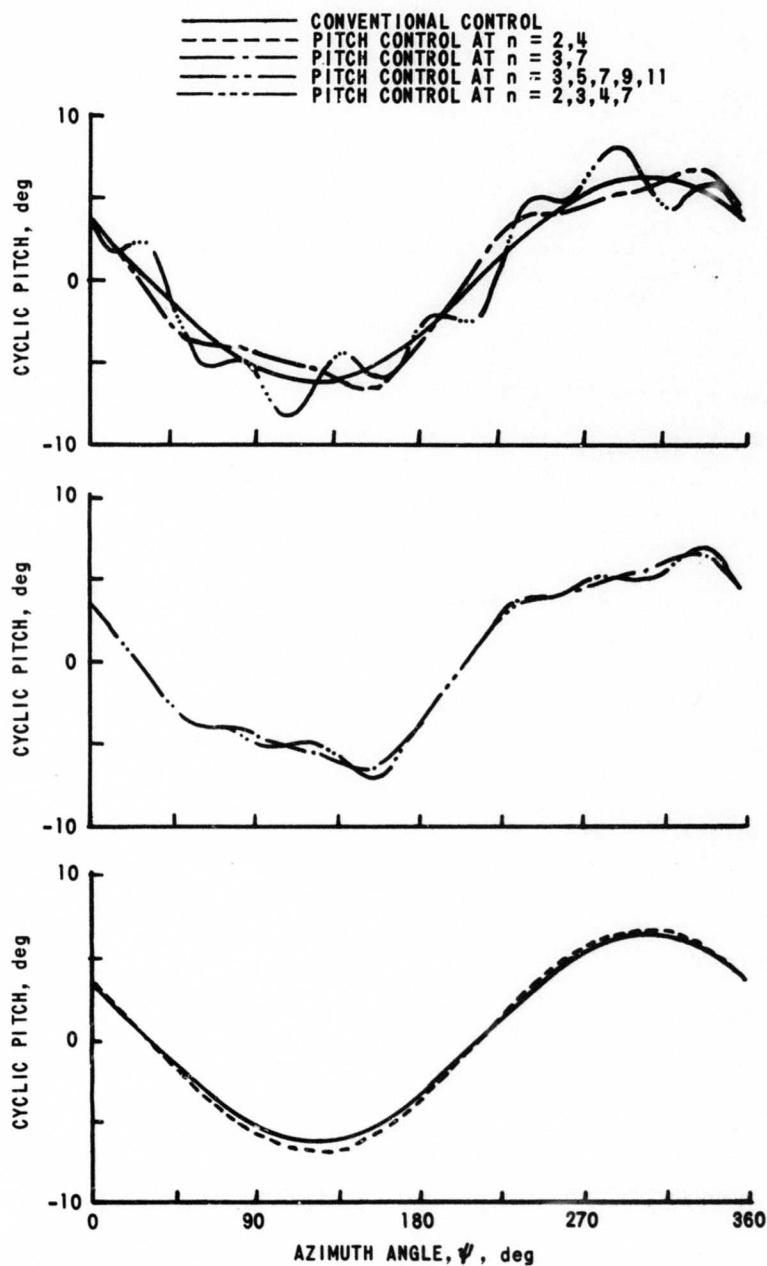VERTICAL ROOT SHEARS – FLIGHT CONDITION DN67A, $\mu = 0.259$
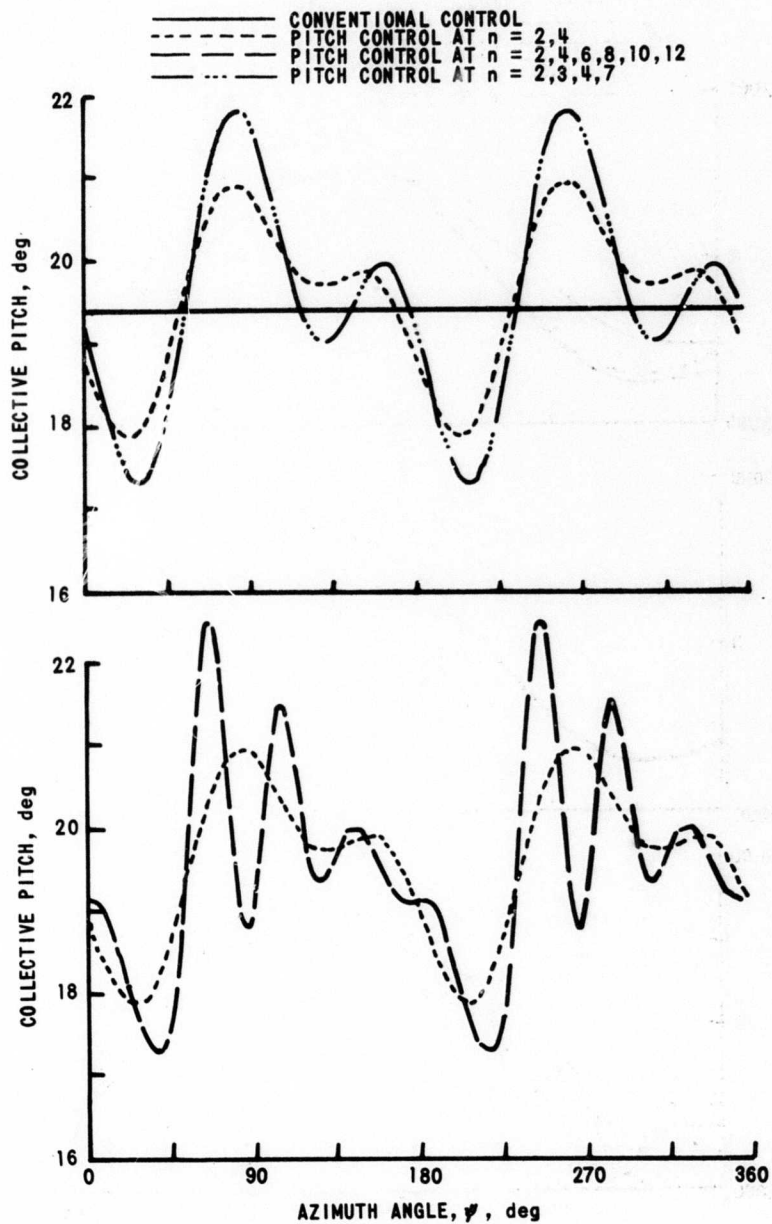
Figure 7. COMPARISONS OF COLLECTIVE PITCH CONTROL SCHEDULES
FOR ELIMINATING NONCANCELING HARMONIC ROOT SHEARS –
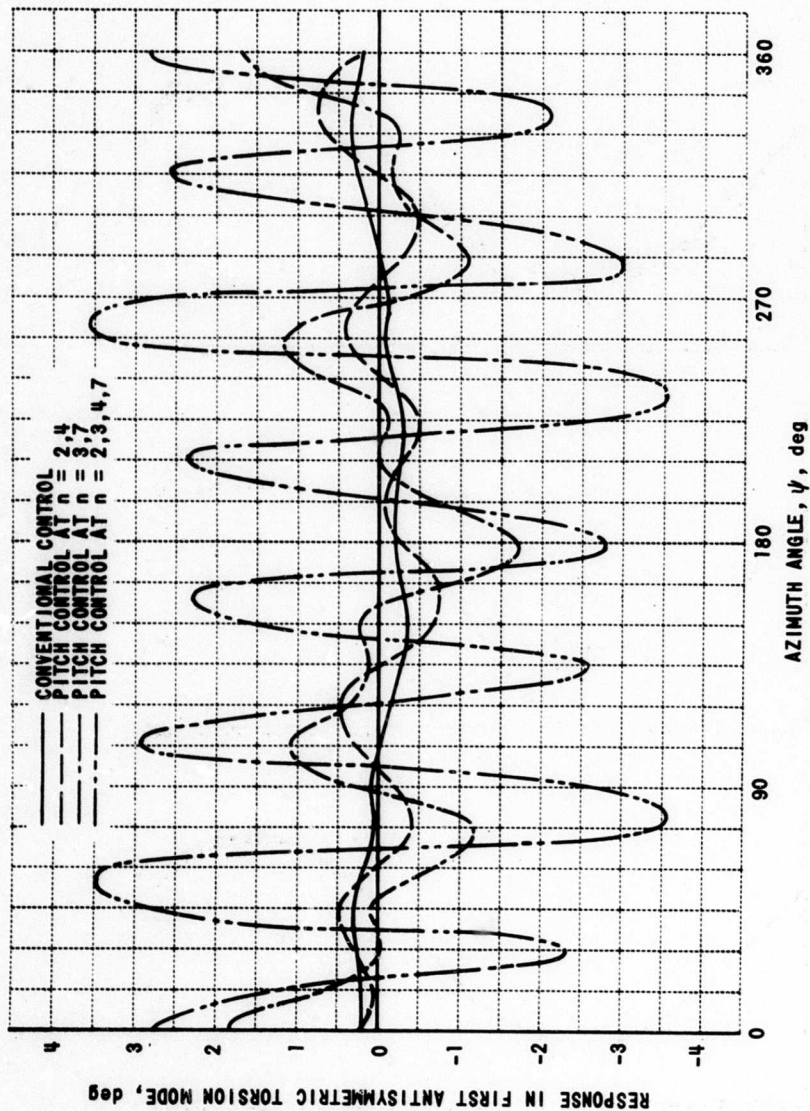FLIGHT CONDITION DN67A, μ = 0.259

53
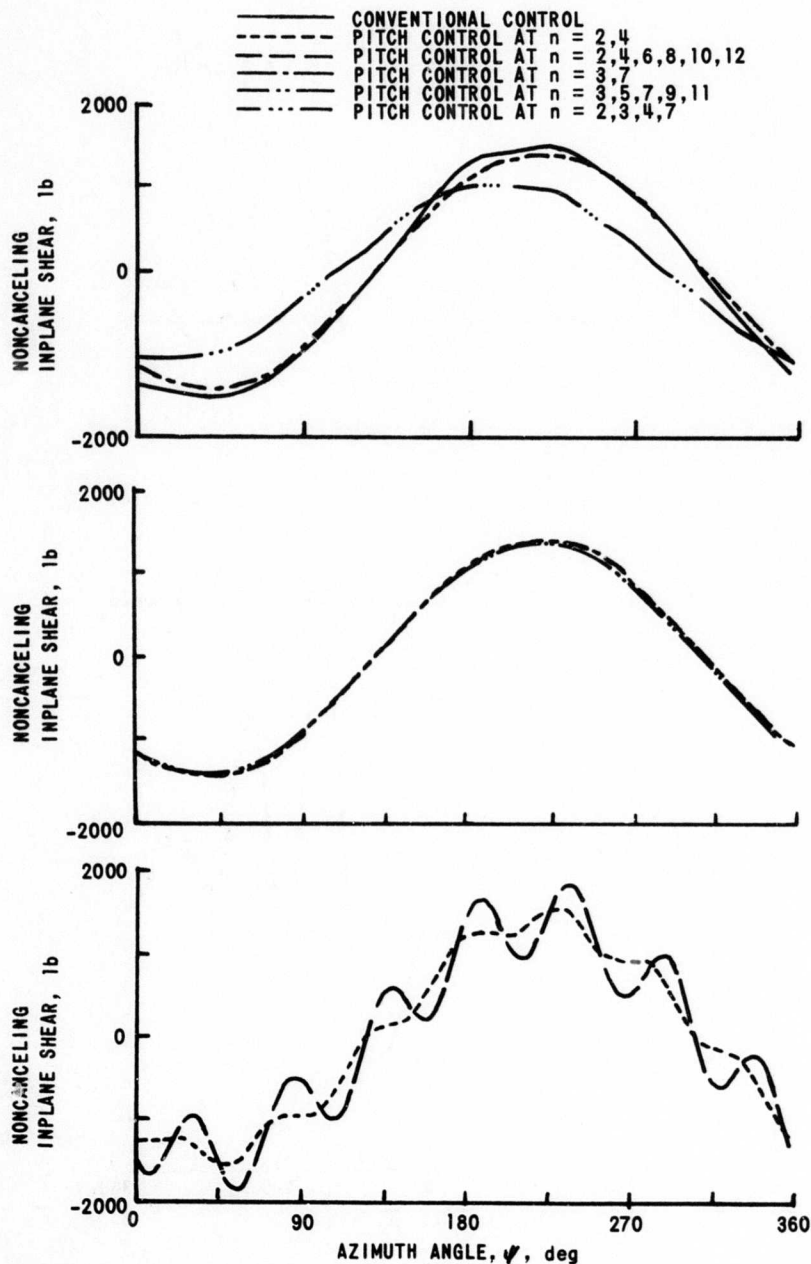
Figure 8. COMPARISONS OF AZIMUTHAL VARIATIONS OF NONCANCELING
INPLANE ROOT SHEARS - FLIGHT CONDITION DN67A, μ = 0.259

54

Figure 9. COMPARISONS OF CYCLIC PITCH CONTROL SCHEDULES FOR ELIMINATING NONCANCELING HARMONIC ROOT SHEARS - FLIGHT CONDITION DN67A, μ = 0.259

55

Figure 10. COMPARISON OF FIRST ANTISYMMETRIC TORSIONAL RESPONSE
FOR CONVENTIONAL CONTROL AND FOR HIGHER HARMONIC
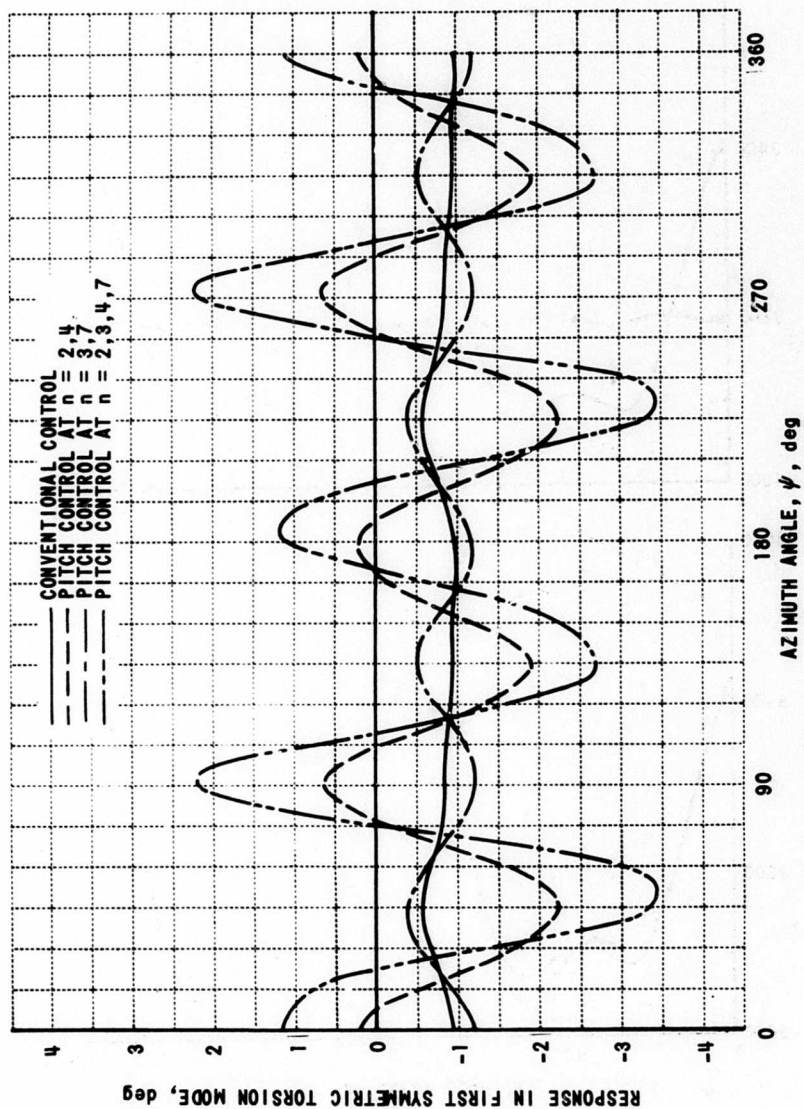PITCH CONTROL AT n = 2, 4; n = 3, 7; AND n = 2, 3, 4, 7

Figure 11. COMPARISON OF FIRST SYMMETRIC TORSIONAL RESPONSE FOR
CONVENTIONAL CONTROL AND FOR HIGHER HARMONIC PITCH
CONTROL AT n = 2, 4; n = 3, 7; AND n = 2, 3, 4, 7

57

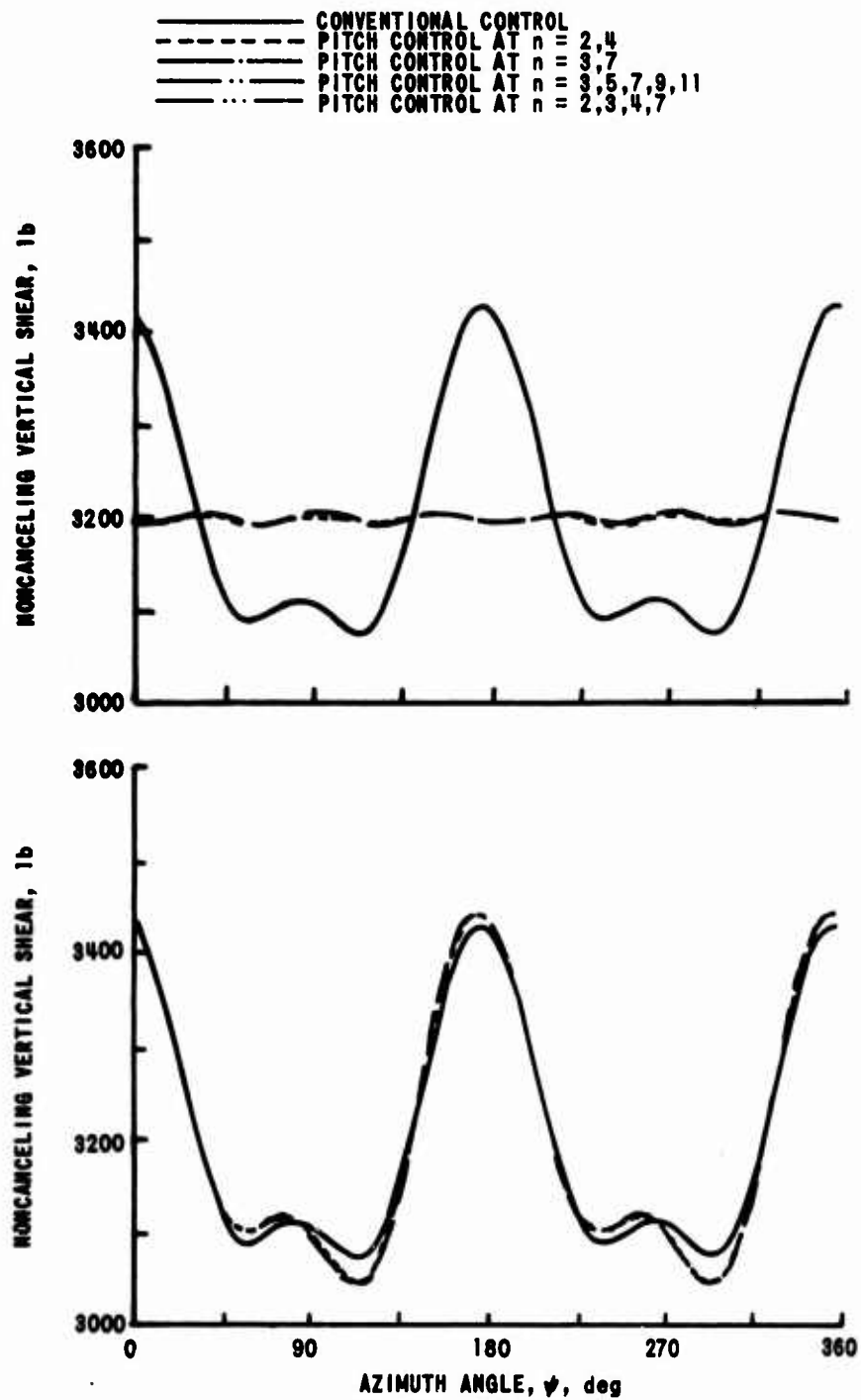Figure 12. COMPARISONS OF AZIMUTHAL VARIATIONS OF NONCANCELING VERTICAL ROOT SHEARS - FLIGHT CONDITION DN65A, μ = 0.076
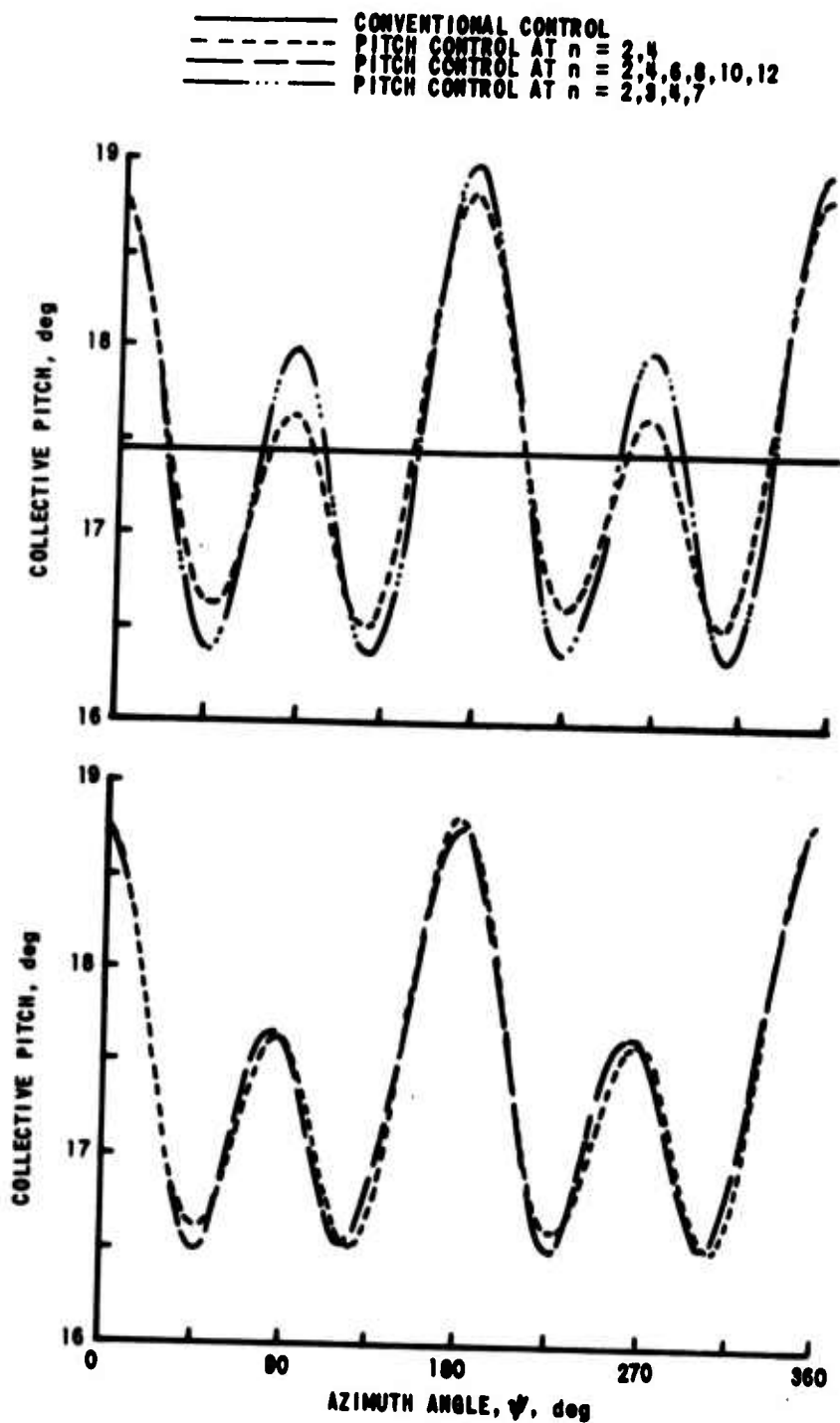
58

Figure 13. COMPARISONS OF COLLECTIVE PITCH CONTROL SCHEDULES
FOR ELIMINATING NONCANCELING HARMONIC ROOT SHEARS -
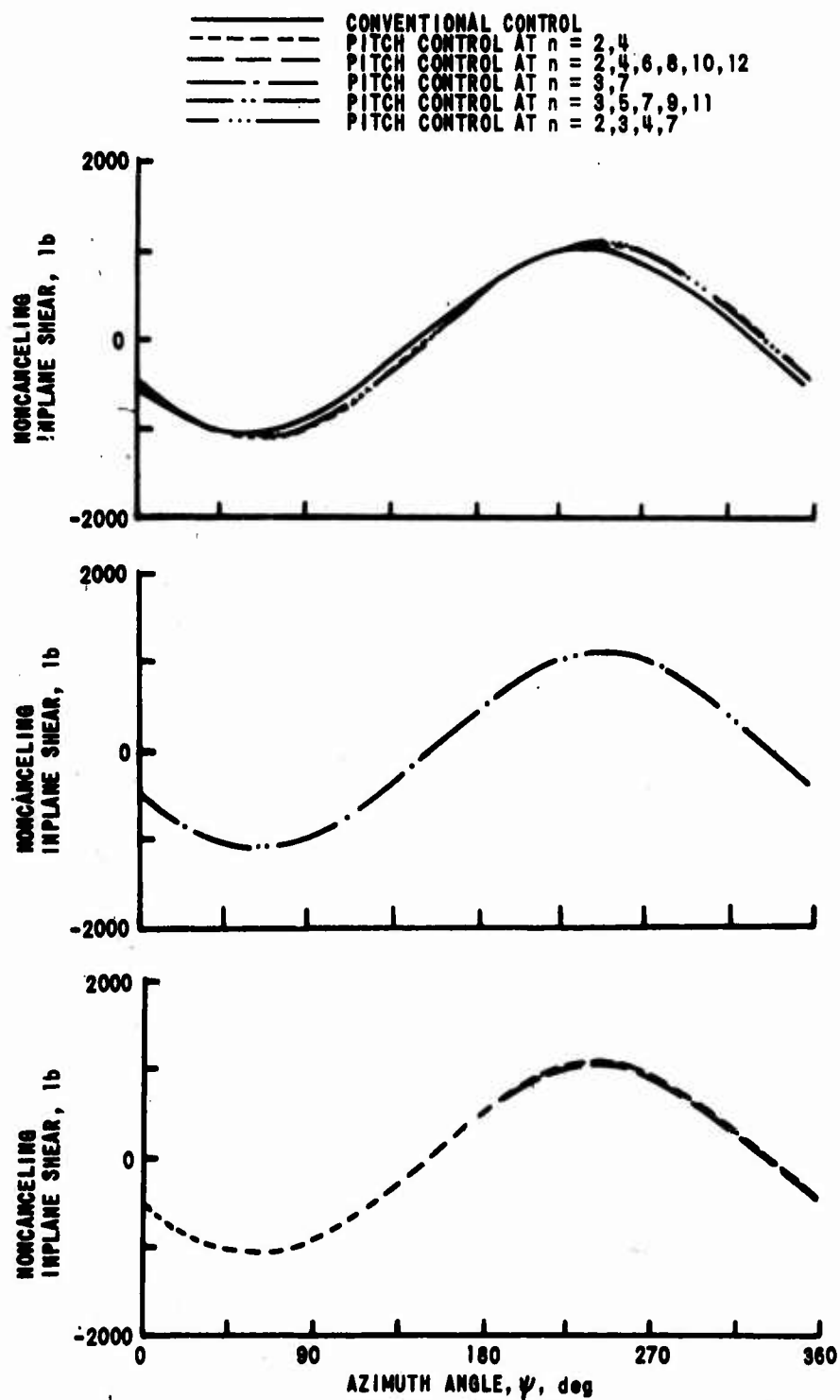FLIGHT CONDITION DN65A, μ = 0.076

Figure 14. COMPARISONS OF AZIMUTHAL VARIATIONS OF NONCANCELING
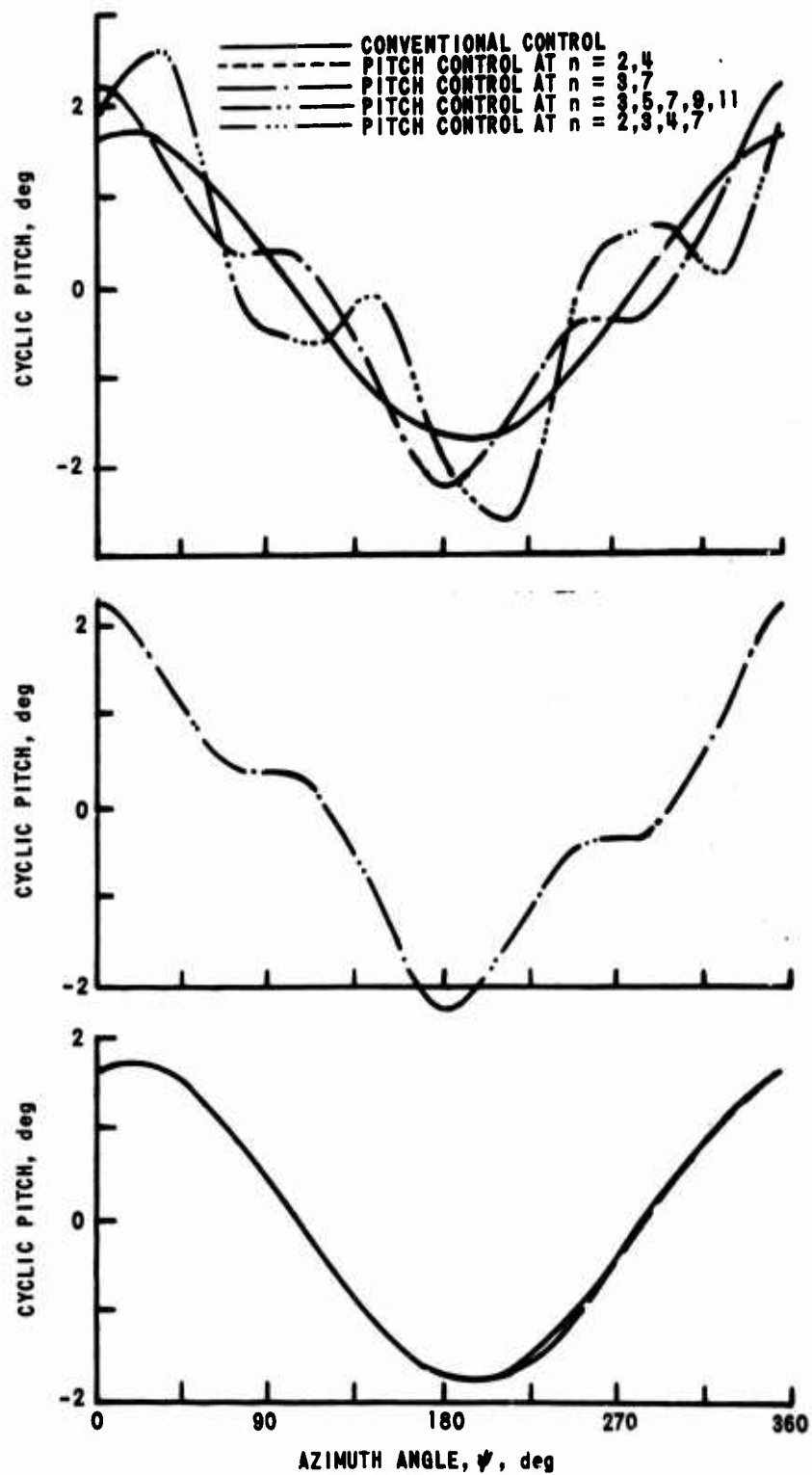INPLANE ROOT SHEARS - FLIGHT CONDITION DN65A, μ = 0.076

60

Figure 15. COMPARISONS OF CYCLIC PITCH CONTROL SCHEDULES FOR
ELIMINATING NONCANCELING HARMONIC ROOT SHEARS -
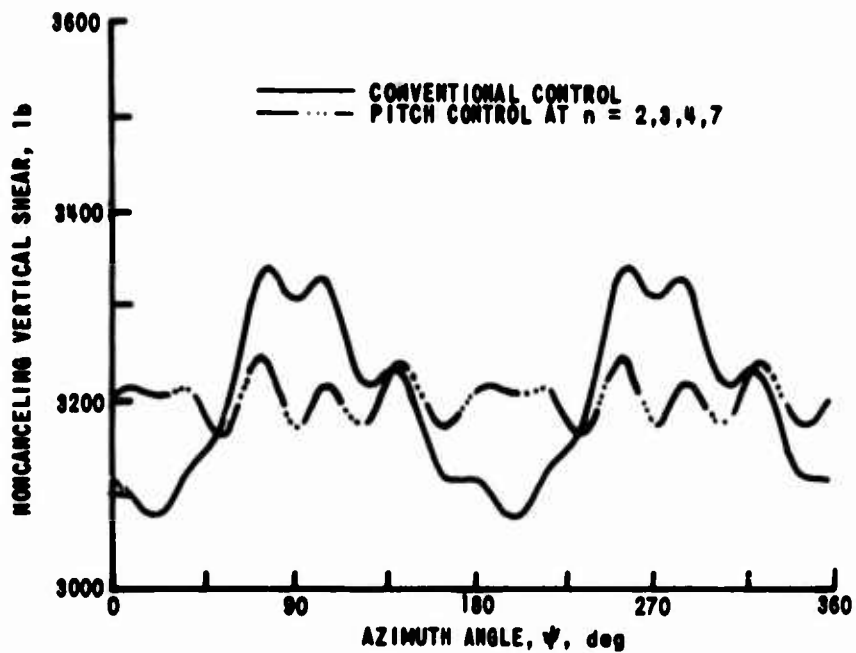FLIGHT CONDITION DN65A, μ = 0.076

61

Figure 16. COMPARISON OF AZIMUTHAL VARIATIONS OF NONCANCELING VERTICAL ROOT SHEARS - FLIGHT CONDITION DN66A, $\mu = 0.215$

Figure 17. COMPARISON OF COLLECTIVE PITCH CONTROL SCHEDULES FOR ELIMINATING NONCANCELING HARMONIC ROOT SHEARS - FLIGHT CONDITION DN66A, $\mu = 0.215$

62

Figure 18. COMPARISON OF AZIMUTHAL VARIATIONS OF NONCANCELING
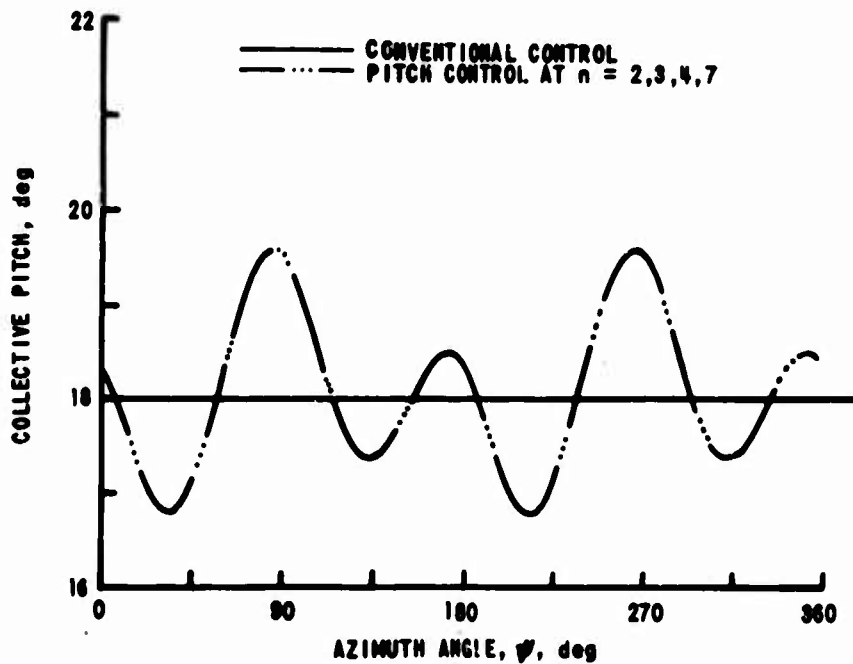INPLANE ROOT SHEARS - FLIGHT CONDITION DN66A, $\mu = 0.215$

Figure 19. COMPARISON OF CYCLIC PITCH CONTROL SCHEDULES FOR
ELIMINATING NONCANCELING HARMONIC ROOT SHEARS -
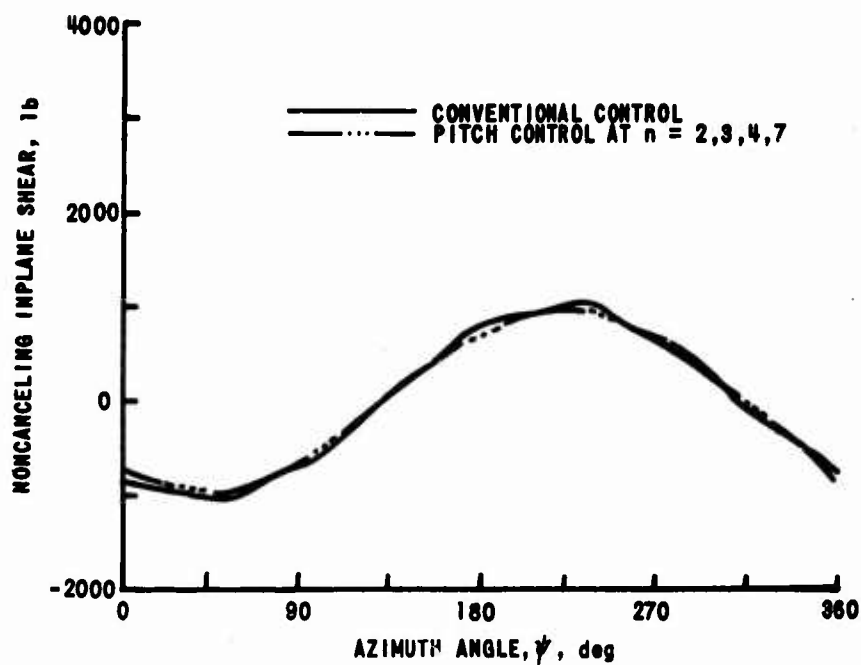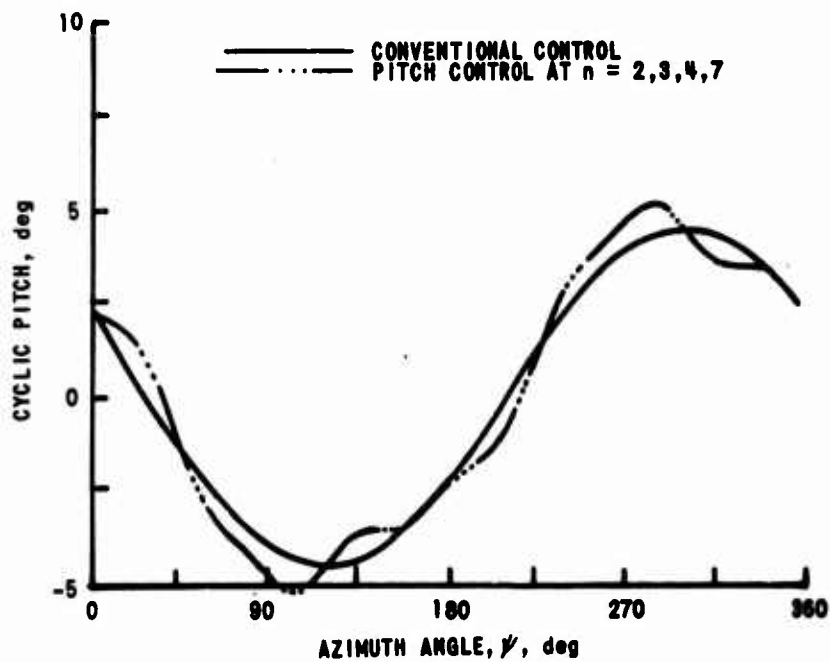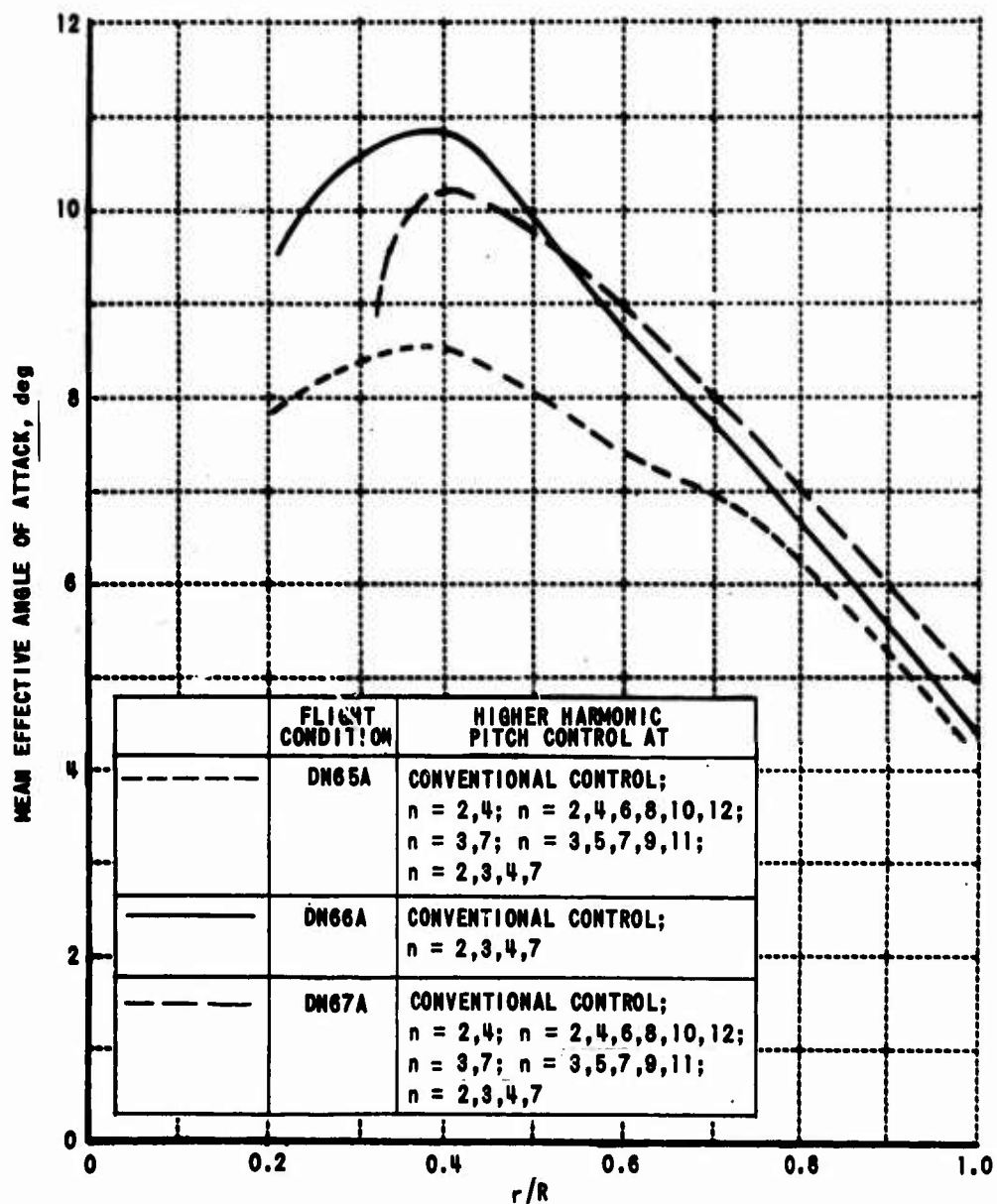FLIGHT CONDITION DN66A, $\mu = 0.215$

63

Figure 20. COMPARISON OF THE RADIAL DISTRIBUTIONS OF THE MEAN EFFECTIVE
ANGLE OF ATTACK - FLIGHT CONDITIONS DN65A, DN66A, AND DN67A

64

APPENDIX I

AERODYNAMICS OF ROTOR-WAKE SYSTEM
AND REPRESENTATION OF DRAG FORCES

The treatment of the aerodynamics of the rotor-wake system was basically the same as that used in Reference 2, and an abbreviated description of the analysis was outlined in Reference 1. Minor modifications of the aerodynamic analysis were made in conjunction with the inclusion of the inplane aerodynamic forces, and a brief description of the complete aerodynamic analysis is included herein for convenience.

The shed and trailing vorticity distributions in the wake of each blade are represented by an arrangement of straight-line vortex filaments as indicated in the sketch below.

EXAMPLE OF WAKE CONFIGURATION
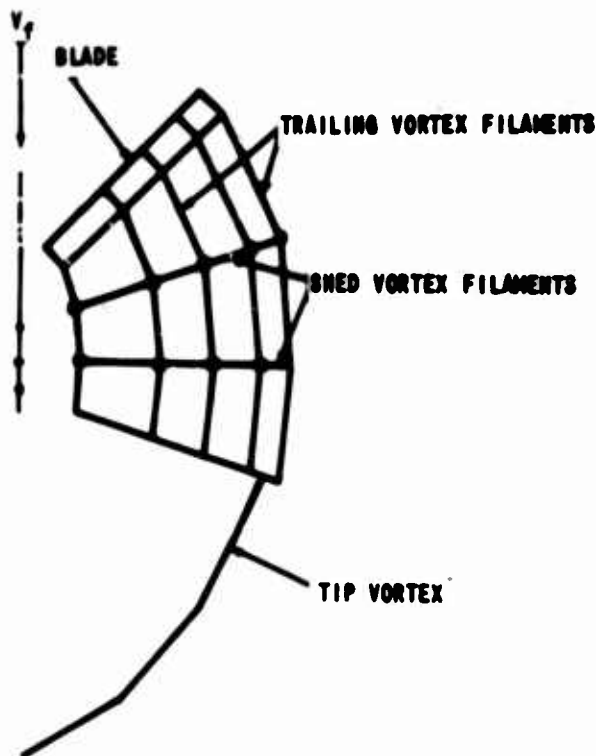
For simplicity, the case of only four radial blade segments is shown on the diagram (i.e., $NR = 4$). Trailing vortex filaments arise only at the ends of the blade segments, since it is assumed that there is no radial variation in bound vorticity along each segment. Shed vorticity is deposited continuously in the wake behind each blade of an actual rotor with an intensity equal to the rate of change of

bound vorticity. However, the numerical solution is carried out discontinuously using discrete time or azimuth angle increments. The discontinuous azimuth angles are denoted by ψ, with a small script letter used as a subscript (e.g., ψ_4 or ψ_j). The equally spaced azimuth angles are given by the formula $\psi_4 = 2\pi(4-1)/(NA)$, where 4 takes on all integer values from one to the total number of azimuth positions (NA). The shed vorticity deposited by each blade segment in a given time increment is lumped into a single shed vortex filament in the computational model as indicated on the sketch. This concentrated vortex filament is shed from the trailing edge at the position corresponding to 70 percent of the time increment. Results in Reference 2 show that this procedure gives a reasonable approximation of the shed wake.

The grid of straight-line vortex filaments representing the shed and trailing vortex filaments can be truncated after a prescribed number of azimuthal increments. Farther aft, the wake is continued as a tip trailing vortex filament representing the rolled-up vortex sheet. Although the computational program permits the use of a distorted wake, the motions of the end points of each wake segment were computed using uniform inflow theory.

In carrying out the solution, boundary conditions are satisfied for NA equally spaced azimuth positions of the rotor at the midpoints of the NR spanwise segments of a given blade. The total bound vorticity or circulation around the airfoil for each of these ($NR \times NA = NRA$) blade segment collocation positions is denoted by Γ with a lower-case letter as a subscript (e.g., Γ_j or Γ_k). The integer subscripts j and k are used to specify successive blade segment collocation positions for the entire rotor disc running from the inboard to the outboard segments at the aft azimuth position and then to the inboard segment at the next azimuth position, etc.

For a periodic problem, the strength of each trailing or shed vortex filament can be expressed by a linear combination of the Γ_j's in the rotor disc as a consequence of the vorticity conservation laws. When the bound vorticity strengths in adjacent blade segments are Γ_j and Γ_{j+1}, the strength of the trailing vortex segment arising at their intersection must be $\Gamma_j - \Gamma_{j+1}$. The strength of the shed vortex filament immediately aft of a given blade segment is equal to the difference of the bound vorticities of the blade segment at the preceding and current azimuth positions. Similar considerations can be used to find the strengths of all the vortex filaments in a wake representation such as shown in the sketch on page 65.

The strength of the trailing vortex segment produced by the rolling up of the vorticity deposited in the wake between azimuth positions ψ_{4-1} and ψ_4 is denoted by $\bar{\Gamma}_4$. It is assumed that $\bar{\Gamma}_4$ is equal in magnitude to the largest of the bound vorticities (Γ_j's) at

66

azimuth position ψ_k. This amounts to assuming that all the trailing vorticity deposited in the wake outboard of the radial position of maximum bound vorticity is concentrated in the tip vortex.

Each segment of the blade at each discrete azimuth position is represented by a continuous distribution of vorticity aligned in the radial direction and varying in intensity only in the chordwise direction. Using the notation of Reference 2 as indicated in the sketch below, the bound vorticity of a blade segment at collocation position (k) can be expressed by the Glauert series,

$$\gamma_k(\theta) = 2\left[A_{0_k}\cot\frac{\theta}{2} + \sum_{n=1}^{\infty} A_{n_k}\sin n\theta\right],$$
(31)

where

$$x = -b\cos\theta.$$
(32)

$$\Gamma_k = \int_{-b}^{+b}\gamma_k(x)dx$$
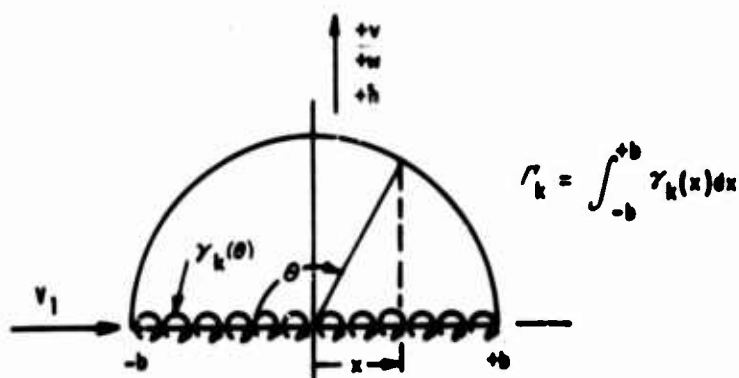
REPRESENTATION OF BLADE SECTION BY CHORDWISE BOUND VORTICITY DISTRIBUTION

The condition for no normal flow through the blade chord at the midspan of a particular blade segment can be expressed as follows:

$$\nu_k(x) + w_k(x) - \frac{1}{2\pi}\int_{-b}^{+b}\frac{\gamma_k(\xi)d\xi}{x-\xi} = 0,$$
(33)

where

$$\nu_k(x) = (-\dot{h} + V_1\alpha_g + \dot{\alpha}_g x)_k$$
(34)

67

and

$$w_k(z) = \sum_{j=1}^{NRA} C_{k_j}(z)\, \Gamma_j \; . \tag{35}$$

The symbol v_k denotes the velocity relative to the surface of the airfoil due to plunging motion ($\dot{h}_k$) and geometric angle of attack (α_{g_k}), while w_k' is the normal velocity induced by the trailing and shed vortex filaments in the wake. It is noted that the expression for w_k can be written in terms of the bound vorticity strengths because the strength of each wake vortex segment is a function of the Γ_j''s. The integral in Equation (33) gives the induced velocity due to the bound vorticity. An approximation for this induced velocity is used which should be reasonable at the midspan of the kth blade segment. It is based on the assumption that the bound vorticity representing the kth blade segment is extended to infinity in both directions. This explains the use of the two-dimensional Biot-Savart law in the integral term.

It is convenient to replace the chordwise variable x in Equations (33), (34), and (35) by the expression defined in Equation (32). Then, the evaluation of the integral in Equation (33) gives the well-known result.

$$\frac{1}{2\pi}\int_{-b}^{b}\frac{\gamma_k(\xi)\,d\xi}{x-\xi} = \frac{-1}{2\pi}\int_{0}^{\pi}\frac{\gamma_k(\phi)\sin\phi\,d\phi}{(\cos\theta-\cos\phi)}$$

$$= A_{0_k} - \sum_{n=1}^{\infty} A_{n_k}\cos n\theta, \tag{36}$$

where the series in Equation (31) has been substituted for $\gamma_k(\phi)$, replacing θ by ϕ. It is also possible to expand w_k' in a cosine series which is written in the form

$$w_k(\theta) = \sum_{j=1}^{NRA}\left(S_{0_{k_j}} + \sum_{n=1}^{\infty} S_{n_{k_j}}\cos n\theta\right)\Gamma_j + \sum_{\ell=1}^{NA}\left(T_{0_{k_\ell}} + \sum_{n=1}^{\infty} T_{n_{k_\ell}}\cos n\theta\right)\bar{\Gamma}_\ell . \tag{37}$$

The following set of equations results from substituting Equations (34), (36), and (37) into Equation (33), and from requiring that the coefficients of each harmonic cosine term be zero separately:

$$A_{0_k} = \left(-\dot{h} + V_1\alpha_g\right)_k + \sum_{j=1}^{NRA} S_{0_{k_j}}\Gamma_j + \sum_{\ell=1}^{NA} T_{0_{k_\ell}}\bar{\Gamma}_\ell ,$$

$$A_{1_k} = \left(+b\dot{\alpha}_g\right)_k - \sum_{j=1}^{NRA} S_{1_{k_j}}\Gamma_j - \sum_{\ell=1}^{NA} T_{1_{k_\ell}}\bar{\Gamma}_\ell ,$$

$$A_{n_k} = -\sum_{j=1}^{NRA} S_{n_{k_j}}\Gamma_j - \sum_{\ell=1}^{NA} T_{n_{k_\ell}}\bar{\Gamma}_\ell ; \qquad n = 2,3,4\cdots \Bigg\} . \tag{38}$$

68

A relationship between the Γ's and A's is required before a solution can be found. This is obtained by integrating the Glauert series for the bound vorticity over the chord, giving the following expression for the total bound vorticity or circulation about blade segment k,

$$\Gamma_k = b_k \int_0^\pi \gamma_k(\theta)\, \sin\theta\, d\theta$$

$$= 2\pi b_k \left(A_0 + \frac{1}{2} A_1\right)_k. \tag{39}$$

Since the theoretical circulation and the theoretical lift-curve slope are not achieved in practice, Equation (39) can be modified as follows:

$$\Gamma_k = b_k \left(C_{\ell_\alpha} A_0 + \pi A_1\right)_k, \tag{40}$$

where $C_{\ell_\alpha}/2\pi$ is an empirical correction factor applied to the theoretical lift-curve slope. The result of combining Equations (40) and (38) is

$$\Gamma_k = I_k + \sum_{j=1}^{NRA} \sigma_{k_j} \Gamma_j + \sum_{\ell=1}^{NA} \tau_{k_\ell} \bar{\Gamma}_\ell, \tag{41}$$

where

$$I_k = \left(C_{\ell_\alpha}\right)_k b_k \left(-\dot{h} + V_1 \alpha_g\right)_k + \pi \left(b^2 \dot{\alpha}_g\right)_k, \tag{42}$$

$$\sigma_{k_j} = \left(C_{\ell_\alpha}\right)_k b_k \left(S_{0_{k_j}}\right) - \pi \left(S_{1_{k_j}}\right) b_k, \tag{43}$$

and

$$\tau_{k_\ell} = \left(C_{\ell_\alpha}\right)_k b_k \left(T_{0_{k_\ell}}\right) - \pi \left(T_{1_{k_\ell}}\right) b_k. \tag{44}$$

Equation (41) represents a set of (NRA) equations which are solved iteratively for the NRA Γ_j's by the Gauss-Seidel method. In each iteration, the Γ_j's for the different spanwise blade segments at a given azimuth angle (ψ_ℓ) must be compared to find their maximum value $\bar{\Gamma}_\ell$.

The definition of stall differs slightly from that used in Reference 2. It is assumed herein that the airfoil is stalled when the effective angle of attack α_e is

$$\alpha_e = \left(\frac{|A_0|}{V_1}\right)_k > \tan \alpha_m, \quad V_{1_k} > 0$$

or

$$\alpha_e = \left(\frac{|A_0|}{|V_1|}\right)_k > \tan(\pi - \alpha_M), \quad V_{1_k} < 0, \tag{45}$$

69

where α_m, α_M are arbitrary stall angles of attack for the airfoil section. For the conditions (45), the circulation Γ is assumed to be

$$\Gamma_k = \pi b_k A_{l_k} + \left(\frac{\alpha_e}{|\alpha_e|} C_{\ell_\alpha} b V_l\right)_k \tan \alpha_m$$

or

$$\Gamma_k = \pi b_k A_{l_k} + \left(\frac{\alpha_e}{|\alpha_e|} C_{\ell_\alpha} b V_l\right)_k \tan (\pi - \alpha_M). \tag{46}$$

This treatment tends to limit the maximum value of Γ_k attainable at each blade segment collocation position, and prevents large, unrealistic values of vorticity from being shed into the wake from sections which are above their assumed stalling angle of attack. For the conditions (45), the effective angle of attack α_e is

$$\alpha_{e_k} = \tan^{-1}\left(\frac{A_o}{|V_l|}\right)_k. \tag{47}$$

Once the set of equations for the Γ's [i.e., Equation (41)] has been solved, the strengths of the bound vortices of the blade segments are known for all collocation positions in the rotor disc. Equation (38) can be used to compute the remaining coefficients (A_2, A_3) of the Glauert expansions of the chordwise vorticity distributions at these positions. The time derivatives of the Glauert coefficients for a given blade segment are also required in the computations. They are determined by assuming that all variables change periodically at steady flight conditions. This assumption makes it possible to express the time derivatives of the Glauert coefficients for a given blade segment at a particular azimuth position in terms of the values of the Glauert coefficients for the blade segment at all of the NA equally spaced azimuth positions which are used in the computations.

The linearized Bernoulli equation for unsteady flow leads to an expression for the chordwise variation in pressure difference on a blade segment as it moves through collocation position (k) in terms of the Glauert coefficients and time rate of change of the Glauert coefficients for the blade segment at position (k). This pressure distribution is used to compute the lift and pitching moment per unit span as a function of the values and time derivatives of the Glauert coefficients of a blade segment at position (k). Empirical correction factors are also introduced in these expressions to allow for the fact that the actual circulation can be less than the theoretical value. Below stall, the expressions for lift and pitching moment (about the midchord) per unit span of a blade segment at collocation position (k) can then be written in the form

$$\mathcal{L}_k = \left\{ b\rho V_l \left(C_{\ell_\alpha} A_o + \pi A_l\right) + \pi b^2 \rho \frac{\partial}{\partial t} \left(3A_o + A_l + \frac{1}{2} A_2\right) \right\}_k. \tag{48}$$

70

$$m_k = \left\{ \frac{1}{2} b^2 \rho V_i \left(C_{\ell_\alpha} A_0 + \pi A_1 \right) + \frac{1}{2} \pi b^2 \rho V_i \left(-A_1 + A_2 \right) - \frac{1}{2} \pi b^3 \rho \frac{\partial}{\partial t} \left(A_0 + \frac{3}{4} A_1 - \frac{1}{4} A_3 \right) \right\}_k \cdot \quad (49)$$

Above stall, the lift and pitching moment are computed in the manner described in Reference 2.

The lift and moment loadings obtained from Equations (48) and (49) are those resulting from the given geometric angles of attack (α_{g_k}), rates of change of geometric angle of attack ($\dot{\alpha}_{g_k}$), and plunging velocities ($\dot{h}_k$) entering in Equations (38) and (42). These quantities must be defined in terms of the geometry and motion of the rotor system.

The shaft-oriented reference system used in the analysis and the deflected blade axis are indicated schematically in Figures 2 and 3, respectively. The following expressions for the velocity components used in the analysis are readily derived by reference to these figures.

$$V_1 = \Omega r + \left(V_f \cos \alpha_s \right) \sin \psi \qquad (50)$$

= component of relative velocity perpendicular to the shaft and to the blade axis.

$$\dot{h} = V_f \sin \alpha_s \cos \left(\frac{dh_m}{dr} \right) + V_f \cos \alpha_s \cos \psi \sin \left(\frac{dh_m}{dr} \right) + \dot{h}_m \cos \left(\frac{dh_m}{dr} \right)$$

= component of velocity perpendicular to V_1 and the blade axis (i.e., velocity of airfoil relative to air excluding induced velocity).

By making use of small-angle approximations,

$$\dot{h} = V_f \sin \alpha_s + V_f \cos \alpha_s \cos \psi \frac{dh_m}{dr} + \dot{h}_m . \qquad (51)$$

Forward velocity is denoted by V_f, shaft angle by α_s, and the distance of the midchord axis above the reference plane by h_m.

Below stall, the drag loading at the collocation position in the disc can be written

$$d_k = \left(\frac{V_1}{|V_1|} \right)_k \rho b_k \left(C_{d_p} V_1^2 - C_{\ell_\alpha} A_0^2 \right)_k + \left(\alpha_g \ell \right)_k , \qquad (52)$$

where C_{d_p} is a profile drag coefficient. The profile drag coefficients are expressed as functions of the geometric angle of attack and Mach number, and are based on the data contained in Reference 5 for the NACA 0015 airfoil section used in the UH-1A rotor blades.

71

Above stall, the drag is simply

$$d_k = (\alpha_g \, l)_k \, .$$

(53)

The expressions used to evaluate rotor torque Q, control moment M, side force Y, and longitudinal force X were based on the analysis of Reference 3. For a teetering rotor, under the assumptions that the rotor blade is mass balanced about the elastic axis, and excluding the dynamic effects of the control system, the expressions of Reference 3 can be written

$$Q = 2C_0$$

(54)

$$M = B_{IC} + 2\Omega^2 \beta_c \sum_j (B_1 H_j) \, \tau_{r_{c_j}} + \Omega^2 \frac{(B_1 h_1)}{R} \sum_j (A_0 H_j) \, \tau_{r_{c_j}}$$

$$- \beta_c C_{IS} - \frac{(B_1 h_1)}{R} C_0 - \Omega^2 \sum_j (B_1 \theta_j) \, J_{\theta_j} - (M_P)_{IS}$$

(55)

$$Y = D_{IC} + 2\Omega^2 \sum_j m_{c_j} (A_1 H_j) - \frac{(B_1 h_1)}{R} L_0$$

$$- \beta_c \left\{ L_{IS} + \Omega^2 \sum_j m_{h_j} (B_1 h_j) \right\}$$

(56)

$$X = -D_{IS} - 2\Omega^2 \sum_j m_{c_j} (B_1 H_j) - \frac{(A_1 h_1)}{R} L_0 - \beta_c \left\{ L_{IC} + \Omega^2 \sum_j m_{h_j} (A_1 h_j) \right\} \, .$$

(57)

The quantities B_{IC}, C_{IS}, D_{IC}, D_{IS}, L_{IS}, and $(M_P)_{IS}$ are the indicated first harmonic cosine or sine components of B, C, D, L, and M_P, while C_0 and L_0 are the steady components of C and L. The expressions for B, C, D, L, and M_P at azimuth position ψ_k are:

$$B_k = \int_0^R (r \, l(r) \, dr)_k \qquad\qquad D_k = \int_0^R (d(r) \, dr)_k$$

$$C_k = \int_0^R (r \, d(r) \, dr)_k \qquad\qquad L_k = \int_0^R (l(r) \, dr)_k$$

$$(M_P)_k = \int_0^R (m_e(r) \, dr)_k$$

where m_e is the aerodynamic pitching moment about the elastic axis. The first harmonic cosine component of B, for example, is determined from the calculated values of B at NA equally spaced azimuth positions. Denoting

$$\psi_k = \frac{k-1}{NA} \pi \quad \cdot \text{ and } \quad B_k = B_\psi = \psi_k \, ,$$

72

$(\ell = 1, 2, \cdots NA)$, B_{1C} is given by

$$B_{1C} = \frac{2}{NA} \sum_{\ell=1}^{NA} B_\ell \cos \psi_\ell .$$

The steady component of C is

$$C_o = \frac{1}{NA} \sum_{\ell=1}^{NA} C_\ell .$$

The quantities (A, H_j), (B, h_j), etc., are given in Equations (7) and (8). Also,

$$\tau_{r_{c_j}} = \int_0^R m r f_{H_j}\, dr ,$$

$$J_{\theta_j} = \int_0^R \left(\frac{dI_x}{dr} + \frac{dI_z}{dr} \right) f_{\theta_j}\, dr ,$$

$$\dot{m}_{c_j} = \int_0^R m f_{H_j}\, dr ,$$

$$m_{h_j} = \int_0^R m f_{h_j}\, dr ,$$

where m, (dI_x/dr), and (dI_z/dr) are as defined in Appendix II.

APPENDIX II
BLADE PARAMETERS USED IN COMPUTATIONS

GEOMETRIC PROPERTIES

The blade planform considered in the computations is shown in the sketch below. The blade was assumed to possess a preconing angle of 3.0 degrees and a built-in twist (θ_β) varying linearly from zero at $r = 23.0$ inches to -11.0 degrees at the blade tip.

UH-1A BLADE PLANFORM

ASSUMED LOCATION OF BLADE PITCHING AND ELASTIC AXES
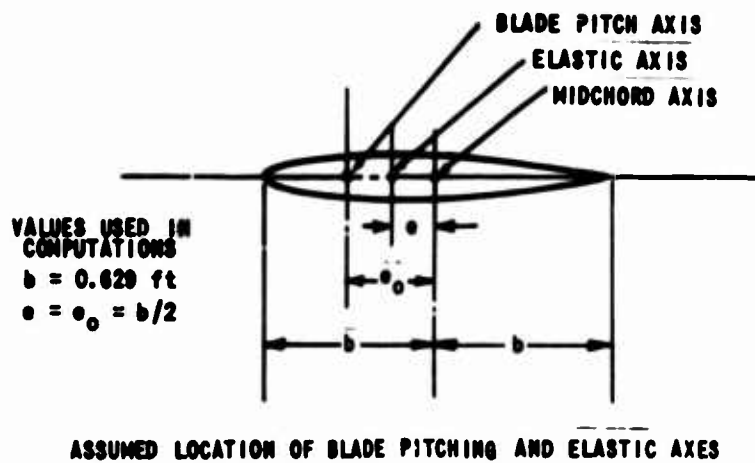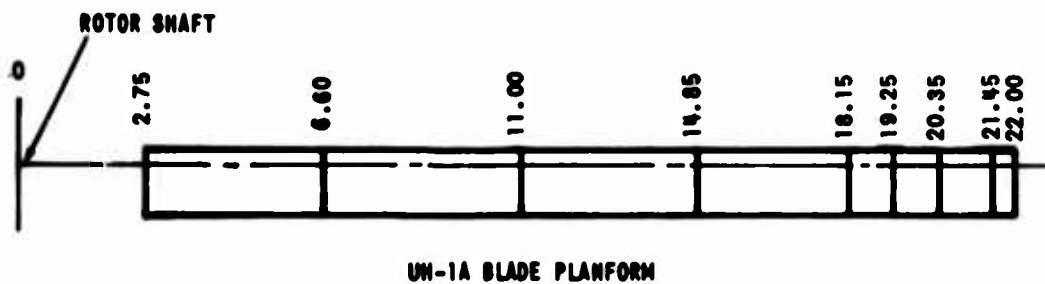
MODES AND FREQUENCIES OF ROTOR BLADE

Uncoupled flapwise and chordwise bending modes and frequencies for the rotating blade were based on the computations using the associated matrix method of Reference 4. The torsional frequencies were obtained from a Holzer-type computation. The blade frequencies were assumed to be identical for the three flight conditions analyzed, since

74

the rotational speed of the rotor was invariant for these cases. As in Reference 1, the frequency and mode shape of the third symmetric bending mode were not computed, and the deflections in this mode were assumed to be zero in the numerical computations. The rotor blade frequencies are summarized in the table below.

Table X
MODAL FREQUENCIES OF ROTOR BLADE

MODE	FREQUENCY ω_{q_i} rad/sec	$\dfrac{\omega_{q_i}}{\Omega}$
ω_{h_2} - 1st SYMMETRIC FLAPWISE BENDING	38.8	1.18
ω_{h_4} - 2nd SYMMETRIC FLAPWISE BENDING	112.8	3.43
ω_{h_6} - 3rd SYMMETRIC FLAPWISE BENDING	--	--
ω_{θ_2} - 1st SYMMETRIC TORSION	168.8	5.14
ω_{θ_4} - 2nd SYMMETRIC TORSION	440.9	13.40
ω_{H_2} - 1st SYMMETRIC CHORDWISE BENDING	39.1	1.19
ω_{H_4} - 2nd SYMMETRIC CHORDWISE BENDING	236.4	7.19
ω_{h_3} - 1st ANTISYMMETRIC FLAPWISE BENDING	96.4	2.94
ω_{h_5} - 2nd ANTISYMMETRIC FLAPWISE BENDING	171.6	5.23
ω_{θ_1} - 1st ANTISYMMETRIC TORSION	168.8	5.14
ω_{θ_3} - 2nd ANTISYMMETRIC TORSION	440.9	13.40
ω_{H_1} - 1st ANTISYMMETRIC CHORDWISE BENDING	39.1	1.19
ω_{H_3} - 2nd ANTISYMMETRIC CHORDWISE BENDING	236.4	7.19

COEFFICIENTS IN EQUATIONS OF MOTION

The coefficients in the equations of motion neglecting the chordwise deformations of the blade are identical to those in Reference 1. The assumptions, listed below, which were made in the computations encompass those of Reference 1, and they were extended to include the chordwise deformations of the blade.

1. The relatively small gyroscopic coupling terms were neglected.

2. The elastic and pitch axes are assumed to be coincident and to intersect with the shaft axis.

3. The blade is assumed to be mass balanced about the elastic axis.

4. It is assumed that there is no elastic coupling between:

   a. the flapwise bending and torsion modes

   b. the chordwise bending and torsion modes

   c. the flapwise bending and chordwise bending modes.

Under these assumptions, the expressions for the mass, centrifugal force, and stiffness coefficients take the form

$$M_{h_i h_i} = \int_o^R f_{h_i}^2 \, m \, dr + \left[\left(\frac{df_{h_i}}{dr}\right)_{r=o}\right]^2 I_z \text{ (root fitting)}.$$

$$T_{h_i h_i} = -\int_o^R \left(\frac{df_{h_i}}{dr}\right)^2 \left[\int_r^R r \, m \, dr\right] dr + \left[\left(\frac{df_{h_i}}{dr}\right)_{r=o}\right]^2 I_z \text{ (root fitting)},$$

$$K_{h_i h_i} = \Omega^2 T_{h_i h_i} + \omega_{h_i}^2 M_{h_i h_i},$$

$$M_{H_i H_i} = \int_o^R f_{H_i}^2 \, m \, dr,$$

$$T_{H_i H_i} = M_{H_i H_i} - \int_o^R \left(\frac{df_{H_i}}{dr}\right)^2 \left(\int_r^R m r \, dr\right) dr,$$

$$K_{H_i H_i} = \Omega^2 T_{H_i H_i} + \omega_{H_i}^2 M_{H_i H_i},$$

$$M_{h_o h_j} = \int_o^R m f_{h_j} \, dr \quad ; \qquad j \geq 1,$$

$$M_{H_o H_j} = T_{H_o H_j} = \int_o^R m f_{H_j} \, dr \; ; \; j \geq 1,$$

76

$$M_{\theta_i \theta_i} = \int_0^R \left(\frac{dI_x}{dr} + \frac{dI_z}{dr}\right) f_{\theta_i}^2 \, dr, \qquad M_{\theta_i c_j} = \int_0^R \left(\frac{dI_x}{dr} + \frac{dI_z}{dr}\right) f_{\theta_i} f_{c_j} \, dr,$$

$$T_{\theta_i \theta_i} = \int_0^R \left(\frac{dI_z}{dr} - \frac{dI_x}{dr}\right) f_{\theta_i}^2 \, dr, \qquad T_{\theta_i c_j} = \int_0^R \left(\frac{dI_z}{dr} - \frac{dI_x}{dr}\right) f_{\theta_i} f_{c_j} \, dr.$$

$$K_{\theta_i \theta_i} = \Omega^2 T_{\theta_i \theta_i} + \omega_{\theta_i}^2 M_{\theta_i \theta_i},$$

where m is the mass per foot, dI_x/dx is the moment of inertia per foot about the elastic axis due to the horizontal distribution of mass, and dI_z/dx is the moment of inertia per foot about the elastic axis due to the vertical distribution of mass. The vertical distribution of mass is neglected in treating the bending modes except for the contribution of the root fitting.

The numerical values of the nonzero coefficients which were used in the computations are summarized below.

Table XI
MASS, CENTRIFUGAL FORCE, AND STIFFNESS COEFFICIENTS
FOR TEETERING AND BENDING MODES

MODE	$M_{h_i h_i}/M_{H_i H_i}$ lb-sec^2/ft	$M_{h_0 h_i}/M_{H_0 H_i}$ lb-sec^2/ft	$T_{h_i h_i}/T_{H_i H_i}$ lb-sec^2/ft	$K_{h_i h_i}/K_{H_i H_i}$ lb/ft
h_1 – TEETERING	1.972	2.847	– 1.972	0
h_3 – 1st ANTISYMMETRIC FLAPWISE BENDING	1.359	-0.891	-10.610	1143.0
h_5 – 2nd ANTISYMMETRIC FLAPWISE BENDING	1.327	0.470	-27.580	9236.0
H_1 – 1st ANTISYMMETRIC CHORDWISE BENDING	1.607	2.415	– 0.388	2040.0
H_3 – 2nd ANTISYMMETRIC CHORDWISE BENDING	1.769	-1.495	-12.460	85310.0
h_2 – 1st SYMMETRIC FLAPWISE BENDING	1.553	2.248	– 2.107	57.5
h_4 – 2nd SYMMETRIC FLAPWISE BENDING	1.060	-0.780	-10.190	2450.0
H_2 – 1st SYMMETRIC CHORDWISE BENDING	1.607	2.415	– 0.388	2040.0
H_4 – 2nd SYMMETRIC CHORDWISE BENDING	1.769	-1.495	-12.460	85310.0

Table XII

MASS, CENTRIFUGAL FORCE, AND STIFFNESS COEFFICIENTS
FOR TORSION AND CONTROL MODES

	$M_{\theta_i \theta_i}$ lb-ft sec^2	$T_{\theta_i \theta_i}$ lb-ft sec^2	$K_{\theta_i \theta_i}$ lb-ft/rad
θ_1 - 1st ANTISYMMETRIC TORSION	0.2179	-0.2294	5961
θ_2 - 1st SYMMETRIC TORSION	0.2179	-0.2294	5961
θ_3 - 2nd ANTISYMMETRIC TORSION	0.2466	-1.646	46156
θ_4 - 2nd SYMMETRIC TORSION	0.2466	-1.646	46156

$$M_{\theta_1 C_1} = 0.2965 \text{ lb-ft-sec}^2 \qquad T_{\theta_1 C_1} = -0.2965 \text{ lb-ft-sec}^2$$

$$M_{\theta_2 C_2} = 0.2965 \qquad\qquad\quad T_{\theta_2 C_2} = -0.2965$$

$$M_{\theta_3 C_1} = -0.1373 \qquad\qquad T_{\theta_3 C_1} = 0.1373$$

$$M_{\theta_4 C_2} = -0.1373 \qquad\qquad T_{\theta_4 C_2} = 0.1373$$

THE STRUCTURAL DAMPING COEFFICIENT IS ASSUMED TO BE g = 0.03 IN ALL BENDING AND TORSION MODES.

78

APPENDIX III

EXPRESSIONS FOR ELEMENTS IN [E] MATRIX

In estimating the increments in the generalized aerodynamic forces from one iteration to the next of the computational procedure, the following expressions are used for the quasi-steady lift and pitching moment loadings:

$$\ell = 2\pi \rho b \left\{ \frac{c_{\ell_\alpha}}{2\pi}\left(V_1^2 \alpha - V_1 h_1 + \frac{b}{2}V_1\dot{\alpha}\right) + \frac{b}{2}\left(V_1\dot{\alpha} - \ddot{h}\right)\right\} \quad . \quad (58)$$

$$m\ (about\ midchord) = \pi \rho b^2 \left\{ V_1^2 \alpha - V_1 h_1 - \frac{1}{8}b^2\ddot{\alpha} \right\} \quad . \quad (59)$$

where V_1, α, $\dot{\alpha}$, and $\dot{h}$ are given by Equations (50), (15), (16), and (17), respectively. The drag, on the other hand, can be written approximately in terms of a drag coefficient slope as

$$d = \rho V_1^2 b \bar{C}_{d_\alpha} \alpha , \quad (60)$$

where $\bar{C}_{d_\alpha}$ is a mean sectional drag coefficient slope assumed, for a rough estimate, to be independent of r and ψ. $\bar{C}_{d_\alpha}$ can be evaluated on the basis of finite wing theory as being approximately equal to the overall lift coefficient C_L, written here as $W_b/\rho \Omega^2 \int r^2 b dr$. The resultant value of $\bar{C}_{d_\alpha}$ for the flight conditions considered was 0.615.

The incremental generalized forces due to these loadings are computed by a procedure similar to that used in Reference 7 and can be expressed in the form

$$\Delta^{(t)} G_{q_i} = \sum_j \left\{ A_{q_i \ddot{q}_i} \Delta^{(t)}\ddot{q}_j + \Omega A_{q_i \dot{q}_i} \Delta^{(t)}\dot{q}_j + \Omega^2 A_{q_i q_i} \Delta^{(t)} q_j \right\}, \quad (61)$$

where only terms independent of μ are retained. The symbol $\Delta^{(t)}$ preceding the symbol for a given quantity is again used to denote the change in that quantity from the $(t-1)^{th}$ to the $(t)^{th}$ approximation of the iterative solution.

Only one-half of the modes of the two-bladed teetering rotor need be included in the summation in Equation (61) because the terms involving the other modes are zero from symmetry considerations; i.e., the only q_j modes to be included in this group are those having the same symmetry as the q_i mode.

79

In the case of periodic motion, each variable in Equation (61) can be expressed in the form of Equation (1), leading to the following equations for the harmonic coefficients of $\Delta^{(t)}G_{q_i}$:

$$\frac{1}{n^2}\Delta^{(t)}(A_n G_{q_i}) = \sum_j \left\{ \left(-n^2 A_{q_i \ddot{q}_j} + A_{q_i q_j}\right)\Delta^{(t)}(A_n q_j) + \left(n A_{q_i \dot{q}_j}\right)\Delta^{(t)}(B_n q_j) \right\} , \quad (62)$$

$$\frac{1}{n^2}\Delta^{(t)}(B_n G_{q_i}) = \sum_j \left\{ \left(-n A_{q_i \dot{q}_j}\right)\Delta^{(t)}(A_n q_j) + \left(-n^2 A_{q_i \ddot{q}_j} + A_{q_i q_j}\right)\Delta^{(t)}(B_n q_j) \right\} . \quad (63)$$

These equations are combined into the following matrix form for convenience in the computer solution:

$$\frac{1}{n^2}\left[\Delta^{(t)}G(n,I)\right] = -\left[E(I,J,n)\right]\left[\Delta^{(t)}X(n,J)\right] . \quad (64)$$

In this expression, $[X(n,J)]$ is the column matrix which lists the harmonic cosine and sine coefficients of the root shear and the generalized coordinates representing the blade motions. [The forms for even and odd n are given explicitly in Equations (7) and (8)].

The form of the 22-by-22 [E] matrix is indicated below by writing the expressions for typical terms in the submatrices obtained by partitioning. In each matrix, the first and ninth columns are zero because the root shears do not appear in Equations (62) and (63). Also, the seventh, eighth, fifteenth, and sixteenth rows are zero since the corresponding equations are constraint equations rather than an expression of the equilibrium of generalized forces in the control modes. Moreover, the quasi-steady generalized forces in the vertical and torsion modes are independent of the generalized coordinates in the inplane modes. The quasi-steady generalized forces in the inplane modes are coupled by steady terms only to the torsion and control modes, as can be seen from Equation (60).

When the transmitted inplane shears are not being suppressed, the inplane generalized coordinates are essentially calculated after the generalized coordinates in the bending, torsion, and control modes. Thus, it is unnecessary to provide the $A_{H_i q_j}$ elements, and the computer program does not do so. When the transmitted inplane shears are suppressed, though, the inplane generalized coordinates must be calculated simultaneously with the others. The $A_{H_i q_j}$ elements are provided then.

$$[E(I,J,n)] = \begin{bmatrix} [0] & \left[n^2 A_{q_i \ddot{q}_j} - A_{q_i q_j}\right] & [0] & \left[-\,n A_{q_i \dot{q}_j}\right] & [0] \\ & [0] & & [0] & [0] \\ [0] & \left[n A_{q_i \dot{q}_j}\right] & [0] & \left[n^2 A_{q_i \ddot{q}_j} - A_{q_i q_j}\right] & [0] \\ & [0] & & [0] & [0] \\ \left[-A_{H_i q_j}\right] & & [0] & & [0] \\ [0] & & \left[-A_{H_i q_j}\right] & & [0] \end{bmatrix}$$

Expressions are given below for the A coefficients in terms of the blade parameters. These coefficients are automatically calculated in the computer program.

$$A_{h_i \ddot{h}_j} = -\pi\rho \int b^2 f_{h_i} f_{h_j}\, dr$$

$$A_{h_i \ddot{\theta}_j} = \pi\rho \int b^2 e f_{h_i} f_{\theta_j}\, dr$$

$$A_{h_i \ddot{c}_j} = \pi\rho \int b^2 e_o f_{h_i} f_{c_j}\, dr$$

$$A_{\theta_i \ddot{h}_j} = \pi\rho \int b^2 e f_{\theta_i} f_{h_j}\, dr$$

$$A_{\theta_i \ddot{\theta}_j} = -\pi\rho \int b^2 \left(e^2 + \frac{b^2}{8}\right) f_{\theta_i} f_{\theta_j}\, dr$$

81

$$A_{\theta_i \ddot{c}_j} = -\pi\rho \int b^2\left(ce_o + \frac{b^2}{8}\right) f_{\theta_i} f_{c_j}\, dr$$

$$A_{h_i \ddot{h}_j} = -\rho \int c_{\ell_\alpha} b r\, f_{h_i} f_{h_j}\, dr$$

$$A_{h_i \dot{\theta}_j} = 2\pi\rho \int b\left\{\frac{c_{\ell_\alpha}}{2\pi}\left(\frac{b}{2}+e\right)+\frac{b}{2}\right\} r f_{h_i} f_{\theta_j}\, dr$$

$$A_{h_i \dot{c}_j} = 2\pi\rho \int b\left\{\frac{c_{\ell_\alpha}}{2\pi}\left(\frac{b}{2}+e_o\right)+\frac{b}{2}\right\} r f_{h_i} f_{c_j}\, dr$$

$$A_{\theta_i \dot{h}_j} = -2\pi\rho \int b\left(\frac{b}{2}-\frac{c_{\ell_\alpha}}{2\pi}e\right) r f_{\theta_i} f_{h_j}\, dr$$

$$A_{\theta_i \dot{\theta}_j} = -\rho \int c_{\ell_\alpha} e\left(\frac{b}{2}+e\right) b r f_{\theta_i} f_{\theta_j}\, dr$$

$$A_{\theta_i \dot{c}_j} = -2\pi\rho \int \left\{\frac{c_{\ell_\alpha}}{2\pi}e\left(\frac{b}{2}+e_o\right)-\left(e_o-e\right)\frac{b}{2}\right\} b r f_{\theta_i} f_{c_j}\, dr$$

$$A_{h_i h_j} = 0$$

$$A_{h_i \theta_j} = \rho \int c_{\ell_\alpha} b r^2 f_{h_i} f_{\theta_j}\, dr$$

$$A_{h_i c_j} = \rho \int c_{\ell_\alpha} b r^2 f_{h_i} f_{c_j}\, dr$$

$$A_{\theta_i h_j} = 0$$

$$A_{\theta_i \theta_j} = 2\pi \rho \int b \left(\frac{b}{2} - \frac{c_{l_\alpha}}{2\pi} e \right) r^2 f_{\theta_i} f_{\theta_j} \, dr$$

$$A_{\theta_i c_j} = 2\pi \rho \int b \left(\frac{b}{2} - \frac{c_{l_\alpha}}{2\pi} e \right) r^2 f_{\theta_i} f_{c_j} \, dr$$

$$A_{H_i h_j} = 0$$

$$A_{H_i \theta_j} = -\rho \bar{c}_{d_\alpha} \int b r^2 f_{H_i} f_{\theta_j} \, dr$$

$$A_{H_i c_j} = -\rho \bar{c}_{d_\alpha} \int b r^2 f_{H_i} f_{c_j} \, dr .$$

APPENDIX IV

PROCEDURES USED FOR SOLUTIONS AT FLIGHT CONDITION DN67A

The procedures for using iteration factors and improved initial conditions in obtaining solutions can be clarified by examining the manner in which the various cases at Flight Condition DN67A (i. e., $\mu = 0.259$) were treated.

CASE 1 - CONVENTIONAL CONTROL (RUNS E2A TO E2C)

This was the basic case for this flight condition. For initial conditions, no dynamic blade response was assumed except for an estimate of the first harmonic flapping. Convergence was achieved in eight iterations with all iteration factors ϕ_c and ϕ_χ equal to 1.0. The results checked closely with Run B-6 of Reference 1.

CASE 2 - PITCH CONTROL AT SECOND AND FOURTH HARMONICS (RUNS E4A TO E4E)

In this case, the two largest transmitted vertical shears (the second and fourth harmonics) were eliminated. For initial conditions, the converged generalized forces and coordinates from Case 1 (Run E2C) were used. Fourteen iterations in five separate runs were necessary to achieve convergence. The modes which caused the most difficulty were the second antisymmetric bending mode and all antisymmetric and symmetric torsion modes. ϕ_c values of 0.5 in these modes led to convergence. The torsional response in the first antisymmetric and symmetric torsion modes are presented in Figures 10 and 11, respectively. As compared with the torsional response to conventional control, it can be seen that the response is much greater here, especially in the symmetric mode. Moreover, the angles involved are quite large and rapidly fluctuating and, thus, have a profound effect on the aerodynamic loading. This is a principal reason, it is believed, that convergence is so difficult to attain.

CASE 3 - PITCH CONTROL AT ALL EVEN HARMONICS (RUNS E3A TO E3E)

In this case, all the higher harmonic transmitted vertical shears (i. e., the second through the twelfth) were eliminated. Initial conditions were the converged generalized forces and coordinates from Case 2 (Run E4E). Fourteen iterations in five separate runs were again needed. Difficulty was encountered chiefly in the two symmetric torsion modes, but ϕ_c values of 0.75 were adequate.

84

CASE 4 - PITCH CONTROL AT THIRD AND SEVENTH HARMONICS (RUNS E6A TO E6C)

Here, the two largest transmitted inplane shears that can be suppressed with root pitch control (the third and seventh harmonics) were eliminated. Initial conditions for the generalized forces and coordinates were taken again from Case 1 (Run E2C). Nine iterations were necessary in three runs. There was very little difficulty with the symmetric modes, but the antisymmetric second bending and both torsion modes converged slowly. ϕ_x values of 0.5 and ϕ_θ values of 0.75 in these modes were used successfully. The resulting first torsional mode responses are also given in Figures 10 and 11. From these results, it can be seen that the antisymmetric torsional response is quite different from the corresponding response to conventional control and is likely to be a source of slow convergence.

CASE 5 - PITCH CONTROL AT ALL ODD HARMONICS (RUNS E7A TO E7C)

In this case, all the higher harmonic transmitted inplane shears that can be suppressed with root pitch control (the third through eleventh) were eliminated. Case 4 (Run E6C) was used for the initial conditions on the generalized forces and coordinates. Eleven iterations in three runs were required. The symmetric modes were rapidly convergent, and ϕ_G and ϕ_x values of 0.75 permitted convergence of the antisymmetric second bending and second torsion modes.

CASE 6 - PITCH CONTROL AT SECOND, THIRD, FOURTH, AND SEVENTH HARMONICS (RUNS E8A TO E8D)

Here, the two largest transmitted vertical shears (the second and fourth harmonics) and the two largest transmitted inplane shears that can be suppressed by root pitch control (the third and seventh harmonics) were eliminated. Initial conditions for the generalized forces and coordinates were found from Case 2 (Run E4E). Sixteen iterations were necessary in four runs. Symmetric and antisymmetric modes were slowly converging; namely, both torsion modes of the former and the first and second bending, and both torsion modes of the latter. On the basis of indications from Run E8A, several of the ϕ_G were changed from unity in an attempt to improve the rate of convergence. Using these values and the results of E8A for initial conditions, four additional iterations were run as E8B, but they actually indicated a slow divergence. The ϕ_G were, therefore, reset to unity, and the results of E8A were again used for initial conditions. A successful iteration was thus resumed, with convergence being attained ultimately using ϕ_x values of 0.5 in all modes. The converged torsional response in the first symmetric mode is close in phase, if not in magnitude, to Case 2 (see Figure 11). This led, in part, to the more rapid convergence of this mode than of the first

85

antisymmetric torsional mode, the response of which is significantly different in character from Case 2 (see Figure 10). Also, here, both even and odd harmonics are being controlled and fairly strong inter-harmonic aerodynamic coupling (of order μ) exists between adjacent harmonics.

At the other flight conditions, the various cases were iterated in the same general manner with some differences in choice of ϕ_θ and ϕ_x as required. No fixed rules can be given at this time for guaranteeing in advance the success of a given iteration. The judgment of the user must be inserted frequently into the iteration.

DOCUMENT CONTROL DATA - R & D

(Security classification of title, body of abstract and indexing annotation must be entered when the overall report is classified)

1. ORIGINATING ACTIVITY (Corporate author)	2a. REPORT SECURITY CLASSIFICATION
Cornell Aeronautical Laboratory, Inc. Buffalo, New York	Unclassified
	2b. GROUP

3. REPORT TITLE

SUPPRESSION OF TRANSMITTED HARMONIC VERTICAL AND INPLANE ROTOR LOADS BY BLADE PITCH CONTROL

4. DESCRIPTIVE NOTES (Type of report and inclusive dates)

Final Report - July 1967 - November 1968

5. AUTHOR(S) (First name, middle initial, last name)

John C. Balcerak and John C. Erickson, Jr.

6. REPORT DATE	7a. TOTAL NO. OF PAGES	7b. NO. OF REFS
July 1969	101	7

8a. CONTRACT OR GRANT NO. DAAJ02-67-C-0096	9a. ORIGINATOR'S REPORT NUMBER(S)
b. PROJECT NO. Task 1F162204A14604	USAAVLABS Technical Report 69-39
c.	9b. OTHER REPORT NO(S) (Any other numbers that may be assigned this report)
d.	BB-2496-S-1

10. DISTRIBUTION STATEMENT

This document is subject to special export controls and each transmittal to foreign governments or foreign nationals may be made only with prior approval of US Army Aviation Materiel Laboratories, Fort Eustis, Virginia 23604.

11. SUPPLEMENTARY NOTES	12. SPONSORING MILITARY ACTIVITY
	U. S. Army Aviation Materiel Laboratories, Fort Eustis, Virginia

13. ABSTRACT

A method was developed to study the possibility of using higher harmonic pitch-angle inputs to eliminate the transmission of oscillatory vertical and inplane forces from a helicopter rotor to its driving shaft. The aerodynamic loads are computed by using a realistic model which represents the rotor blades by bound vorticity distributions and the wake by a mesh of segmented vortex filaments.

Computed results are presented for a two-bladed teetering rotor which was approximately the same as that of the UH-1A configuration except for the assumed differences in pitch control. The required pitch-angle inputs were determined for eliminating various combinations of harmonic root shears for three flight conditions.

DD FORM 1473 REPLACES DD FORM 1473, 1 JAN 64, WHICH IS OBSOLETE FOR ARMY USE.

14. KEY WORDS	LINK A		LINK B		LINK C	
	ROLE	WT	ROLE	WT	ROLE	WT
Transmitted Harmonic Rotor Loads						
Higher Harmonic Pitch Control						